Wave overtopping in harbour areas

MSc thesis by:

M.R.A. Gensen

March 2017

TU Delft

HKV LIJN IN WATER

Front cover image:
Violent wave overtopping at Samphire Hoe
Photograph courtesy of Eurotunnel and the White Cliffs Countryside Project
Retrieved January 27th 2017 from: http://www.clash.ugent.be/

Wave overtopping inside harbours

On how to model wave overtopping discharges in harbour areas under the influence of wave penetration and locally generated waves

Thesis by:

M.R.A. Gensen

Master of Science thesis
Master Civil Engineering; track Hydraulic Engineering
Delft University of Technology

Delft, March 2017

Graduation committee

Prof.dr.ir. Uijttewaal, W.S.J. (Wim)	Delft University of Technology
Ir. Botterhuis, A.A.J. (Ton)	HKV Lijn in Water B.V.
Dr.ir. Van Vuren, S. (Saskia)	Delft University of Technology
Dr. Tissier, M.F.S. (Marion)	Delft University of Technology

Preface

Before you lies the thesis 'Wave overtopping in harbour areas', the product of a research on the methodology to predict wave overtopping discharges in a harbour area which is under the combined influence of locally generated waves and penetrated wave action. The initial question was posed by the Dutch consultancy company HKV Lijn in Water.

This thesis is the final requirement for obtaining a master's degree in Civil Engineering, with a specialisation in the field of Hydraulic Engineering, at the Delft University of Technology. The research with this thesis report as a result represents forty European Credits (ECTS).

The first words of gratitude go out to my graduation committee members for their time, guidance and critical review during the course of the thesis; Wim Uijttewaal for his scientific view on the rather practical topic; Ton Botterhuis from HKV for his practical guidance and his help in streamlining the working method during the course of the thesis; Saskia van Vuren for the initial contact with HKV and her in-depth feedback and Marion Tissier for her interest in the topic and her specific help with the topic of waves.

Secondly I really appreciate the opportunity that HKV Lijn in Water has given me to perform my thesis at their company. They facilitated this thesis by providing guidance and work space at its locations in Lelystad and Delft. The professional input and pleasant environment my colleagues and fellow students at HKV gave me during work time, at the lunch table and during the after-lunch walks were very helpful during the course of the research.

Finally I would like to thank anyone who has answered one of my questions; and of course my family, housemates and friends for their unconditional support during the entire course of my thesis.

Matthijs Gensen,
Delft, March 2017

Abstract

Wave overtopping in harbour areas is a fairly untreated topic in the context of flood risk analyses. Pragmatic approaches were undertaken to evaluate the possible influence of wave overtopping on the frequency of flooding. However no consensus was reached on how wave overtopping in a harbour area could be quantified. Therefore it is also difficult to determine whether wave overtopping should be accounted for in a flood risk assessment or not.

This master thesis seeks to find an answer on the question which method is best suitable to quantify wave overtopping in harbour areas. Along the way it is studied which wave processes play a role and how available models take into account these processes. Subsequently a choice for a certain method or model can be made. Using this approach the question whether the effect wave overtopping might be significant in a flood risk analysis is answered.

At first a theory study is undertaken which consists of two parts. The first part examines the theory on the wave processes which play a role in the nearshore and inside harbours. The second part explores the capabilities and limitations of empirical and numerical modelling of wave heights and wave overtopping in harbour areas.

It was chosen to develop a non-numerical model within the scope of this thesis. The available numerical models are either not capable of modelling all relevant wave processes or model an entire harbour area in a sufficiently efficient way. These considerations might change by future updates of the discussed numerical models or the development of a new and suitable numerical model. Furthermore the computational speed is expected to keep growing, such that the problem of a lack of computational efficiency might decrease in the future.

The developed non-numerical WGPO model considers the most relevant processes, namely: **w**ave **g**eneration, wave **p**enetration and wave **o**vertopping. Wave generation is estimated using the empirical Bretschneider formula. Wave diffraction and wave transmission and the interaction between the two are the considered components to determine the contribution of penetrated waves. The wave diffraction pattern is determined using the analytically derived Goda diffraction diagrams. Finally the expected amount of wave overtopping over the quay walls of the harbour is estimated using the empirical EurOtop formulas. Using the case of the *Vlissingen Buitenhaven* the performance of the WGPO model was verified with respect to earlier researches. Due to the assumptions which lie at the basis of the model it is not (yet) possible to model complex harbour geometries. This would require improvements to the WGPO model or the application of a numerical wave model.

By applying the model to the case of the *Brittaniëhaven* in the *Botlek* area of the harbour of Rotterdam the influence of wave overtopping on the probability of flooding was estimated. It appears that the frequency of flooding of the harbour areas may double. In conclusion, this case study of the Brittaniëhaven thus shows the importance of taking into account wave overtopping in a flood risk analysis of a harbour case.

Table of Contents

1. Introduction

1.1. Research motivation

In the Netherlands more than 115,000 people live in (partly) unembanked areas experiencing flood risk (Dutch: *buitendijks gebied*). They live on the water side of the primary flood protections. In general these are the floodplains of the major Dutch rivers. Unembanked areas cover approximately 4 percent of the country's area in total (Rijkswaterstaat, 2012), see Figure 1.1. They have different functions: nature areas, agriculture, industry and residential areas.

Most of the unembanked areas are fairly uninhabited and have a low economic value. The major exception is the Rijnmond-Drechtsteden region in the western Rhine delta (Figure 1.2). The unembanked areas in this region are populated by approximately 65,000 people. One of these areas is the Noordereiland in Rotterdam, see Figure 1.3. Furthermore extensive industrial areas with large economic values are located in this region, including the port of Rotterdam. The port of Rotterdam is the largest port in Europe with an annual cargo tonnage of over 400 million. It consists of several distinct harbour areas which stretch out over forty kilometres, from the historic harbour areas inside the city centre to the newly developed harbour area Maasvlakte 2.

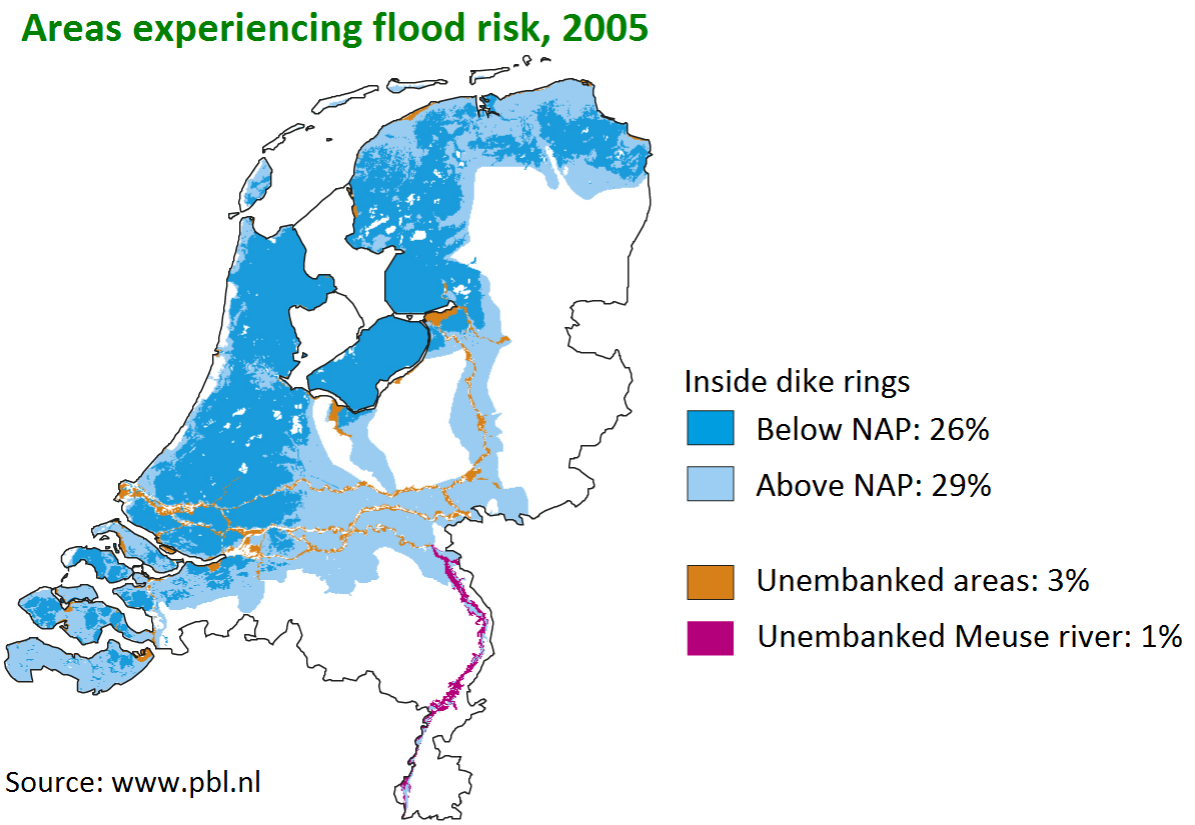

Figure 1.1: Flood prone areas in the Netherlands including unembanked areas. It can be seen that most unembanked areas are found along the main rivers and in the Rotterdam harbour area (Planbureau voor de Leefomgeving, 2009)

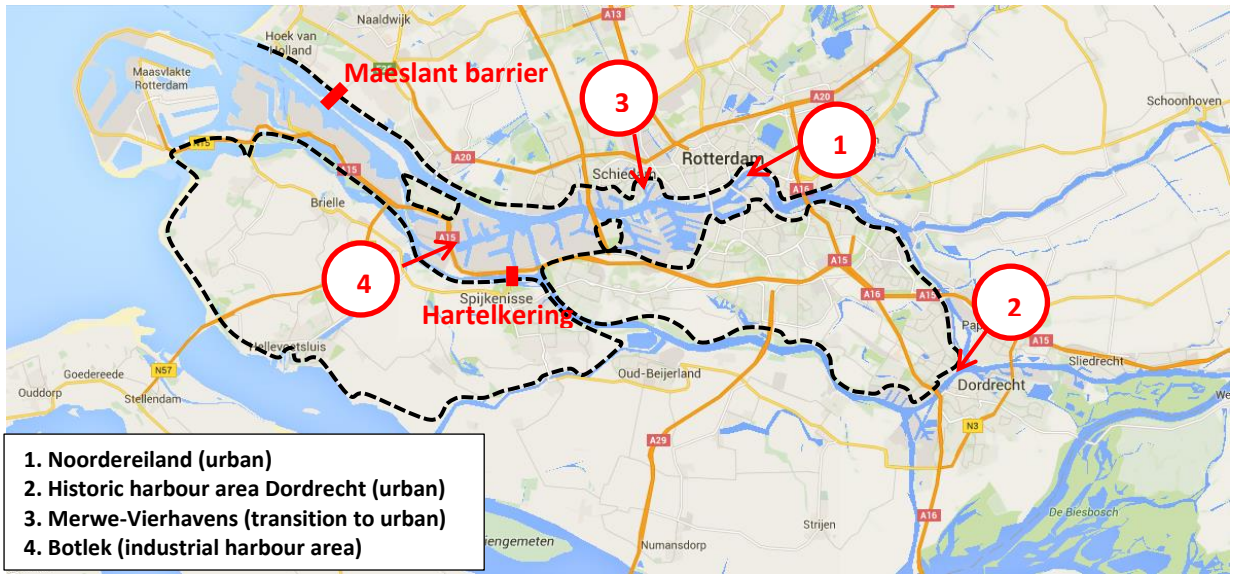

Figure 1.2: Map of the Rijnmond-Drechtsteden area (Google Maps, 2016). The black dotted lines indicate the primary flood defences in the areas surrounding the harbour of Rotterdam. The locations of the four pilot projects of the 'Strategic adaption agenda for unembanked areas' have been indicated.

Figure 1.3: Noordereiland in Rotterdam; its 3200 inhabitants are prone to flooding on a (nearly) yearly basis. A pilot project has been started as the complexity of the water safety problem is large and the costs to increase the safety level are high. The goal of this pilot project is to generate input for the agenda on unembanked areas in the Rijnmond-Drechtsteden area. Source picture: (ANP, 2016)

These unembanked areas experience flood risk. Flood risk is the product of the probability of a flood event and the consequences of this event. The unembanked floodplains along the main rivers experience regular flooding, but the consequences are very little, leading to an acceptable flood risk.

For the Rijnmond-Drechtsteden region the situation is different. Although high water levels can originate both from sea as from the river, the probability of flooding is rather low (Van Barneveld,

2013) as the ground levels of the unembanked areas are high compared to average and more extreme high water levels. In the Rotterdam region surface elevations are generally around 3 to 3.5 meters above the mean sea level (Van Veelen, 2013). Furthermore the probability of casualties is also relatively low. Extreme high water levels due to high river discharges can be predicted several days in advance, such that inhabitants can be evacuated in time with a safe margin (Elshof, 2014) (Pieterse, Knoop, Nabielek, Pols, & Tennekes, 2009). Threats originating from the sea are far more unpredictable; however the Rijnmond-Drechtsteden area is rather well protected from this threat via various (storm surge) barriers such as the Maeslant barrier and the *'Hartelkering'* (locations indicated in Figure 1.2). A far more important contributor to flood risk in the Rijnmond-Drechtsteden region are the potential economic damages during a flood event (Elshof, 2014). Flooding of the vital infrastructure in the Rotterdam harbour areas may induce large economic damages and societal disruption (Nicolai, et al., 2016) (Elshof, 2014) (Van Barneveld, 2013) (Van Veelen, 2013) (Veerbeek, et al., 2010).

Under future climate change sea levels will rise and storms are expected to become more severe. With a maximum sea level rise of 100 centimetres (KNMI, 2015) average tidal water levels can already be expected to approach the elevation of the unembanked areas. For different climate scenarios an increase of the flood frequency by a factor 10 up to 100 can be expected in these areas (Van Barneveld, 2013) (Veerbeek, et al., 2010). Furthermore consequences of flooding will also increase as the use of the unembanked areas is expected to intensify (Van Buuren, Eshuis, & Van Vliet, 2015) (Elshof, 2014). However not only an increase of economic value will occur; a total population growth in unembanked areas of 60,000 people can be expected in this century (Rijkswaterstaat, 2012). This will lead to an unacceptable situation for several inhabited and uninhabited areas within the Rijnmond-Drechtsteden region (Elshof, 2014).

Inside the primary flood protection system safety from flooding is regulated and guaranteed by the Dutch government. However for unembanked areas this is not the case and protection from flooding is the responsibility of the local residents and the companies themselves. National policy on the flood protection of unembanked areas will not be changed in the near future as is stated in the *'Nationaal Waterplan 2016-2021'* (Rijksoverheid, 2015). Due to the expected unacceptable situation in the future with regards to flood risk in the unembanked areas the Delta Program 2015 (Rijkswaterstaat, 2015) has set the task of mapping and adapting the flood risk for several unembanked areas in the mouth of the river Rhine. This task is placed under the authority of regional and local governments through earlier legislation, i.e. the *'Nationaal Waterplan 2009-2015'* (Rijksoverheid, 2009).

In this context it was agreed that a 'Strategic Adaptation Agenda for unembanked areas' (Dutch: *Strategische adaptatieagenda buitendijks*) will be developed for the Rijnmond-Drechtsteden area (Rijkswaterstaat, 2015). Within this adaptation agenda four pilot projects were defined, see Figure 1.2. (Deltacommissaris, 2016). For each of those locations the water safety issue is complex and the investment costs for solutions are high. Two of the pilot projects have an existing urban function (*Noordereiland* and the *historic harbour area of Dordrecht*). One of the locations is undergoing a gradual transformation from an industrial harbour area to an urban area (*Merwe-vierhavengebied*). The final pilot project location is the Botlek area, being intensively used as an industrial harbour area, see Figure 1.5 for an aerial picture of the Botlek area.

In the 'Pilot water safety Botlek' the probability of a flood event and the consequences of the event are investigated. The first phase of the pilot has resulted in flood maps for the current situation as well as for the future conditions in the years 2050 and 2100 (Gemeente Rotterdam, 2016). During this first phase a very pragmatic approach was applied meaning that wherever necessary risk contributing factors were quantified by expert judgement or simple thumb rules. This simple approach was sufficient in the framework of the pilot project, but for future flood risk estimations a more detailed approach may be necessary. An example is the influence of wave overtopping on flood risk and corresponding inundation. Wave overtopping is the process of water crossing the flood protection over its crest due to wave action, see Figure 1.4. It occurs when the crest levels are not high enough to prevent waves from rushing up against the structure and thereby exceeding the crest level.

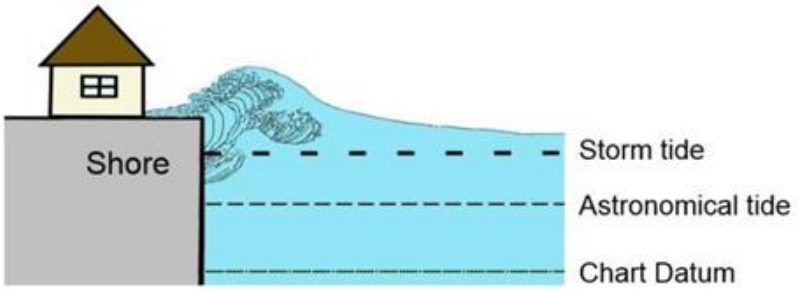

Figure 1.4: Illustration showing the possible flooding of an area due to wave overtopping. The still water level, consisting of several components, does not reach the crest level of the structure. However, due to wave action water still crosses the crest of the structure. (Benítez & Mercado-Irizarry, 2015)

In the determination of the flood maps wave overtopping was taken into account via a simple addition to the still water level mainly based on expert judgement (Botterhuis, Nicolai, & Stijnen, 2015). This simple approach contributed to the overall uncertainty of the determination of the flood maps. A more accurate and physical approach was not undertaken as the topic of wave overtopping was surrounded with too much indistinctness and uncertainty. Research is required to possibly find a more physical and accurate approach to include the effect of wave overtopping in flood risk assessment.

Figure 1.5: Botlek area, extensive harbour area outside of the primary flood defences. Source: (ANP, N.D.)

1.2. Problem definition

In recent flood risk calculations in unembanked areas the contribution of wave overtopping to flood risk is often left unaddressed. Extreme high water levels are carefully determined by combining still water levels, astronomical tides, seiches, harbour oscillations and future sea level rise (Slootjes & Wagenaar, 2015) (Van Barneveld, 2013). Waves are disregarded as is assumed wave heights are relatively low and thus have a little influence on flood risk. Unknown is if this assumption is actually true.

With the described future changes the influence of wave overtopping on flood risk is presumably going to increase. With future sea level rise the water level during an average high tide may already approach the elevation of the urbanized and industrial unembanked areas. With low freeboards overtopping of the quay walls by short waves may occur fairly frequently.

This type of overtopping without overflow (with overflow occurring when the still water level exceeds the crest level) will not directly lead to large inundation depths. While this would not be a serious problem for any other area, it is a problem for the Botlek area. The Botlek area contains a lot of petrochemical industry. Throughout the harbour area pipelines run just above the surface. The pipeline systems are expected to be vulnerable to flooding (Nicolai, et al., 2016) (Elshof, 2014). Failure of the system may occur as a consequence of the failure of the electrical network or from direct contact of salt water with a pipeline. As failure of the pipeline system can have catastrophic consequences, inundation of only a few centimetres is already unwanted. This example illustrates why the recommended maximum wave overtopping in the '*Handbook of quay walls*' is only 0.42 l/s/m (De Gijt & Broeken, 2005). The EurOtop overtopping manual (EurOtop, 2016) suggests even lower tolerable overtopping discharges.

This example shows the likely importance of wave overtopping for an unembanked area in a flood risk calculation. For the design and assessment of (primary) flood defences it is already dealt with, where it is often combined with overflow. In general cases of flood defences a certain freeboard is taken into account in the design of the defence. This freeboard accounts for wave run-up and wave overtopping. Rules of thumb are given for tolerable overtopping discharges from which the required freeboard can be determined.

In practice the amount of wave overtopping is difficult to determine accurately. Often empirical formulas will be applied. Such formulas have been derived from line-fitting to a set of measurements. The formulas have been gathered in the EurOtop overtopping manual (EurOtop, 2016). To apply a formula one must know the wave conditions (significant wave height, wave period and wave direction) and the local geometry (slopes, water depths, freeboards, etc.). For an assessment of a dike the calculated overtopping discharge can be compared to the tolerable discharge.

For unembanked harbour areas several issues are encountered when trying to determine the overtopping discharges. Inside a harbour basin the wave conditions are very difficult to predict. Many different wave processes play a role, e.g. wave diffraction, resonance and reflections. These processes create a very complex two-dimensional wave field. This is different for a coastal setting, where waves are far more unidirectional and less wave processes play a role. Although a deterministic approach exists (Rijkswaterstaat, 2014), its use is restricted to very specific conditions.

A way of finding the (extreme) wave conditions could be by extrapolation of a wave record. However a little amount of measurement campaigns have been undertaken. Even if a long wave record would be available, extrapolation is not straight-forward and might even be invalid for a harbour case. In a harbour more processes come into play under extreme conditions. An example is the submergence of a breakwater when water levels exceed the crest level of the breakwater. In this case the amount of wave transmission increases significantly. When extrapolating a set of measurements this significant increase in the amount of wave transmission is not reflected, such that the predicted extreme wave heights inside the harbour may be too small.

A subsequent complexing factor is the determination of the overtopping rate given the prevailing wave conditions. The empirical formulas given in the EurOtop manual (EurOtop, 2016) are restricted to specific conditions. An example is the wave direction; in the manual it is assumed that all waves have the same direction. However, inside a harbour basin the wave field may be very irregular. Assumptions have to be made in order to be able to apply the formulas. The uncertainty surrounding such assumptions is unknown.

Earlier case studies have largely avoided the mentioned issues by using pragmatic approaches (Botterhuis, Nicolai, & Stijnen, 2015) (Slootjes & Wagenaar, 2015). To assess the accuracy of their approaches the topic of wave overtopping inside harbour areas requires more attention.

1.3. Objective

Several studies have been performed to find the contribution of wave overtopping to flood risk for unembanked areas (Botterhuis, Nicolai, & Stijnen, 2015) (Slootjes & Wagenaar, 2015). However no consensus has been reached on the best method to determine wave heights and associated overtopping discharges and volumes. The objective of this thesis is to find an approach that can be applied to model wave overtopping rates in harbour areas. The knowledge gained during the course of the research can help answering questions concerning wave overtopping in harbour areas. A question in this context is: does wave overtopping have a significant influence on flood risk in harbour areas?

1.4. Research questions

The main research question stated below covers the problem statement and the objective:

What is the best approach to model wave overtopping in a harbour area under the influence of wave penetration and local wave generation and how does it affect flood risk?

Several research questions lie at the base of this main research question:

1. Which processes affect wave propagation, wave penetration into harbour areas and wave overtopping?
2. Which type of approach is likely to be most suitable for determining the combination of wave penetration, agitation and subsequent overtopping?
    - What is the relative influence of the wave processes on the wave field inside the harbour and the overtopping rate over the quay walls?
    - Besides (expected accuracy), which assessment criteria apply?

- Which non-numerical methods have been applied to determine the wave field and wave overtopping discharges in harbours?
- Which numerical methods have been applied to determine the wave field and wave overtopping discharges in harbours?
- Which type of approach is (likely to be) the best approach with regards to meeting the requirements and assessment criteria?

3. What are the characteristics of the final modelling approach?
    - What is the structure of the model?
    - How are the most relevant wave processes dealt with in the model?
    - In which cases can the model be applied?
4. How does wave overtopping affect flood risk in the '*Brittaniëhaven*' case study?
    - Which variables have the most influence on the overtopping discharge?
    - How do wave overtopping rates translate to flood risk?
    - What is the effect of future sea level rise on the wave overtopping discharges and corresponding flood risk?

1.5. Reading guide

The outline of the remainder of this report is visualized in Figure 1.6.

The second chapter of this report contains a theory study on the various wave processes which play a role in the nearshore and inside ports. This chapter is specifically meant for readers without knowledge on wave physics.

The third chapter consists of a theoretical and a practical part. It deals with the modelling of wave penetration, agitation and overtopping in harbour areas. It explores the topic of empirical and numerical modelling in port applications in earlier research. Furthermore it also sets the requirements and assessment criteria for a model. At the end of this chapter a choice is made for a certain modelling approach.

Following the choice for a certain approach, a (semi-empirical) model was built. This model, the **W**ave **G**eneration **P**enetration **O**vertopping model, is described in Chapter 4. This description contains the general philosophy of the WGPO model, the model structure and the model components. Subsequently the model results are verified using the *Vlissingen Buitenhaven* case. Finally this chapter discusses the applicability range of the WGPO model.

Chapter 5 deals with a case study on the *Brittaniëhaven*. Firstly the case will be described, after which the case is implemented into the WGPO model. With this model setup the flood risk of the *Brittaniëhaven* including the effect of wave overtopping is studied. Finally an uncertainty analysis is performed for this specific case in which the consequences on the flood frequency by a change in the model or a change in the input parameters is tested.

The final chapter, Chapter 6, gives a discussion on the methods and results in this thesis. Furthermore a general conclusion is drawn and finally some recommendations with regards to the topic are given.

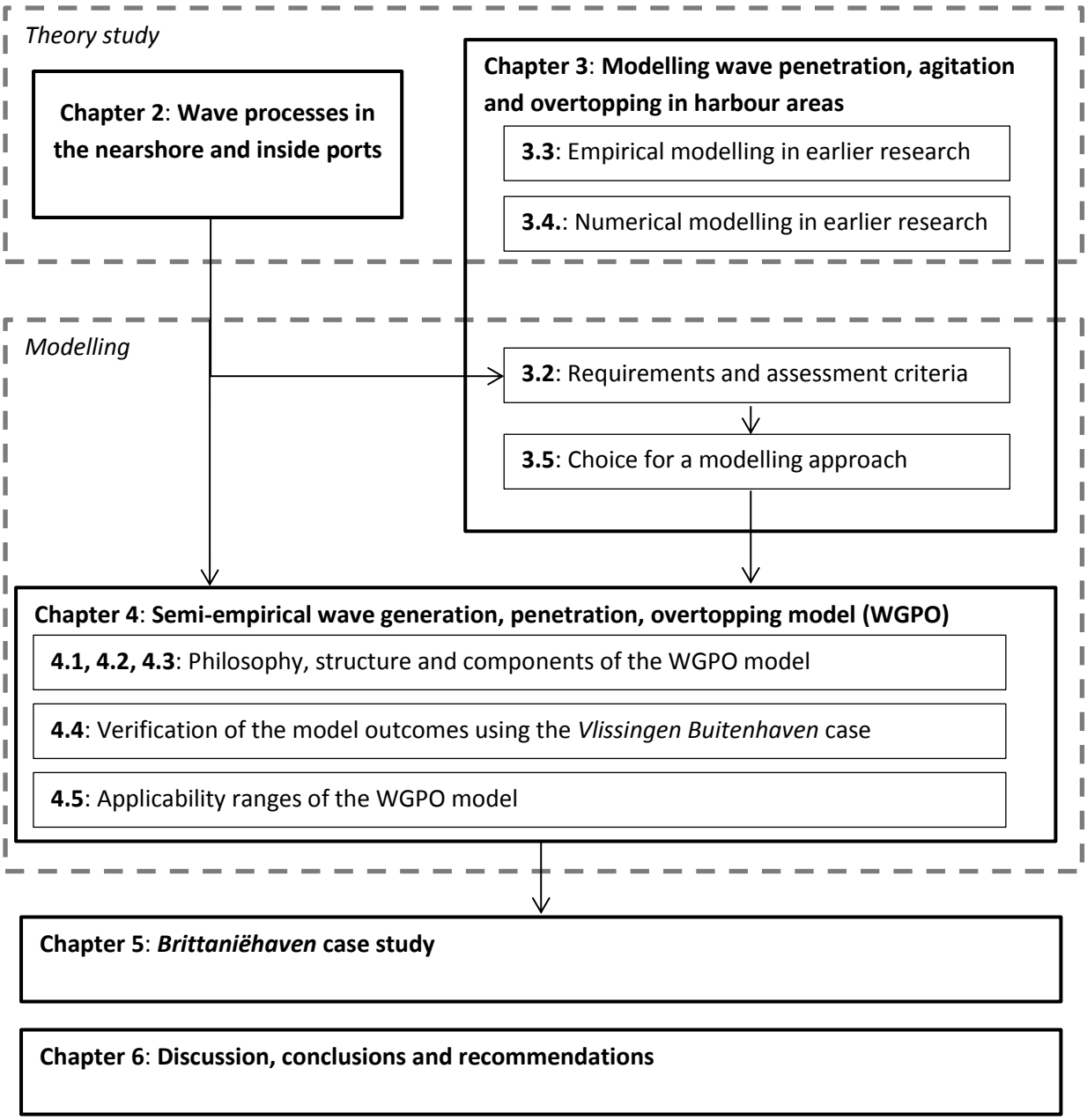

Figure 1.6: Visual representation of the reading guide

2. Wave processes in the nearshore and inside ports

This chapter will give an overview of the most important wave processes in the nearshore and inside ports. Thereby it will answer the first research question:

> *1. Which processes affect wave propagation, wave penetration into harbour areas and wave overtopping?*

Each paragraph gives general descriptions of the various processes. Detailed information and equations for a specific process are given in the grey boxes. Paragraph 2.1 describes some general aspects about wind waves and how they propagate. Paragraph 0 contains the processes that start playing a role in the nearshore where the propagation of waves becomes depth-dependent. Subsequently (Paragraph 2.3) the transfer of energy between waves and the dissipation of wave energy is discussed. The final paragraph (2.4) deals with the processes that are induced by the presence of a coastal structure.

2.1. Generation and propagation of wind waves

The sea is generally a very random pattern of waves. It consists of many different wave components; together making up the entire sea surface. The largest contribution to the spectrum of wave components comes from wind-generated waves. Where wind blows over the sea surface a shear stress is exhibited to the sea surface causing oscillations. Waves have larger wave heights for increasing wind speed, increasing duration of the wind and increasing area over which the wind blows.

Wind-waves can be generated close-by or can originate from far away. Wave fields contain different components depending on the geographical location and the origin of the waves. For a 'young wind sea' a lot of wave energy is added close-by. For this type of sea the wave energy is a function of the local fetch; i.e. the distance over which the wind blows. This type of sea has the most randomness. When local wave conditions are dominated by waves generated by a storm further away very regular swell waves with lower frequencies will arrive at the coast. Due to frequency dispersion longer waves will arrive earlier at the coast than shorter waves, although they may originate from the same time and place. The wave length can be determined using the dispersion relation. It is a function of the local water depth and the wave period. It is a dominant variable in many processes. For instance bottom-induced wave processes, such as energy dissipation by friction, have a larger effect on waves with a large wave length.

Frequency dispersion

Waves of different wavelengths and frequencies travel with different phase speed; this phenomenon is called frequency dispersion. Phase speed is not the velocity of the water particles under the wave, but the propagation velocity of the wave itself. Longer waves with a low frequency travel faster than shorter waves with a high frequency. This can be found by using the dispersion relation for linear surface gravity waves (U.S. Army Corps Of Engineers, 2008) (Holthuijsen, 2007):

$$\omega^2 = gk\tanh(kh) \quad or \quad \lambda = \frac{g}{2\pi}T^2\tanh\left(2\pi\frac{h}{\lambda}\right) \qquad \textbf{Equation 2-1}$$

With:

ω	=	Angular frequency (in radians per second)
k	=	Wave number (in radians per meter)
h	=	Water depth (in meters)
λ	=	Wave length (in meters)
T	=	Wave period (in seconds)

In this case of linear waves the phase velocity can be expressed as follows (U.S. Army Corps Of Engineers, 2008):

$$c_p = \frac{\lambda}{T} = \frac{\omega}{k} \qquad \textbf{Equation 2-2}$$

Wave length and relative water deepness

The wave length of a wave with a certain frequency can be determined using the dispersion relation. As the dispersion relation is an implicit expression in terms of the wave length (or wave number k), iterations are required. For deep and shallow water the dispersion relation can be simplified (Holthuijsen, 2007):

$$\omega = \sqrt{gk} \quad or \quad \lambda = \frac{gT^2}{2\pi} \qquad for\ deep\ water:\ kh \to \infty \qquad \textbf{Equation 2-3}$$

$$\omega = k\sqrt{gh} \quad or \quad \lambda = T\sqrt{gh} \qquad for\ shallow\ water:\ kh \to 0 \qquad \textbf{Equation 2-4}$$

In practice the relative water deepness (kh or h/L) can also be seen as an indicator for the influence of depth-dependent processes such as shoaling and bottom friction. In general wave-induced particle motions can be found up to a depth of halve of the wave length (U.S. Army Corps Of Engineers, 2008).

Any wave field can be summarized in a wave spectrum. The spectrum presents the amount of wave energy for a certain wave frequency. Any linear wave field can be represented in a one-or two-dimensional wave spectrum by sampling the waves.

Wave energy

The energy of a wave system is the sum of the kinetic and the potential energy. The kinetic energy is associated with the motion of the water particles under the wave whereas the potential energy is the energy stored in a wave as a result of its position relative to the still water level. Under the assumption of linear wave theory and thus strictly harmonic waves the time-averaged potential and kinetic energy are equal and amount (U.S. Army Corps Of Engineers, 2008):

$$\overline{E_k} = \overline{E_p} = \frac{1}{16}\rho g H^2 \qquad \textbf{Equation 2-5}$$

The total time-averaged (specific) wave energy per unit surface area (unit: J/m^2) is then:

$$\bar{E} = \frac{1}{8}\rho g H^2 \qquad \textbf{Equation 2-6}$$

Theoretical wave spectra have been developed for different types of seas. Examples of these theoretical spectra are the Pearson-Moskowitz spectrum and the JONSWAP spectrum. These theories are closely related to theory on local wave generation.

Local wave generation

The process of generation and growth of waves is not straightforward. Starting with an entirely flat sea surface, three processes will cause the generation and growth of waves at short fetches. The first two processes are related to the energy input by wind. Turbulent winds cause pressure fluctuations just above the sea surface. These pressure differences induce small-amplitude short

waves via resonance with the sea surface (Philips, 1957). Subsequently these waves may grow due to a wave-wind feedback mechanism. The wind pattern above the just formed wave changes with over pressures at the windward side and under pressures at the leeside (Miles, 1957). The wind distribution changes along with the sea surface, thereby transferring energy to the wave. For larger waves the distortion of the wind pattern is larger and as of such larger waves will also induce a larger energy transfer. Therefore wave growth due to the feedback mechanism with the wind shows exponential growth in time. The third process which causes wave growth of newly formed waves is the (non-linear) interaction between several wave components. This process is discussed separately.

In reality the combination of these three mechanisms cause the generation and growth of waves. Therefore no formulation based on physical grounds exists. Also no single empirical formulation can describe wave growth accurately for any given circumstances. Different empirical formulas exist for varying circumstances (e.g. fetch-limited wave growth or depth-limited wave growth) The most relevant parameters in (most) empirical formulas are:

F = Fetch (in meters)
U_{10} = Wind speed at ten meters height (in meters per second)
h = Water depth (in meters)
H_s = Significant wave height (in meters)

Some widely used examples of empirical formulas for wave growth are:
Bretschneider formula (U.S. Army Coastal Engineering Research Center, 1975)*:*

$$H_s = \frac{0.283 * U_{10}^2 * \tanh\left[0.530\left(\frac{gh}{U_{10}^2}\right)^{0.75}\right]}{g} * \tanh\left(\frac{0.0125}{\tanh\left[0.530\left(\frac{gh}{U_{10}^2}\right)^{0.75}\right]}\left(\frac{gF}{U_{10}^2}\right)^{0.42}\right) \qquad \textbf{Equation 2-7}$$

Young and Verhagen (1996) *:*

$$H_s = \frac{0.241 * U_{10}^2 * \tanh\left[0.493\left(\frac{gh}{U_{10}^2}\right)^{0.747}\right]^{0.87}}{g} * \tanh\left(\frac{3.133 * 10^{-3}}{\tanh\left[0.493\left(\frac{gh}{U_{10}^2}\right)^{0.747}\right]}\left(\frac{gF}{U_{10}^2}\right)^{0.575}\right)^{0.87} \qquad \textbf{Equation 2-8}$$

Breugem and Holthuijsen formula (Breugem & Holthuijsen, 2007)*:*

$$H_s = \frac{0.240 * U_{10}^2 * \tanh\left[0.343\left(\frac{gh}{U_{10}^2}\right)^{1.141}\right]^{0.572}}{g} * \tanh\left(\frac{4.410 * 10^{-4}}{\tanh\left[0.343\left(\frac{gh}{U_{10}^2}\right)^{1.141}\right]}\left(\frac{gF}{U_{10}^2}\right)^{0.790}\right)^{0.572} \qquad \textbf{Equation 2-9}$$

All formulas use the same variables and a similar structure of the formula, but the parameters vary. It is difficult, if not impossible, to choose the right formula for arbitrary circumstances (Nederpel & Van Balen, 2015). Too little measurements have been done for varying circumstances, water body types and geometries. Another additional uncertainty is the already present variability of the natural process (Nederpel & Van Balen, 2015).

2.2. Wave processes in the nearshore

When waves travel into shallower water various mechanisms will change the height, length and shape of the waves. Non-linear processes will become more dominant. For these reasons the propagation of waves in the nearshore is more difficult to predict compared to deep water wave propagation.

One of the primary wave transformation processes in the nearshore is (linear) shoaling. Shoaling is the phenomenon of increasing wave height due to a reduction of the group velocity of the waves. Shoaling plays a very dominant role in areas with bottom gradients.

Shoaling

Shoaling occurs as energy fluxes have to be conserved in a stationary situation if all dissipative mechanisms are neglected. Energy fluxes are a function of the energy density times the velocity. The velocity is the group velocity of the waves as the energy is transported with the wave groups. For energy conservation reasons; if the group velocity increases or decreases the energy density has to decrease or increase respectively. When waves travel from deep water to shallower water the propagation velocity decreases (follows from dispersion relation: Equation 2-1) Thus with decreasing group velocity the energy per surface area has to increase. As the wave height is directly related to wave energy, wave height increases. The shoaling processes can be captured in the following partial derivative (valid for normally incident waves in x-direction and parallel depth contours):

$$\frac{d}{dx}\left(c_g * E\right) = 0 \qquad \textbf{Equation 2-10}$$

For small amplitude waves this formula can be applied using linear wave theory as it can be assumed that non-linear effects will not play a dominant role (Holthuijsen, 2007). For higher amplitude waves more complex phenomena start playing a role; for instance the generation of higher order waves.

Shoaling may also occur due to ambient currents in the (opposite) direction of the propagation.

Wave refraction is closely related to wave shoaling. It also involves a change of wave energy density as waves travel over a non-flat bed. However with refraction oblique waves are involved. While travelling over a bottom gradient the waves will start turning. This leads to bundling or spreading of the wave energy. As of such refraction can both cause the wave height to increase and decrease.

Refraction

Similar to shoaling, the phenomenon of refraction is also related to energy flux conservation. However oblique waves are involved now. Wherever the depth contours are not perpendicular to the wave rays, the waves will start turning and wave heights will change as a consequence of refraction. This can either concern an increase or a decrease of the wave height. Refraction occurs due to the depth variation along a wave crest such that the phase speed along the crest is variable. Refraction can be expressed with the following partial differential equation (Holthuijsen, 2007):

$$\left(\frac{d\theta}{dt}\right)_{refraction} = -\frac{c_g}{c}\frac{\partial c}{\partial m} \qquad \textbf{Equation 2-11}$$

In which:

$\frac{d\theta}{dt}$	=	Turning rate of the wave crest in time in a frame moving with the group velocity
c	=	Phase speed (in meters per second)

c_g	=	Group velocity (in meters per second)
∂m	=	Distance along a wave crest

Similar to shoaling wave refraction may also occur due to ambient currents. In the case of refraction the direction of the ambient current should be under an angle with the wave propagation direction in order to occur.

Whereas refraction involves bending of the wave crests due to water depth fluctuations, diffraction is the phenomenon of bending waves due to a discontinuity in the wave height along the crest. This may for instance occur due to obstructions in the path of the wave ray. Similar to sound waves, surface waves can travel around corners and barriers. Behind obstacles wave energy will penetrate into the undisturbed area. The effect of diffraction increases with increasing wave length.

Diffraction

After a wave passes an obstacle or travels through an opening wave directions will change as waves are able to travel around corners. The bending (and extension of the wave crest) will cause the wave heights to decrease in the original propagation direction. The sea surface behind the obstacle is however disturbed and will now show some wave action. The curvature of the wave ray which is affected by diffraction can be expressed as follows (Holthuijsen, 2007):

$$\left(\frac{d\theta}{dn}\right)_{diffraction} = -\frac{1}{2(1+\delta_a)}\frac{\partial \delta_a}{\partial m} \qquad \textbf{Equation 2-12}$$

In which:

$\frac{d\theta}{dn}$	=	Turning rate of the wave ray
δ_a	=	Diffraction parameter (function of the wave amplitude)
∂m	=	Distance along a wave crest
∂n	=	Distance along a wave ray

Generally this function is impossible to solve as the computation of the wave rays requires the wave amplitude and vice-versa. Analytical solutions and empirical solutions exist for simple cases with a flat bed and a semi-infinite straight breakwater or a gap between two straight breakwaters. Both the analytical solution by Sommerfeld as the empirical diffraction diagrams are presented by Goda, Takayama, & Suzuki (1978). For more complex cases a numerical approach is usually required.

In the nearshore waves will start breaking (see paragraphs on wave breaking in section 2.3). In first instance the larger waves will break. In cases where wave groups were present in the offshore conditions (very) long waves may become relevant near the coast. These long waves can penetrate easily into harbours due to their large wave lengths (see paragraph on diffraction).

Bound and free long waves

Wave groups are the set of waves which together make up the oscillating wave amplitude. Bound long waves are generated by differences in radiation stress within such a wave group. Under high amplitude waves a higher water level is present; with the reversed effect for low amplitude waves. This pattern creates a long wave, also called an infragravity wave, which is bound to the wave group; it travels with the group velocity. Only in shallow water the amplitude of this long wave is significant. Typically the wave period of such waves is in the range of 20 to 200 seconds.

Near the coast the individual waves making up the wave group will start breaking. This will cause the bound long wave to be released from the wave group. It will then behave like a normal wave and will also be affected by wave processes such as shoaling, refraction and diffraction. With their lengths they will diffract easily and will therefore penetrate deep into harbour basins and therefore may become relevant in the scope of this thesis.

2.3. Wave energy transfer and dissipation

In the previous two paragraphs the two topics of wave energy generation and energy transfer within a wave have been discussed. This section will discuss the dissipation of wave energy and the transfer of energy between waves (wave-wave interactions). Various processes can cause these energy transfers and energy dissipation. However, they may tend to be dominant and negligible compared to other processes under varying circumstances.

Bottom friction is often one of the largest sources of wave energy dissipation in the nearshore. It is concerned with the complex mechanisms in the turbulent boundary layer at the bottom under the influence of the water particle motions. Wave energy is dissipated when it is transferred into turbulent motion.

Energy dissipation through bottom friction

The amount of wave energy dissipation due to bottom friction is dependent on rather complicated processes near the bottom. Instead of dissipation it is actually a transfer of energy from wave energy into turbulent motion. The amount of energy transfer is influenced by the waves and the characteristics of the bottom. A complicating factor is the interdependency between the waves and the bottom in a small layer near the bottom. A general formulation for the time-averaged dissipation rate is:

$$\overline{D_{bfr}} = -\overline{\tau_b u_b} \qquad \textbf{Equation 2-13}$$

In which:

D_{bfr} = Energy dissipation rate by bottom friction per unit bottom area (in kg ·s^{-3})

τ_b = Magnitude of the shear stress (in pascals = kg·m^{-1}·s^{-2})

u_b = Magnitude of the particle velocity at the bottom (in meters/second)

Several options are available to find this energy dissipation rate (Guillou, 2014). The influence of bottom friction on the wave field mainly depends on the water depth and characteristics of the wave. For deep water (h>L/2) wave height reduction due to bottom friction is irrelevant as the particle motion does not extend to the bottom (U.S. Army Corps Of Engineers, 2008). But also for intermediate water depths as for instance is the case for many harbour basins, bottom friction may also be neglected.

Another dissipating mechanism is wave breaking. There are two types of wave breaking: steepness-induced wave breaking (whitecapping) and depth-induced wave breaking. Both cause wave energy to be transferred into turbulent energy. Generally whitecapping is the dominant breaking mechanism in deep water whereas depth-induced wave breaking is dominant in shallow water.

Wave breaking – Whitecapping

The term whitecapping is concerned with all dissipating mechanisms that produce a white cap on the sea surface. It occurs when the particle velocity in the wave crest travels faster than the propagation velocity of the wave crest itself. This process involves the steepness of the wave; an absolute maximum wave steepness (wave height/wave length) is approximately 0.14. Locally

whitecapping is a very nonlinear process. In practice the approximation of Hasselmann (Hasselmann, 1974) is used (Holthuijsen, 2007). In his theory the whitecap takes energy from the sea surface on the front side of the wave as it exerts a downward pressure. Although whitecapping is highly variable and locally has a large influence, Hasselmann assumes a weak effect on the mean sea surface. In this fashion a linear dissipation term is created. Although highly desirable a more physical description and modelling approach is not available (The WISE Group, 2007).

Wave breaking – Depth-induced breaking

When waves approach the coast the sea becomes shallower. At a certain moment the wave height is too large compared to the water depth after which the waves will start breaking. As a rule of thumb often an 80% fraction of the water depth is taken as the maximum wave height. To model this highly nonlinear process often the average energy dissipation rate is taken similar to a hydraulic bore. This leads to the following dissipation term:

$$D_{surf-break} = -\frac{1}{4}\alpha_{BJ}\rho g f_0 H_{br}^2 \qquad \textbf{Equation 2-14}$$

In which:

α_{BJ} = Coefficient

f_0 = Wave frequency; inverse of the wave period (in seconds^{-1})

H_{br} = Wave height of the breaking wave (in meters)

Besides energy transfer from wave energy to turbulence, energy can also be transferred between waves. Two of the primary processes are triad and quadruplet wave-wave interactions. Quadruplet wave-wave interaction is found in (relatively) deep water when two diamond wave patterns resonate with each other. It thus contains four wave components. The process transfers energy from the higher frequency waves towards the lower frequency waves. Triad wave-wave interaction can only occur in relatively shallow water in which it transfers energy from (or near to) the peak frequency to the double (or higher) frequency.

(Nonlinear) quadruplet and triad wave-wave interactions

Nonlinear wave-wave interactions occur as different (sets of) wave components resonate with each other. No direct dissipation occurs as the energy is only being transferred between wave components. Indirect dissipation may occur as the transformed wave may be influenced more by bottom friction (in case of a shift to lower frequencies) or whitecapping (in case of a shift to higher frequencies).

The four-wave interaction is a nonlinear process in which four different wave components resonate. The interaction involves an energy transfer amongst the four wave components. It occurs if the following conditions are met:

$$\begin{aligned} f_1 + f_2 &= f_3 + f_4 \\ \overrightarrow{k_1} + \overrightarrow{k_2} &= \overrightarrow{k_3} + \overrightarrow{k_4} \end{aligned} \qquad \textbf{Equation 2-15}$$

In which:

f_i = Wave frequency (in seconds^{-1})

$\overrightarrow{k_i}$ = Wave number (in meters^{-1})

The equation for the energy transfer is given by Hasselmann (Holthuijsen, 2007). The influence of quadruplet wave-wave interaction is largest for young seas where much wave energy is present at higher frequencies (Holthuijsen, 2007) (Rijkswaterstaat, 2014). In these cases quadruplet wave-wave interactions cause energy to be shifted to lower frequencies. As a result of its natural occurrence during measurement campaigns on wave growth the process is often implicitly taken

into account when using empirical wave growth formulas (Rijkswaterstaat, 2014).

The triad wave-wave interaction has a similar resonance condition as the quadruplets, however now only consisting of three components:

$$\begin{matrix} f_1 + f_2 = f_3 \\ \overrightarrow{k_1} + \overrightarrow{k_2} = \overrightarrow{k_3} \end{matrix} \qquad \textbf{Equation 2-16}$$

These resonance conditions cannot be met in deep water. Therefore triad wave-wave interaction only occurs in shallow water. Approximations of the sources and sinks caused by triad wave-wave interactions exist (Holthuijsen, 2007).

2.4. Structure-induced wave processes

Inside a harbour basin some additional processes will play a role on top of the nearshore processes. Reflection is the process of wave energy being reflected when waves hit a structure or coast. The amount of reflected wave energy strongly depends on the material and geometry of the structure. In harbours many vertical quay walls are present, which reflect nearly all wave energy. The incoming angle of the wave rays will equal the outgoing angle of the reflected wave rays. Typically the amount of reflection reduces as the incoming wave angle becomes more oblique. Reflected waves will interfere with incoming waves and this interference may cause a standing wave pattern.

In a semi-enclosed or closed basin reflection also enables resonance to occur. For resonance to occur the frequency of certain wave components should match the eigenfrequency of a harbour basin. Frequencies at which resonance occurs are generally fairly small such that only long waves in the order of several kilometres may cause resonance. Seiches is a similar phenomenon but those are caused by meteorological circumstances. Amplitudes of seiches and harbour oscillations often amount several decimetres to over a meter.

Harbour oscillations and seiches

Two typical causes can be distinguished for the occurrence of long wave resonance in a semi-enclosed body of water. The first is the penetration of long waves into the basin which have a frequency equal or close to the eigenfrequency of the basin. For a semi-enclosed basin these resonance periods equal (simplified equation):

$$T_n = \frac{4L}{(2n+1)\sqrt{gh}} \qquad \textbf{Equation 2-17}$$

In which:

T_n = Natural period for which resonance occurs (in seconds)
L = Basin length (in meters)
n = Order of the resonant mode
h = Water depth (in meters)

If the frequency of the incoming wave matches this eigenfrequency, harbour oscillations will occur. The seiches phenomenon occur due to meteorological circumstances: e.g. differences in atmospheric pressure. If the corresponding fluctuations in wind patterns correspond to eigenfrequencies again resonance may cause an amplification of the oscillation. Impulsive seiches generation can also occur. A sudden increase of wind speeds may for instance cause an impulse to the water mass which contains the eigenfrequency of the basin (Rijkswaterstaat, N.D.).

The opposite process of wave reflection is wave transmission. It is described as the amount of wave energy transmitted over or through a porous or non-porous structure. An example of wave transmission is the passage of wave energy through a breakwater at the seaside of a harbour. Also inside a harbour wave transmission can occur. This happens when not all wave energy is reflected off a quay wall, but instead overtops the structure. Part of the wave energy is then propagated on top of the structure.

Wave transmission

Wave transmission through or over structures is a phenomenon that affects the amount of wave energy, the wave height and the wave period inside the harbour. The influence of wave transmission is very dependent on the type and characteristics of the structure. Therefore no analytical solution is available. Instead many empirical formulations are available. In practice the approach of Goda is often used (Rijkswaterstaat, 2014). His solution for the fraction of transmitted wave energy is (Goda, Takeda, & Moriya, 1967):

$$\frac{R_C}{H_S} \leq -\propto -\beta \quad \rightarrow K_T = 1$$

$$-\propto -\beta \leq \frac{R_C}{H_S} \leq \propto -\beta \quad \rightarrow K_T = \frac{1}{2}\left[1 - \sin\left(\frac{\pi}{2}\frac{\frac{R_C}{H_S} + \beta}{\alpha}\right)\right] \qquad \textbf{Equation 2-18}$$

$$\frac{R_C}{H_S} > \propto -\beta \quad \rightarrow K_T = 0$$

In which:

R_C	=	Freeboard = crest level – still water level (in meters)
H_S	=	Significant wave height (in meters)
K_T	=	Wave transmission coefficient
α	=	Coefficient determined by structure type (Goda, Takeda, & Moriya, 1967)
β	=	Coefficient determined by structure type (Goda, Takeda, & Moriya, 1967)

For specific cases (e.g. a smooth non-porous vertical wall) the EurOtop manual (EurOtop, 2016) gives different formulations.

In cases where crests of structures are not high above the water level wave overtopping (and thus wave transmission) may occur. Wave overtopping is a main concern for several kinds of (coastal) hydraulic structures. Two types of overtopping can be distinguished. 'Green' wave overtopping occurs when the crest of the wave at the structure exceeds the crest level of the structure. This type of overtopping is non-impulsive and often concerns large overtopping volumes. The other type of overtopping is impulsive 'white' overtopping. When breaking or broken waves hit the structure water is diverted upwards possibly causing splash to overtop the structure. This type of overtopping has a strong dependence on wind direction; e.g. onshore wind transports splash onshore.

Wave overtopping

Wave overtopping is the process of water crossing the flood protection over its crest due to wave action. The quantity of wave overtopping depends on wave characteristics, such as height and period and the characteristics and geometry of the structure. A lot of knowledge on wave overtopping has been collected in the EurOtop manual (EurOtop, 2016). This manual helps predicting wave overtopping discharges from given conditions. Several other topics are also addressed in the EurOtop manual, such as wave transmission, wave reflection, overtopping volumes and number of overtopping waves in a storm.

For wave overtopping over a vertical structure, e.g. a harbour quay wall, several empirical formulations exist based on several data sets. The distinction between impulsive ('white') and non-impulsive ('green') wave attack has to be made to be able to choose the most suitable formula. For quay walls inside a harbour non-impulsive conditions will occur as the water is relatively deep. Still the formulas of Allsop and Franco can be used (EurOtop, 2016) (Van der Meer & Bruce, 2014), where the formula of Franco would be applied for non-impulsive conditions. These formulas can also be replaced by one single formula which is valid for the entire range of impulsive to non-impulsive conditions (EurOtop, 2016). This formula reads as follows (EurOtop, 2016):

$$\frac{q}{\sqrt{g \cdot H_{m0}^3}} = 0.047 \cdot \exp\left[-\left(\frac{2.35}{\gamma_\beta}\frac{R_C}{H_{m0}}\right)^{1.3}\right] \qquad \textbf{Equation 2-19}$$

The reliability of this formula is given by the standard deviations of the two coefficients: $\sigma(0.047) = 0.007$ and $\sigma(2.35) = 0.23$. In case of a design or assessment calculation the coefficients are tuned with one standard deviation each.

The parameters in formula Equation 2-19 are:

q	=	Specific overtopping discharge (in cubic meters per second per meter width)
g	=	Gravitational acceleration (in meters per second squared)
H_{m0}	=	Spectral significant wave height ($\approx H_s$ in deep water (EurOtop, 2016), in meters)
γ_β	=	Influencing factor for oblique wave attack
R_C	=	Freeboard measured from the still water level (in meters)

3. Modelling wave penetration, agitation and overtopping in harbour areas

3.1. Introduction

Wave modelling inside harbour domains is a fairly untreated topic. Often the focus is on efficiency and workability of ships in the navigation channels and inside the harbour basins. During severe action it may be prohibited for ships to enter the harbour or that ships cannot be loaded and unloaded at the quay. These factors then determine the possible downtime of the port. Extreme cases where waves overtop the quay walls in large volumes are left mostly unaddressed as the port would most certainly not be in operation.

In any case it is definitely not straight-forward to determine the wave field inside a harbour as was already stated in the introduction. Chapter 2 has discussed the many wave processes that might play an important role in the development of the wave field inside the harbour. To be able to describe all these processes and the possible interaction between them sets many requirements for any model.

Often the wave climate under extreme conditions will be estimated using measurements, thereby avoiding the use of any analytical, empirical or numerical model. Long records of wave data should create the possibility to determine wave extremes in a probabilistic manner. However, for harbour areas not many measurement campaigns have been undertaken (Reijmerink, 2012). The measurements also need to show a sufficient amount of detail with regards to wave heights, periods and directions. Especially for harbour areas this might be a problem as the wave field consists of a large amount of (multiply) diffracted and reflected components. A final restriction to the ability of using probabilistic techniques to determine extreme wave conditions is the large dependency the water level has on the wave height. The problem statement in the introduction (section 1.2) stated the example of the significant increase of wave transmission over a breakwater when water levels exceed the crown of the breakwater. Another example is the flooding of low-lying (harbour) areas. This again causes an increase of wave transmission towards the hinterland. Another effect is the increase of the fetch for locally generated wind-waves.

A different approach is thus required. One alternative is the physical modelling of the entire harbour area (Gruwez, Bolle, Verwaest, & Hassan, 2011). This enables a very thorough analysis of the agitation of waves under different circumstances. Obviously this costs a lot of time and resources, but as it is often the only option; physical modelling is often an important tool in estimating the wave climate for the design of (future) ports. For assessment purposes such as in the Botlek area it is likely that the required resources are too large to weigh up to the benefits.

Remaining possibilities are empirical modelling and numerical modelling of the wave penetration and subsequent overtopping. For both types of modelling practical examples are available. However, little research up to date has combined the topic of wave penetration into ports with wave overtopping resulting from the local wave action.

Before exploring previous research the next section will discuss the primary and secondary requirements or criteria. The subsequent two sections will discuss the empirical (3.3) and numerical (3.4) modelling of wave penetration and wave overtopping. The final paragraph of this chapter will

discuss the methods with respect to the requirements and criteria set in section 3.2. This will lead to a choice for a certain approach. This section will seek answers the second research question:

2. Which type of approach is likely to be most suitable for modelling the combination of wave penetration, agitation and subsequent overtopping?

- *What is the relative influence of the wave processes on the wave field inside the harbour and the overtopping rate over the quay walls?* **(3.2.1)**
- *Which secondary assessment criteria apply?* **(3.2.2)**
- *Which non-numerical methods have been applied to determine the wave field and wave overtopping discharges in harbours?* **(3.3)**
- *Which numerical methods have been applied to determine the wave field and wave overtopping discharges in harbours?* **(3.4)**
- *Which type of approach is (likely to be) the best approach with regards to meeting the requirements and secondary criteria?* **(3.4)**

A model for the chosen approach will be discussed, presented and validated in Chapter 4.

3.2. Model requirements and assessment criteria

This paragraph will go into the requirements and assessment criteria that a model is ought to comply with. The choice for the approach that will be followed in this thesis is done based on these requirements and criteria, see section 3.5.

3.2.1. Model requirements

The requirements that a model is ought to comply with consist of the most important wave processes. These processes have been explained and discussed in the previous chapter (Chapter 2). Table 3.1 below lists all processes and indicate their relative influence on the (extreme) wave field inside a harbour area. The table is an adapted version from the list that is found in "*Waves in oceanic and coastal waters"* (Holthuijsen, 2007); the difference being that the list in the table below is meant for extreme wave conditions for which wave overtopping is likely to occur.

Table 3.1: The relative influence of the wave processes discussed in Chapter 2 on the characteristics of the extreme wave field and the amount of overtopping inside an arbitrary harbour (adapted version of the list in "*Waves in oceanic and coastal waters"* (Holthuijsen, 2007)

#	Process:	Relative influence
1	Wave overtopping	**+++**
2	Diffraction	**+++**
3	Local wind-wave generation	**+++**
4	Reflection	**++**
5	Transmission	**++**
6	Quadruplet wave-wave interactions	**+**
7	(Bound and free) long waves	**+**
8	Energy dissipation through bottom friction	**+**
9	Whitecapping	**+**
10	Resonance/harbour oscillations	**+**
11	Refraction and shoaling	**+**
12	Frequency dispersion	**+**
13	Depth-induced wave breaking	**-**
14	Triad wave-wave interactions	**-**

+++ = Dominant, ++ = Significant, + = Minor influence, - = Very little influence thus negligible

Table 3.1 only serves as guidance; the reason being that the relative importance of a process depends to a large extent on the specific location and geometry of the harbour. Therefore this list is not static and it may occur that for a specific harbour a process with minor influence (as seen in Table 3.1) still needs to be taken into account. Appendix A (*Relative influence of various wave processes and phenomena*) describes how the relative influences were chosen for the wave processes.

3.2.2. Assessment criteria

Besides the technical requirements of a certain model, secondary criteria influence the choice for a certain model (type). These secondary criteria mainly focus on the practicality of the method. Preferably the model is simple to use and thereby does not require a large set-up time for every different harbour case. Currently required computational effort is also a limiting factor to the practicality of the model; by future developments this limit decreases. Furthermore it might be possible that little data is available, this should preferably not limit the possibility to use the model.

Obviously expected accuracy and certainty is an important factor as well. This mainly revolves around the way the model takes into account the processes from Table 3.1 and how it combines them to find the overtopping discharges over the quay walls. This criterion likely contradicts with the easiness of using the model. This might lead to the conclusion that a model which takes into account less processes, thereby reducing accuracy, might still be the preferred option.

As mentioned the (un)certainty in the final model is also relevant. As every harbour is different uncertainty exists if the model works for each case. No wave measurements are available to test the accuracy and performance of the model. Therefore expert judgement will always be required to evaluate the (uncertainty of the) outcome. Therefore the results should be easily interpretable and must follow logically from the way the wave processes have been taken into account. In the line of this argumentation a 'white-box' model is clearly preferred over a 'black-box' model.

To summarize, the following assessment criteria have been mentioned:

1. Meeting the requirements with respect to wave modelling (Table 3.1)
2. Expected model accuracy and certainty in a harbour case
3. Applicability range
4. Practicality of the model:
    - Simplicity
    - Required (computational) effort
    - Required data availability
5. Interpretability of the results

3.3. Empirical modelling of wave penetration and overtopping in previous research

This section will explore previous research on non-numerical methods to evaluate the wave action and wave overtopping in harbour areas. The term 'empirical' model does not capture the essence of what is meant in the context of this thesis. A strict definition of an empirical model is a model being based upon observations instead of mathematical formulations. In the light of this thesis it is rather used as the name for the collection of non-numerical methods; for instance deterministic models and

pragmatic end-to-end methods. These approaches do not rely upon a numerical model which would solve the equations of motion. Reference is made to section 3.4 for an analysis of such numerical models.

As stated in the introduction of this thesis the influence wave overtopping has been addressed in flood risk studies in the Botlek area (Botterhuis, Nicolai, & Stijnen, 2015) (Slootjes & Wagenaar, 2015), see Figure 3.1 for a map of the study areas. The main focus of these studies were not to find exact overflow and overtopping amounts, but rather the extent, area and depth of inundation of the Botlek area. Slootjes and Wagenaar followed a rather deterministic approach; quantifying all relevant parameters in logical order (e.g. water level → seiches → waves) to find the results. The wave heights, periods and directions were extracted from *Hydra-zoet* (Duits & Kuijper, 2012). In *Hydra-Zoet* the wave direction is equal to the governing wind direction. These are all relevant parameters in waver overtopping formula, see chapter 2. Unknown is whether the assumption of constant wave direction might lead to a significant over- or underestimation of the wave overtopping discharge where waves might turn, as for instance in a harbour. This would be the case when the angle of incidence at the structure under consideration increases and decreases respectively compared to the wind direction. Furthermore, no waves penetrate into the *Hartelkanaal* (3), which was the main origin of flooding in their study. No approach is suggested for cases where waves do penetrate into the area of interest. Unclear is thus whether and how it is possible to take these penetrated waves into account. In a brief study on the *Brittaniëhaven* (2) the possible influence of overtopping waves was not considered. Slootjes and Wagenaar addressed and estimated the effect of overtopping waves based on expertise.

Figure 3.1: Map of the Botlek area. Indicated are the locations and water bodies of interest in the mentioned studies (Botterhuis, Nicolai, & Stijnen, 2015) (Slootjes & Wagenaar, 2015). Source: Google Maps (2016). See Appendix H for a larger map of the western part of the Rotterdam harbour.

A different, more pragmatic approach can also be applied to include the influence of wave overtopping. After consultation within their project group, Botterhuis, Nicolai and Stijnen (2015) increased the (still) water level by a certain value in order to account for the effect of waves. A more complex approach was suggested. In this suggested approach the waves would be quantified in a

probabilistic or deterministic fashion. This suggestion has led to the initiation of this thesis and thus little attempts have been undertaken to adopt the more complex approach prior to this thesis.

Both studies (Botterhuis, Nicolai, & Stijnen, 2015) (Slootjes & Wagenaar, 2015) relied upon data gained from numerical SWAN simulations of the entire lower Rhine-influenced riverine area (Chbab, 2012). This type of modelling will be addressed in section 3.4. What already should be noted is that the results from the wave modelling in SWAN were not validated against measurements. The simple reason for this being the absence of any measurement data in the area of interest (Chbab, 2012). A different, numerical or non-numerical approach should therefore not be ruled out on forehand.

In case of the Botlek area, where wave penetration from sea is of a smaller influence, an approach in which the waves are estimated solely with empirical wave growth formulas (see chapter 2) might work. Stepping away from this area, finding accurate deterministic ways to find the wave conditions is more difficult as more processes come into play. Attempts have however been made. An updated report originally from the '*Rijksinstituut voor Kust en Zee'* (Rijkswaterstaat, 2014) has described a detailed method in which wave penetration can be taken into account. Empirical formulations and estimations are used to find the effect of local wave growth, wave diffraction and wave transmission. The applicability of this method is restricted to relatively simple geometries. These simple geometries are defined as having no multiple diffraction or transmission patterns when waves enter the harbour. For complex geometries a numerical approach would be required (Rijkswaterstaat, 2014). Besides this method, other sources confirm the complexity of the task of finding the wave climate deterministically by the use of empirical knowledge (Van Mierlo, 2014), (Heuts, 2010), (Van der Meer, Langenberg, Breteler, Hurdle, & Den Heijer, 2002).

3.4. Numerical modelling of wave penetration and overtopping in previous research

Numerical modelling of port applications has been a constant topic of (academic) research as it poses many challenges and complexities. Since many advanced numerical model have become available during the last decade, a fair amount of recent research can be referred to. The first paragraph (3.4.1) gives a short general description of numerical wave modelling and lists several numerical wave model types. Subsequently previous research on the numerical modelling of wave penetration into harbours and wave overtopping will be explored. To date no research can be referred to which combines wave penetration modelling with wave overtopping. Therefore these topics will be treated in separate paragraphs, 3.4.2 and 3.4.3 respectively.

3.4.1. Numerical wave model types

In essence all numerical wave models are based on the Navier Stokes equations for motion. Until present no model is able to capture the full Navier Stokes equations as its governing equations are too complex to solve in an efficient manner. For different purposes, different assumptions are made. With these simplifications, the ability to correctly represent all physical processes will get lost.

Several types of numerical wave models can be distinguished. All have their capabilities and inabilities, strengths and weaknesses. A more comprehensive discussion of wave model types is found in Appendix B: *Numerical wave models*. Below follows the list of discussed wave model types and their most important characteristic.

- Shallow water models; This type of model based on the shallow water equations models long waves for relatively large domains.
- Spectral wave models; The spectral wave model calculates the wave spectrum by solving the energy balance taking into account several wave processes including energy input by wind.
- Boussinesq-type models; The Boussinesq equations are based on the potential flow equations. The accuracy can be increased by adding more terms in the series expansion.
- Mild slope models; The mild slope model is derived in a fairly similar fashion as the Boussinesq models. However the equations are now more computational efficient and its particular use is now for cases where diffraction and refraction are the most dominant processes.
- Nonlinear shallow water model; This type of model accounts for nonlinear effects such that larger perturbations can be modelled more accurate. A non-hydrostatic pressure term can also be added to the horizontal momentum equations. It can then handle rapidly varying flow conditions, for which the hydrostatic pressure assumption is invalid.
- Reynolds averaged wave models; This type of model is based on the Reynolds averaged Navier Stokes (RANS) equations. As the only averaging occurs over the turbulent motion it can capture nearly any flow phenomenon.
- SPH solvers; The SPH model solves the flow problem in a Lagrangian fashion. It simulates and follows fluid particles on their paths.

These model types have often been applied in practice. An outline of some research on the topic of wave penetration and wave overtopping can be found in the next two paragraphs.

3.4.2. Numerical modelling of wave conditions in harbour domains

The wave climate inside ports depends on many factors: outside wave climate, local wave generation and geometry. The many processes, see 3.2, create several numerical conditions to be met. In previous research the topic of wave penetration has been dealt with. Comparative studies have been undertaken which show the possibilities to successfully model the wave conditions inside the port.

One of the seemingly most complete researches on wave penetration is Van Mierlo's thesis, *'Numerical modelling of wave penetration in ports'* (Van Mierlo, 2014). Van Mierlo compared the performance of three different numerical models to each other and to physical model outcomes. In that fashion he was able to draw conclusions on specific strong of weak points of each model. It was shown that all three models, the mild slope model PHAROS (Deltares, N.D.), the Boussinesq-type model TRITON (Deltares, 2008) and the nonlinear shallow water model SWASH (SWASH team, 2010), accurately reproduced relevant processes such as shoaling and diffraction. PHAROS, a mild slope model, appeared to be a good tool for a quick estimation of the wave field, while the more complex models SWASH and TRITON can be used to attain more accurate results. All three model types could therefore be successfully used to model wave penetration.

More researches show the good performance of the nonlinear model SWASH in harbour domains. Being a non-hydrostatic phase-resolving model, SWASH solves the sea surface in time. In this framework (partial) reflection and diffraction are modelled accurately (Dusseljee, Klopman, Van Vledder, & Riezebos, 2014) (Van Vledder & Zijlema, 2014). The phase-resolving character of the

model does create a restraint on the size of the domain. However, due to constraints on the size of the grid cells and the time step, the computational demand of the model for a harbour case is very large (Van Mierlo, 2014). Also Boussinesq-type models, TRITON and a comparable model such as MIKE21BW (DHI Group, N.D.), have been successfully applied to model the propagation of waves into harbour domains (Boeyinga, 2010). (Suzuki, Gruwez, Bolle, Verwaest, & Mostaert, 2012) (Kofoed-Hansen, Kerper, Sørensen, & Kirkegaard, 2005).

The mentioned models (PHAROS, SWASH, TRITON and MIKE21BW) have been proven to meet the required abilities with respect to wave penetration. However, none of these models is able to account for locally wind-generated waves. Being very relevant to the wave conditions inside the harbour (indicated in section 3.2 and explained in Appendix A); the applicability of the numerical models is limited. This requires the need of a different approach.

One of the models that can generate waves within the domain is the SWAN model (SWAN Team, 2016). As discussed in paragraph B.2 (Appendix B) this type of model solves the water surface on a wave group scale only. However, being a phase-averaged model, SWAN cannot model phase-dependent processes accurately (SWAN Team, 2016) (Enet, Nahon, Van Vledder, & Hurdle, 2006). Examples of phase-dependent processes are diffraction and reflection. Due to the dominance of these processes in a harbour case SWAN should then not be applied (SWAN Team, 2016).

Individually none of the discussed models can meet the requirements of accurate wave penetration and wind-wave generation modelling. Coupling of two models might be the solution. Although it is not a straight-forward procedure, it has proven to be fairly accurate for some case studies (Alabart, Sánchez-Arcilla, & Van Vledder, 2014) (Dusseljee, Klopman, Van Vledder, & Riezebos, 2014) (Gruwez, Bolle, Verwaest, & Hassan, 2011). The formula which is the basis of this coupling is as follows: (Van der Meer, Langenberg, Breteler, Hurdle, & Den Heijer, 2002):

$$H_{total} = \sqrt{H_{local}^2 + H_{penetration}^2}$$

This formula is valid for a random set of harmonic (sinusoidal) waves. The use of it is limited to linear waves. This linear wave theory is valid under the condition that the waves are not too steep and that the water depth is relatively large (Holthuijsen, 2007). These conditions are likely met for the case of harbours as they are usually protected from the highest waves by breakwaters.

3.4.3. Numerical modelling of wave overtopping over vertical walls

Numerical modelling of wave overtopping is a fairly unexplored topic, especially at vertical (quay) walls. Therefore it is difficult to judge the performance of different models in overtopping cases. Already many models can be ruled out as they cannot handle a sudden contraction of the water depth. An example is the mild slope model type.

From the previous paragraph it was found that a nonlinear model such as SWASH is able to model waves until the shoreline and as such also until quay walls in the harbour areas reasonably well. Overtopping of the quay walls could also be implemented directly into the model. An accurate performance of SWASH in an overtopping case on a purely vertical wall has not yet been proven. An attempt has been made for a case with a wide foreshore (Vanneste, Altomare, Suzuki, Troch, &

Verwaest, 2014) and case with a steep dike front (Suzuki, et al., 2011). For these specific cases fairly accurate results have been attained. When the relative freeboard (freeboard over wave height) increases, the performance of the model decreases (Suzuki, et al., 2011).

In a general sense the results given by SWASH must be treated carefully. Vanneste et al. (2014) and Suzuki et al. (2011) ran SWASH in depth-average mode. Under waves the highest velocities are found near the surface. In depth-averaged sense velocities are lower in this region, thus likely underestimating the velocity on top of the wall, see Figure 3.2. It may thus be possible the good results are just a coincidence.

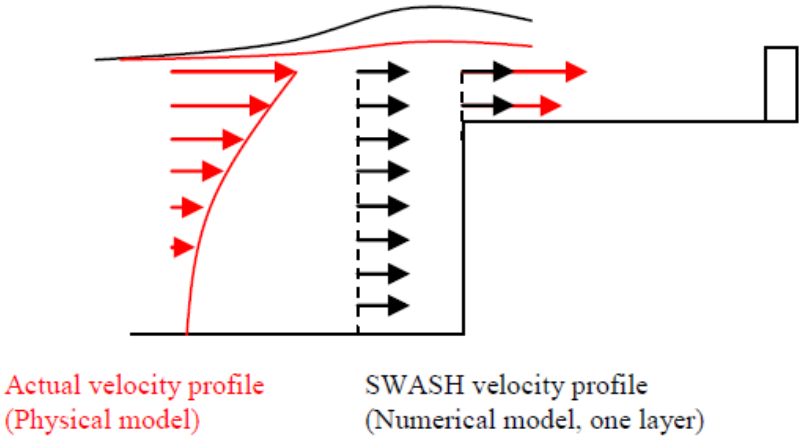

Figure 3.2: Velocity profiles in front of the vertical wall; comparison between reality and the SWASH model if only one layer is used. Source: Vanneste, Altomare, Suzuki, Troch, & Verwaest (2014)

To solve this apparent issue, SWASH can be run with multiple vertical layers. This has also been attempted, but this lead to critical instabilities (Vanneste, Altomare, Suzuki, Troch, & Verwaest, 2014). Furthermore the computational effort also increases further. It is thus uncertain if SWASH is applicable for the overtopping case.

3.4.4. Conclusions on numerical modelling of wave penetration and wave overtopping for port applications

The previous two paragraphs have discussed the theory study conducted to explore the performance of numerical models in a port domain. The two main topics, wave penetration and propagation in harbour domains and wave overtopping, have been discussed (in paragraphs 3.4.2 and 3.4.3 respectively). It appeared that none of the discussed models meet all requirements, see Table 3.2.

More comprehensive numerical models, also listed in Table 3.2, might meet more or all requirements with respect to the modelling of the various processes. Examples are the Reynolds Averaged Navier Stokes (RANS) FLOW-3D model (Flow Science, N.D.) or the Smoothed-particle hydrodynamics (SPH) solver SPHysics (Gesteira, Rogers, Dalrymple, Crespo, & Narayanaswamy, 2010). Still, these types of models are not considered for this thesis. Due to their large complexity, the limited availability (licensing) and the large computational demand the models do not comply with the secondary assessment criteria (section 3.2) and are therefore not suitable for this thesis.

Table 3.2: Capabilities and limitations of numerical models with respect to the requirements set in this thesis

Representative model	Model type	Short waves	Solves sea surface in time	Diffraction/ Reflection	Internal wind-wave generation	Wave overtopping
Delft3D	Shallow water model	✗	✓	✗	✗	✗
SWAN	Spectral wave model	✓	✗	✓/✗[1]	✓	✗
TRITON	Boussinesq-type	✓	✓	✓	✗	✓
PHAROS	Mild slope	✓	✓	✓	✗	✗
SWASH	Non-hydrostatic	✓	✓	✓	✗	✓/✗[2]
XBeach (non-hydr.)	Non-hydrostatic	✓	✓	✓	✗	✓/✗[2]
FLOW-3D	Reynolds-averaged	✓	✓	✓	✓	✓
DualSPHysics	SPH solver	✓	✓	✓	✗	✓

Remarks:
[1] A diffraction module is included in SWAN, but it is not meant for harbour cases, see paragraph B.2 of the appendices.
[2] Wave overtopping in SWASH and XBeach non-hydrostatic has not been thoroughly validated for varying wave conditions and geometries

During the literature study it was found that the nonlinear and non-hydrostatic shallow water wave model SWASH may model wave overtopping accurately. In that case the model could be applied in an integral fashion: simulating the waves from the boundary up to and the including the locations where the waves would overtop. This would require assumptions on the locally generated waves (e.g. several runs with varying wave boundary conditions in which the locally generated waves would be accounted for).

The potential of this method is high; but in order to actually function, SWASH should be able to model wave overtopping over vertical walls. The performance of SWASH on wave overtopping cases is uncertain (see 3.4.3). Because of the potential of SWASH, a validity research on wave overtopping in SWASH has been conducted within the scope of this thesis. The results of this validity research are shown and discussed in Appendix C: *Validity of SWASH for wave overtopping*. It appears that SWASH indeed produces overtopping discharges which match to measurements. However the validity range is limited. Extreme conditions (e.g. high waves or high freeboard) cannot be modelled as for these cases the model experiences critical instabilities. No clear explanation for these instabilities was found. They occur very sudden at seemingly random moments during the model run. This leads to the conclusion that currently SWASH cannot be used for overtopping scenarios for which no measurements are unavailable.

3.5. Choice for a modelling approach

The previous two sections (3.3 and 3.4) discussed the modelling of wave penetration, generation and overtopping in previous research. It appeared that the combination between the wave modelling and the wave overtopping is an untreated topic. Table 3.3 below shows the capabilities and limitations of some of the discussed methods with respect to the set requirements (3.2, Table 3.2).

Table 3.3: Capabilities and limitations of the discussed numerical and non-numerical methods with respect to the set requirements. Listed methods are: a physical scale model of a harbour (paragraph 3.1), a deterministic (paragraph 3.3, e.g. Slootjes & Wagenaar, 2015), a pragmatic approach (paragraph 3.3, e.g. Botterhuis, Nicolai, & Stijnen, 2015) and three numerical methods (paragraph 3.4)

#	Process:	Physical model	Deterministic approach	Pragmatic approach	SWASH	SWASH+SWAN coupling	RANS model or SPH solver
		Non-numerical			Numerical		
1	Wave overtopping	✓	✓	✓	✗	✗	✓
2	Diffraction	✓	✓	✗	✓	✓	✓
3	Local wind-wave generation	✓/✗[1]	✓	✓	✗	✓	✓
4	Reflection	✓	✗	✗	✓	✓	✓
5	Transmission	✓	✓	✗	✓	✓	✓
6	Quadruplet wave-wave interactions	✓	✓/✗[2]	✗	✓	✓	✓
7	(Bound and free) long waves	✓/✗[1]	✓[3]	✗	✓	✓	✓
8	Energy dissipation through bottom friction	✓	✓	✗	✓	✓	✓
9	Whitecapping	✓	✓/✗[2]	✗	✓	✓	✓
10	Resonance/harbour oscillations	✓	✓[3]	✗	✓	✓	✓
11	Refraction and shoaling	✓	✓/✗[4]	✗	✓	✓	✓
12	Frequency dispersion	✓	✗	✗	✓	✓	✓
13	Depth-induced wave breaking	✓	✓/✗[4]	✗	✓	✓	✓
14	Triad wave-wave interactions	✓	✗	✗	✓	✓	✓

Remarks:
[1]Scaling effects increase when modelling both short and long waves (Hughes, 1993)
[2]Implicitly via wave growth formula
[3]Practically it can only be taken into account as a contribution to the still water level
[4]Practical approaches via (linearity) assumptions

The choice for a method is not solely based on how well the method meets the requirements. Section 3.2 also set some secondary assessment criteria. Table 3.4 below gives informal scores on a scale from 0 to 3 (3 is 'best' and 0 is 'worst') on how well the model scores on the criterion. A short explanation on the choice for these scores is given in Appendix D.

Table 3.4: Scoring of the methods on the various assessment criteria on a scale from 0 to 3.

	Physical model	Deterministic approach	Pragmatic approach	SWASH	SWASH+SWAN coupling	RANS model or SPH solver
Assessment criterion:	Non-numerical			Numerical		
Meeting the requirements (Table 3.3)	3	2	0	1	2	3
Expected accuracy in a harbour domain	3	1	0	2	2	3
Applicability range	2	1	3	2	3	2
Practicality: simplicity	3	3	3	1	0	0
Practicality: required (computational) effort	0	3	3	1	1	0
Practicality: required data availability	3	2	3	0	0	0
Interpretability of the results	3	3	0	2	1	1

Remarks:
The scores may contain a degree of subjectivity as it is difficult to estimate the performance of a method with respect to the criterion on forehand. Therefore in a re-analysis of the methodology, different conclusions may be drawn. It may also occur that by future development (e.g. increase of numerical capabilities and increase of computational power) the scores will change, also stated in the Discussion in Chapter 6.1.

The scores on the assessment criteria show a large spread in the strengths and weaknesses of the methods. Generally the numerical methods score well on meeting the requirements, accuracy and applicability. However practicality and efficiency being important factors as well, the total scores of the numerical models are insufficient compared to a non-numerical approach. SWASH could be an exception. This numerical model has been validated for harbour applications, but it cannot model local wave generation yet and it shows large uncertainty with respect to wave overtopping modelling. These two aspects are very important within the scope of this thesis (see Table 3.1), thereby ruling out the integral use of SWASH. At the end of this thesis the possible use of SWASH is discussed and recommendations are given for future applications of SWASH within this topic (paragraphs 6.1 and 6.3).

Generally non-numerical deterministic models will produce less accurate results. They rely heavily on simplifications and assumptions. The main exception is the physical modelling. However, the amount of required resources to set up a physical harbour model is well beyond the possibilities in simple flood risk study. Due to the practicality and simplicity of a deterministic and (semi-) empirical model it is expected to be the best tool within the scope and objective of this thesis. The main limitation of this approach is the applicability range of the method. This applicability range is described in 0 at the end of the next chapter. In the final chapter (6), on the discussion of this thesis and the main recommendations, suggestions are given on how cases which fall outside of the applicability range could still be modelled.

4. Semi-empirical wave generation, penetration, overtopping model

This chapter describes the deterministic method that will be applied to model wave generation, penetration and overtopping for a port application. Thereby it will answer the research question 3 including its sub-questions:

3. What are the characteristics of the final modelling approach?
- *What is the structure of the model?*
- *How are the most relevant wave processes dealt with in the model?*
- *In which cases can the model be applied?*

The first paragraph states the general philosophy behind the approach. Section 4.2 will show the structure of the model. Subsequently, section **Error! Reference source not found.** describes the approach for the various subcomponents of the model; i.e. how different processes will be quantified in the model. Paragraph 4.4 will validate the model using the '*Vlissingen Buitenhaven*' case. Finally section 0 goes into the applicability of the empirical model. From now on the model will be referred to as the 'WGPO model': **W**(*ave*) **G**(*eneration*) **P**(*enetration*) **O**(*vertopping*).

4.1. General model philosophy and description

Chapter 3 described the arguments which stood at the base of the choice to build and use an empirical/deterministic model during this thesis. This paragraph will describe the main characteristics of the WGPO model and the main simplifications and assumptions which lie at its base. The grey box below summarizes the model and its assumptions.

Main elements of the WGPO model:
- The WGPO model is meant for assessment purposes only: it gives a conservative result with respect to wave heights and wave overtopping rates
- Wave reflection and water depth-induced processes such as shoaling are not accounted for
- The water level and the bottom elevation in the basin are assumed to be constant; a representative water depth needs to be chosen which gives conservative answers.
- Independence of the wave processes is assumed (except for the interaction between wave diffraction and transmission)
- The model is built in the MATLAB modelling environment for the purpose of this thesis

As stated in the previous chapter the expected accuracy of the model is less than what can be expected from numerical methods. The main reason for this being the way the processes are implemented. The main philosophy of the model are its conservative nature and its stepwise approach in which the considered wave processes are quantified. The conservativeness leads to an estimation of the upper limit to the wave conditions and the wave overtopping discharge. This upper limit is of interest in the assessment of the flood risk in the harbour. Due to the possibly large conservativeness the model is not appropriate for design purposes. In the case study of the '*Brittaniëhaven*' in Chapter 5 the degree of conservativeness is reflected upon.

For reasons of the simplicity, transparency and interpretability of the model, several wave processes are neglected, see Table 4.1. The neglected processes would generally reduce the amount of wave

energy and wave overtopping in harbours (see Appendix A for a discussion on the relative influence of the processes). The main exception is the process of wave reflection. The complexity of the resulting (multiple) reflection pattern is the main reason for not implementing it into the model. This limits the applicability of the model, see paragraph 0.

Table 4.1: List of wave processes, similar to Table 3.1. Strikethroughs indicate the neglected processes.

#	Process:	Relative influence
1	Wave overtopping	**+++**
2	Diffraction	**+++**
3	Local wind-wave generation	**+++**
	~~Reflection~~	**++**
5	Transmission	**++**
6	Quadruplet wave-wave interactions[1]	**+**
7	(Bound and free) long waves[2]	**+**
	~~Energy dissipation through bottom friction~~	**+**
9	Whitecapping[1]	**+**
10	Resonance/harbour oscillations[2]	**+**
	~~Refraction and shoaling~~	**+**
	~~Frequency dispersion~~	**+**
	~~Depth-induced wave breaking~~	**-**
	~~Triad wave-wave interactions~~	**-**

+++ = Dominant, ++ = Significant, + = Minor influence, - = Very little influence thus negligible

Remarks:
[1] Taken into account implicitly via a wave growth formula in which the processes whitecapping and quadruplet wave-wave interaction play a role
[2] Depending on the given boundary conditions it is taken into account via an addition to the still water level

One of the main assumptions is the assumption of constant water depth. This eliminates water depth-induced processes such as shoaling and refraction. For harbour cases this assumption is likely to be valid as generally harbour areas are dredged to guarantee a certain minimum water depth. A requirement which comes with this approach is the choice for the most conservative representative bottom elevation.

For shoaling local shallow areas in the harbour might lead to local energy bundling, which might harm the conservativeness of the results. However, such shallow areas are not likely to be found in a harbour area for workability reasons (guaranteed minimum water level). In the '*RIKZ*' report (Rijkswaterstaat, 2014) it is shown that refraction generally reduces the wave height inside the harbour basin if the water depth in the navigation channel is larger than outside the channel. Therefore assuming a constant water depth (which equals the maximum water depth in the harbour) can be regarded as conservative, see also paragraph A.3 of Appendix A. However, careful judgement of the situation is always required to check whether the assumption of a constant representative water level is justifiable.

Another assumption is the independency of the various wave processes with the exception of the interaction between transmission and diffraction (see 4.3.4). Generally this will not harm the conservativeness principle; e.g. the interaction between existing high-frequency wave energy (by wave transmission for instance) and wave growth reduces the combined wave height of the two

components compared to the case of independence (Rijkswaterstaat, 2014). The assumption of independence is necessary to reduce the demanded complexity of the model.

The model will be in line with the 'RIKZ' method (Rijkswaterstaat, 2014). An obvious difference between this model and the method of 'RIKZ' is the extension to wave overtopping. Furthermore a continuous outcome will be modelled instead of a discontinuous, point-based calculation. This continuous pattern will help interpret the model outcomes. It then becomes a more helpful tool in the assessment of flood risk. The model is built in the modelling environment MATLAB, version 2016a (MathWorks, 2017). This platform supports computational mathematics and the built-in graphics allow clear data visualizing. The choice for MATLAB is based on the author's experience with the software. The same model can be created within other modelling environments such as Python or Fortran.

4.2. Model structure

Figure 4.1 visualizes the model structure of the WGPO model in the form of a flow chart. The model components are discussed in the next section (**Error! Reference source not found.**).

4.3. Model components

Following the model structure in the previous section, this paragraph discusses the individual model components. These components have been numbered in the flowchart in Figure 4.1 and those numbers correspond to the sub-sections in this paragraph. At the start of every sub-section a summary is given of the assumptions and main elements of the approach. Subsequently a more comprehensive description and an explanation of the model choices and assumptions are given.

4.3.1. Wave generation by wind

Main elements of the model component '*wind-wave generation*':

- Governing conditions in a harbour: relatively deep water and short fetches
- The wave growth formula of Bretschneider will be applied
- The fetch in Bretschneider is taken as the maximum fetch occurring in a sector of 60 degrees around the principle wind direction (conservative approach)
- The water depth in Bretschneider is taken as the maximum water depth occurring in the area of interest

Wind-wave generation is physically a very complex process. Research on the topic has largely revolved around finding fitting empirical formulas. Extensive measurement campaigns have been undertaken for various circumstances. The performance of a formula depends on the local circumstances at the measurement campaign (Nederpel & Van Balen, 2015). In a harbour the water depth will be relatively large (wave length over water depth is a large number). Furthermore, in general, unobstructed fetches will tend to be relatively small. The wave height dependency on the duration of the specific wind conditions are neglected; this would only be relevant for long fetches. This sets the conditions for the choice of a formula. Figure 4.2 plots several wave height formulas for deep water conditions (d=15m) and short fetches (<3000m).

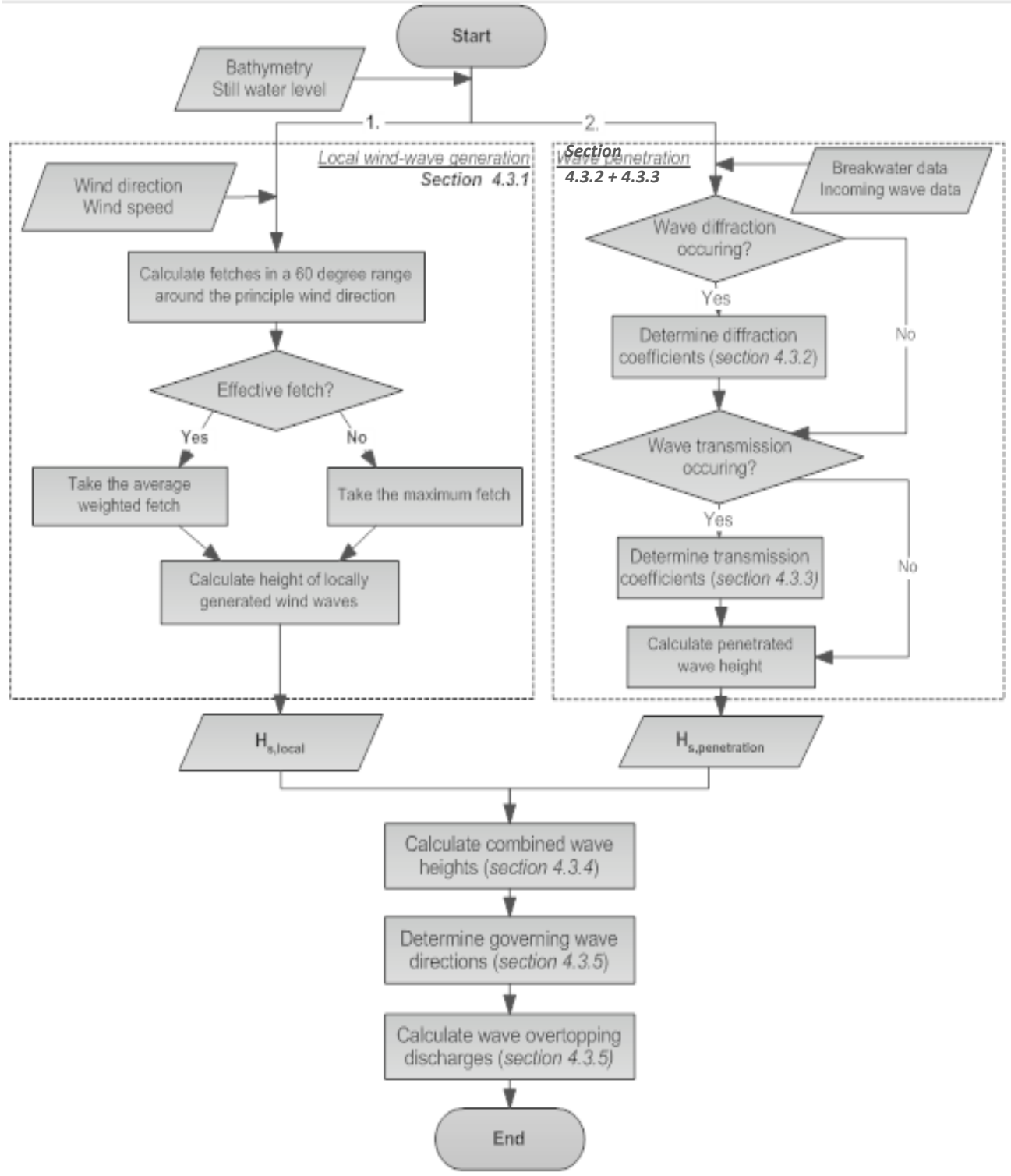

Figure 4.1: Flowchart of the model structure of the WGPO model

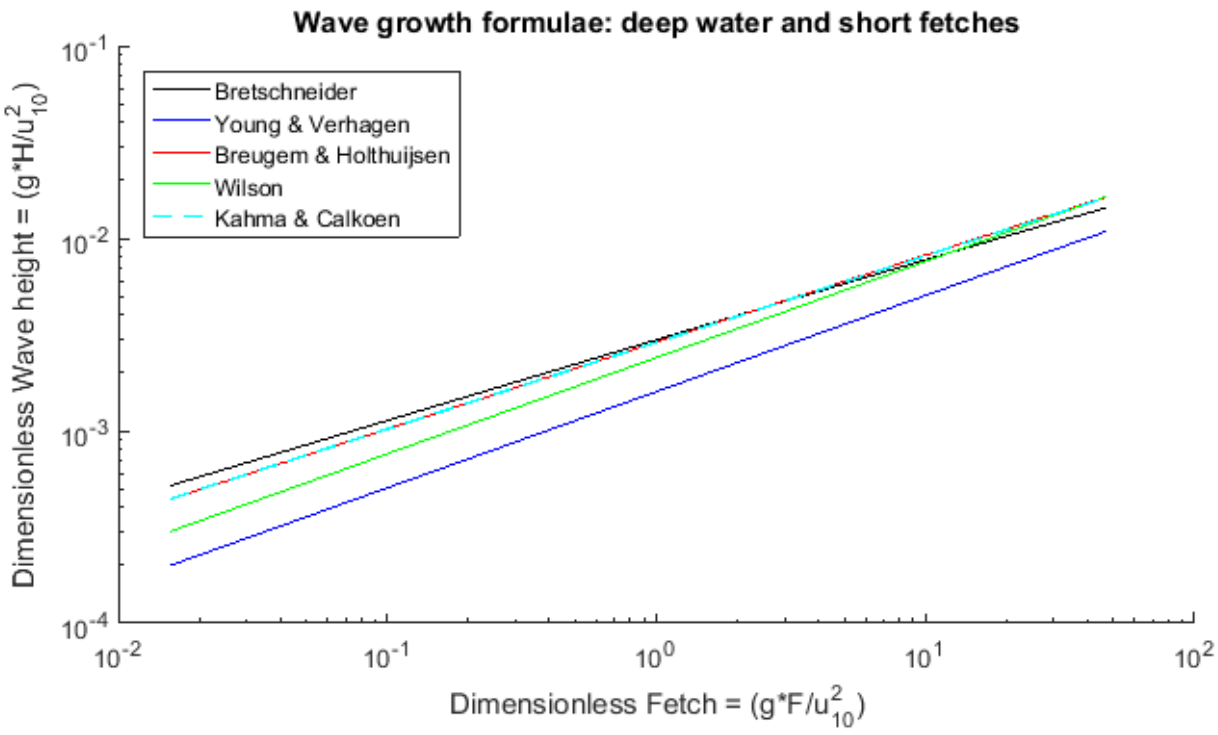

Figure 4.2: Wave growth formulae in relatively deep water for short fetches (d = 15m & u_{10} = 25 m/s). The following formulas have been plotted: Bretschneider (U.S. Army Coastal Engineering Research Center, 1975), Young & Verhagen (1996), Breugem & Holthuijsen (2007), Wilson (1965) and Kahma & Calkoen (1992)

The formula of Bretschneider (U.S. Army Coastal Engineering Research Center, 1975) is worldwide an often applied empirical formula to determine wave growth. It has a good performance for a wide range of conditions although its derivation is based upon deep water and long fetch conditions (Nederpel & Van Balen, 2015). Similar to Young & Verhagen (1996) and Breugem & Holthuijsen (2007), the formula of Bretschneider contains a depth-dependent wave growth. The formula of Young & Verhagen has been fitted to data from a large measurement campaign at Lake George, Australia. This lake is shallow and the fetches are in the order of ten to almost thirty kilometres. These conditions deviate from the harbour case with larger water depths and shorter fetches. The formula of Breugem & Holthuijsen (2007) is based upon a reanalysis of the Lake George dataset. Only for larger fetches it gives the same values as Young & Verhagen; for smaller fetches it matches Kahma & Calkoen (1992). Kahma & Calkoen developed the formula with the use of an extensive dataset. Its validity is limited to large dimensionless fetches (in the order of 100) and deep water. Furthermore, it does not contain a depth-dependency. The final formula that has been considered is Wilson's (1965). This formula is developed specifically for short fetches and deep water. These conditions match the case of a harbour, but the formula again does not contain a depth-dependency.

It is difficult to choose the most suitable formula. However, the uncertainty concerned with choosing a formula is considerably less than the uncertainty revolving around the input parameters, e.g. representative water depth and constant wind speed (Nederpel & Van Balen, 2015). For this reason any of the remaining formulas could be chosen, beyond the fact that two of the formulas are not depth-dependent. This dependency is not large in deep water, but it seen as a decisive factor when choosing between very similar formulas. In practice often the formulation of Bretschneider is used.

Therefore, in line with Nederpel & Van Balen, it is opted to use Bretschneider. This formula is repeated from Equation 2-7:

$$H_s = \frac{0.283 * U_{10}^2 * \tanh\left[0.530\left(\frac{gh}{U_{10}^2}\right)^{0.75}\right]}{g} * \tanh\left(\frac{0.0125}{\tanh\left[0.530\left(\frac{gh}{U_{10}^2}\right)^{0.75}\right]}\left(\frac{gF}{U_{10}^2}\right)^{0.42}\right) \qquad \textbf{Equation 4-1}$$

The variables in Equation 4-1 are:

- F = Fetch (in meters)
- U_{10} = Wind speed at ten meters height (in meters per second)
- h = Water depth (in meters)
- H_s = Significant wave height (in meters)

The uncertainty revolved with choosing a single wave growth formula is analysed for the case study of the *Brittaniëhaven* (paragraph 5.4.1).

Fetch

The fetch is the distance over which the wind blows in the area of interest. Waves are not purely generated in the direction parallel to the wind direction, but also in directions which have a certain small angle with the principle wind direction. Therefore in an area with an irregular geometry the effective fetch can exceed the fetch parallel to the governing wind direction. The principle of any method to determine such effective fetches is the weighting of the fetches in a certain sector around the principle wind direction (Bottema & Van Vledder, 2008) (Holthuijsen, 2007). The effect of the wind under an angle with the principle wind direction is reduced by the cosine of that angle. For a sector of directions (with a step of Δ degrees between the various directions) this results in the following formula for effective fetch (Rijkswaterstaat, 2014):

$$F_{Eff} = \frac{\sum_i \cos^2(\Delta_i) F_{\theta,i}}{\sum_i \cos(\Delta_i)} \qquad \textbf{Equation 4-2}$$

For certain areas within the harbour using the principle of effective fetch would result in the application of a lower fetch (compared to the parallel fetch) and thus lower wave heights. This can be the case for locations close to the edge of the harbour. This harms the conservativeness of the method. Therefore similar to the *'RIKZ'* method (Rijkswaterstaat, 2014) instead of the effective fetch, the maximum fetch in a sector around the principle wind direction is used to calculate the height of the local wind-generated waves, see Figure 4.3. The total sector in which this maximum fetch can occur consists of 60 degrees around the principle wind direction, i.e. 30 degrees on both side of the wind direction. The influence of this conservative approach is analysed in paragraph 5.4.1.

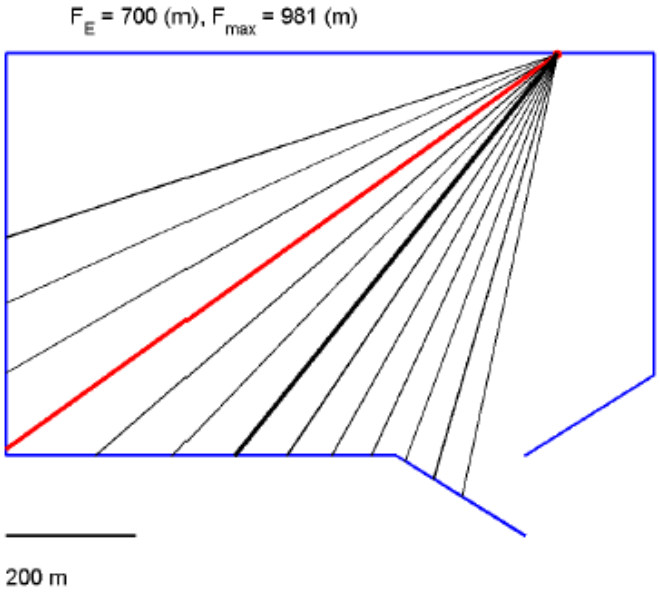

Figure 4.3: Principle of the maximum and the effective fetch. The blue lines indicate the boundaries of the harbour geometry, the thick black line indicates the fetch in the principle wind direction. The red line gives the maximum fetch in the surrounding sector. Source: Rijkswaterstaat (2014)

Water depth

The Bretschneider formula, Equation 4-1, contains a dependency on the local water depth. This dependency is illustrated in Figure 4.4.

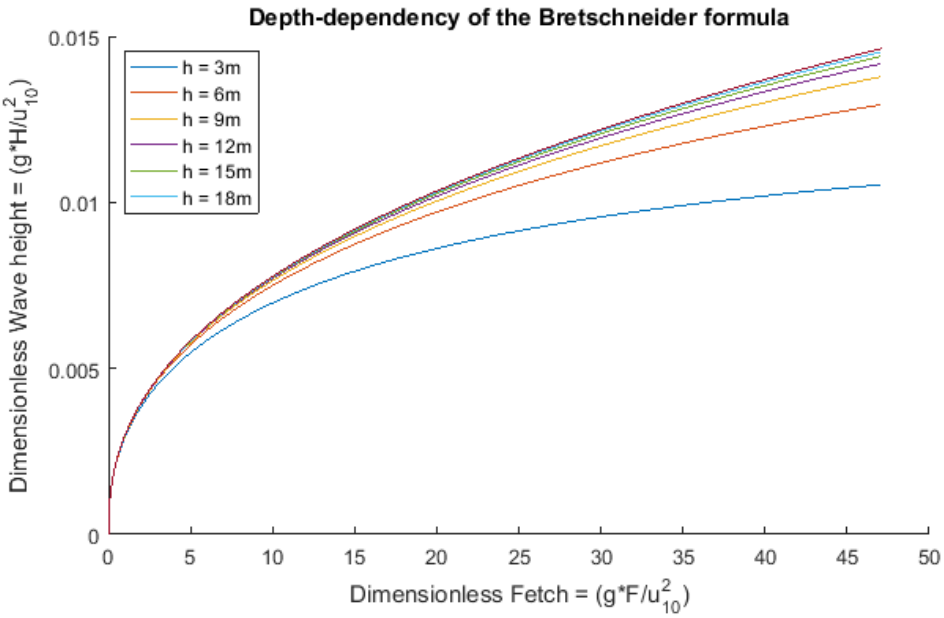

Figure 4.4: Depth-dependency of the Bretschneider formula (u_{10} = 25 m/s)

To apply the formula one single value for the water depth is required. From the above figure can be deduced that the depth-dependency on the wave height is marginal for water depths approximately larger than ten meters. A more important observation is the very little depth-dependency for dimensionless fetches up to 5 (≈300 meters for a wind speed of 25 m/s). Therefore the

representative depth should not be reduced by averaging the maximum water depth with the water depths on shallow areas, e.g. a flooded foreshore or harbour area. This averaging could cause an underestimation of the actual wave height at dimensionless fetches larger than 5. Instead the maximum water depth in the harbour area should always be taken. This implicates some conservativeness, but as seen Figure 4.4 this conservative effect is little for water depths above approximately ten meters.

4.3.2. Diffraction

Main elements of the model component *'Wave diffraction'*:

- Diffraction tables are used to find the diffraction pattern inside the harbour (Rijkswaterstaat, 2014)
- No multiple diffraction may occur; the geometry of the harbour is restricted
- For an inland harbour without any breakwaters the same diffraction diagrams can be applied

Wave diffraction is the process of turning and spreading of wave energy into areas with little wave energy. In harbours this is (one of) the most dominant processes. Analytical solutions of wave diffraction are based on the Sommerfeld solution for a semi-infinite straight breakwater or for a set of two semi-infinite breakwaters (Goda, Takayama, & Suzuki, 1978). Goda et al. applied this Sommerfeld solution for multi-directional waves; i.e. a wave spectrum. To construct the (analytical) solution for irregular waves Goda et al. integrated the individual solutions over various directions and frequencies. The results were summarized in diffraction diagrams. For the purpose of the updated 'RIKZ' method (Rijkswaterstaat, 2014) a re-calculation of the Goda method was done by Svašek Hydraulics to increase the accuracy of the diffraction diagrams. The resulting tables are found in the RIKZ manual *'Golfbelastingen in havens en afgeschermde gebieden'* (Rijkswaterstaat, 2014). Such diffraction tables exist for the case of a semi-infinite breakwater as well as for a certain gap in a set of breakwaters. Various tables are given for gap widths in the range of once until eight times the local wave length[1].

The diffraction tables show the diffraction coefficient as a function of the dimensionless coordinates, scaled with the wave length[1], see Figure 4.5 for the visualization of the tables for a semi-infinite breakwater. The origin of the coordinate system (X/L=0 and Y/L=0) lies at the tip of the breakwater. The x,y-coordinate system is rotated such that the y-axis is always parallel to the incoming wave angle. Diagrams for two cases of directional spreading are available: one for high directional spreading as is found at young-wind seas and one for low directional spreading which concerns swell waves. Generally, for harbours in the Netherlands the use of the high directional spreading diagram is advised as the wave conditions are typically related to a young wind-sea (Rijkswaterstaat, 2014). To a large extent the Dutch coast is sheltered from swell waves and is nearly only prone to waves generated on the North sea.

[1] The wave length in the model is calculated by means of iterations of the frequency dispersion relation (Equation 2-1):

$$\lambda = \frac{g}{2\pi} T^2 \tanh\left(2\pi \frac{h}{\lambda}\right)$$

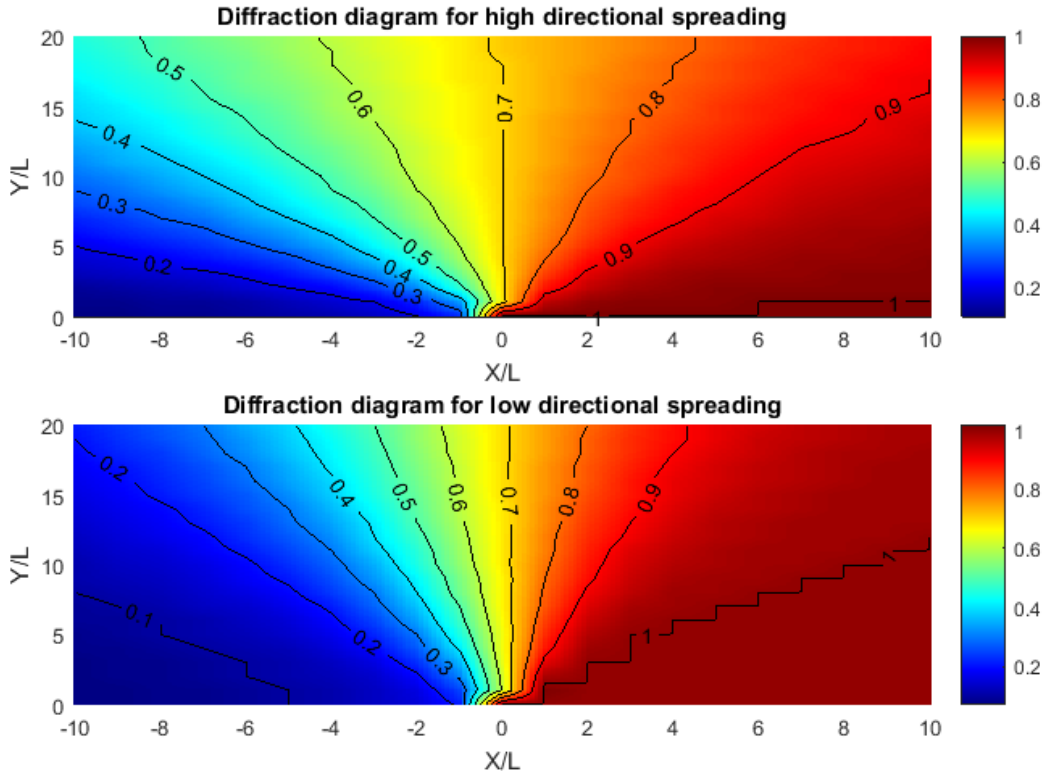

Figure 4.5: Updated Goda diffraction diagrams (by Svašek Hydraulics) for spectra with directional spreading. The semi-infinite breakwater runs on the negative part of the x-axis (at Y/L=0). The figures represent the diagrams for high directional spreading (S_{max} = 10) and low directional spreading (S_{max} = 75). See 'Golfbelastingen in havens en afgeschermde gebieden' (Rijkswaterstaat, 2014) for a more detailed description. Similar diffraction diagrams are available for the case of a set of two breakwaters.

In order to be allowed to use this approach no multiple diffraction may occur. Multiple diffraction occurs if more than one obstruction are found on the straight line between a location inside the harbour to the harbour entrance, see Figure 4.6. In practice this means a restriction on the complexity of the harbour geometry. Figure 4.7 shows a few imaginary harbour geometries for which the diffraction coefficients inside the harbour can be modelled using this approach. For these cases only singular diffraction takes place. This means that for every location in the harbour no more than one obstruction is in the path of the wave towards this location.

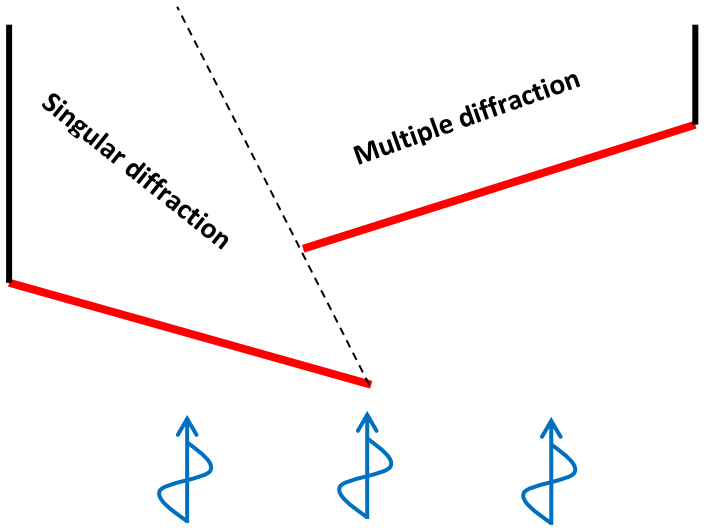

Figure 4.6: Illustration showing the difference between singular and multiple diffraction. The red lines indicate the breakwaters. The black dotted line indicates the boundary between singular and multiple diffraction

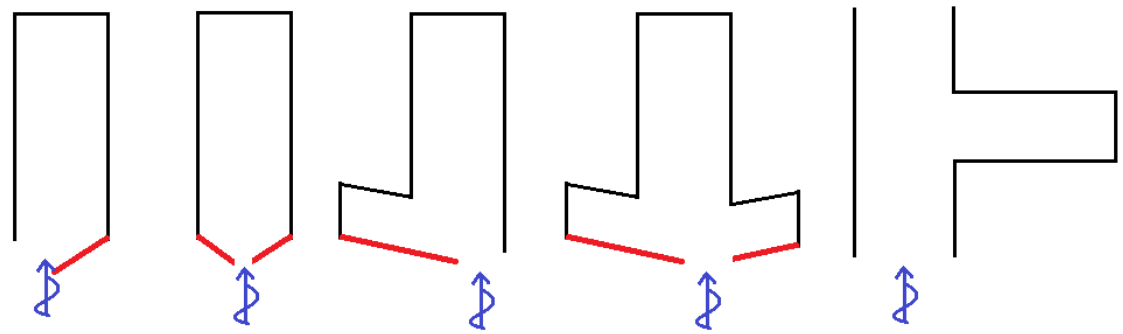

Figure 4.7: Imaginary harbour geometries for which the diffraction coefficients can be determined via the diffraction diagrams. The black lines indicate the quay walls and the red lines indicate a breakwater.

The right-most case in Figure 4.7 shows the (imaginary) case of an inland harbour. For this geometry waves will travel into the harbour via diffraction as well. The analytical Sommerfeld solutions do not exactly match up with this geometry. The analytical solutions have two components: the diffraction of directly transmitted waves and the diffraction of waves reflected of the breakwater (Goda, Takayama, & Suzuki, 1978). The reflected waves can also curl around the breakwater into the shadow zone of a breakwater, thereby slightly increasing the wave energy inside the harbour. It can be expected that this increase of wave energy is small as the required diffraction angle is larger than the diffraction angle of the directly transmitted waves (U.S. Army Corps Of Engineers, 2008).

For inland harbours, or any other harbour that is not protected by breakwaters, this secondary component is non-existent. This automatically leads to an overestimation of the wave height in the basin. If the overestimation is significant the use of the diffraction diagrams has a limited validity for inland harbours. To assess the influence of the reflected wave component on the wave conditions inside the harbour a rough check was done. This check consists of an assessment of the governing solutions and the application of the numerical model SWASH. The SWASH models for the two configurations allow for a quantitative comparison between the case of a (nearly) fully reflective breakwater to the case of an inland harbour configuration. The check on the validity of the diffraction diagrams can be found in Appendix E: *Check on the validity of the diffraction diagrams for inland harbours*. The conclusion is that the overestimation of the wave energy is fairly small when applying the diffraction diagrams for the inland harbour configuration.

4.3.3. Wave transmission

Main elements of the model component '*wave transmission*':

- The distinction between permeable and impermeable breakwaters has to be made
- The wave transmission coefficient is calculated using the method of Goda et al. (1967)
- The limits to the transmission coefficient are 0.0075 and 0.8 (EurOtop, 2016).
- The transmission coefficient is constant in throughout the transmission zone which consists of the area confined by the lines which have a 15 degree angle with the wave direction and their origin at the tip and the beginning of the structure

The penetration of waves by wave transmission through or over a structure is called wave transmission. Such wave transmission in harbours occurs via permeable or impermeable breakwaters and dams. The variety in the natural process of wave transmission is large due to the variety in structure types. Empirical formulations for wave transmission have to deal with this variety.

In first instance the distinction between permeable and impermeable breakwaters must be made. No single empirical formulation used in practice can describe both permeable and impermeable breakwaters. The main difference is the possibility of wave transmission through a permeable breakwater, which is not possible for impermeable breakwaters.

For impermeable dams and breakwaters wave transmission can be estimated using the method of Goda et al. (1967). This method is often used in practice (Rijkswaterstaat, 2014) and is for instance the default option for wave transmission in SWAN (SWAN Team, 2016). The formulas concerned with this method are repeated from Equation 2-18 below and plotted in Figure 4.8:

$$\frac{R_C}{H_S} \leq -\propto -\beta \qquad \rightarrow K_T = 1$$

$$-\propto -\beta \leq \frac{R_C}{H_S} \leq \propto -\beta \qquad \rightarrow K_T = \frac{1}{2}\left[1 - \sin\left(\frac{\pi}{2}\frac{\frac{R_C}{H_S} + \beta}{\alpha}\right)\right]$$

$$\frac{R_C}{H_S} > \propto -\beta \qquad \rightarrow K_T = 0$$

These variables in this formula are:

R_C = Freeboard = crest level – still water level (in meters)
H_S = Significant wave height (in meters)
K_T = Wave transmission coefficient = $H_{trans}/H_{incoming}$

The parameters α and β are structure-dependent parameters and are given in Table B2 of the manual '*Golfbelasting in havens en afgeschermde gebieden*' (Rijkswaterstaat, 2014). Alternative expressions are given in the 'EurOtop manual' (EurOtop, 2016). However, the validity of these formulas is limited to low-crested structures and the complexity of the formula is larger.

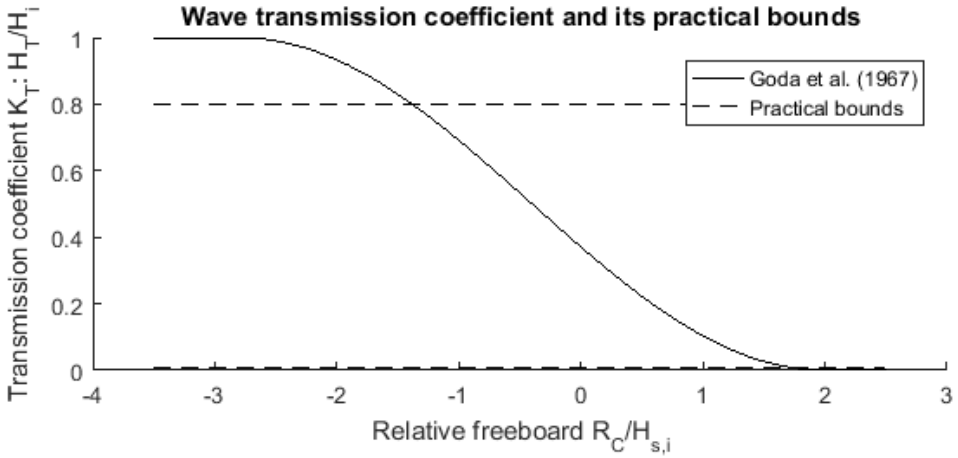

Figure 4.8: Wave transmission coefficient as is given by Goda et al. (1967). The practical bounds given in the EurOtop manual (2016) have been shown as well.

For permeable breakwaters, including a permeable core, usually a numerical approach is required (U.S. Army Corps Of Engineers, 2008). For permeable low-crested structures the formulas by Goda et al. and those given in the EurOtop manual would still give a good estimation. In this case wave

transmission will be dominated by transmission through overtopping waves. The transmission of waves through the breakwater can then be neglected. When the transmission of waves by wave overtopping becomes less dominant a practical minimum of 0.0075 for the transmission coefficient is adopted to account for any other cause of wave transmission (EurOtop, 2016). Furthermore also a practical upper limit to the wave transmission coefficient is applied (EurOtop, 2016).

The area for which wave transmission is accounted for is the wave transmission zone. This area is confined by the lines which make a 15 degree angle with the incoming wave angle from the outer edges of the breakwater or dam, see Rijkswaterstaat (2014). In this entire area the wave transmission coefficient is equal to the value calculated with the method of Goda et al. (1967). The suggestion (Rijkswaterstaat, 2014) to gradually reduce the transmission coefficient outside of the transmission zone has not been adopted in the model.

4.3.4. Combining the processes of local wave generation, diffraction and transmission

Main elements of the model component '*combining wave energy sources*':

- The combined wave height is calculated by means of linear superposition
- Interaction between wave growth and penetrated high-frequency waves is not accounted for
- A reduction of the amount of diffraction due to wave transmission is accounted for, although it is suspected that the approach to deal with this interaction is not entirely accurate.

The combination of the various wave components occurs through superposition. This superposition can done using the following principles (Van der Meer, Langenberg, Breteler, Hurdle, & Den Heijer, 2002):

$$E_{total} = E_{local} + E_{penetration}$$
$$H_{total} = \sqrt{H_{local}^2 + H_{penetration}^2}$$

Using this principle no interaction is accounted for. It may occur that the process of local wave generation is influenced by the presence of high-frequency waves (Rijkswaterstaat, 2014). This can be explained by a changed energy transfer from the wind to the waves when waves already exist (wind-wave feedback mechanism described by Miles, 1957). Unclear is what this influence will mean for the wave height in the basin. Therefore it was chosen to not implement the possible interaction between high-frequency waves and wave growth.

The interaction between wave transmission and wave diffraction of incoming waves is more evident. Wave diffraction occurs due to a gradient in the amount of wave energy present along the crest of a wave. The diffraction rate (the speed at which the crest of the wave turns) increases for a larger gradient in the wave energy. When wave energy is present in the shadow zone due to the process of wave transmission, the amount of diffraction towards this area decreases. The reduction of the diffraction can be estimated by superposition of the wave energies (Yu & Togashi, 1996) (Rijkswaterstaat, 2014). This is expressed in the formula for the combined diffraction-transmission coefficient:

$$K_{D,T} = \sqrt{(1 - K_T)^2 * K_D^2 + K_T^2}$$

While this formula will be applied in the model, the author of this thesis suspects an inaccuracy when using this approach. The formula for the combined diffraction-transmission coefficient expresses the reduction of diffraction inside the transmission zone. At the same time this reduction of the diffraction inside the shadow zone behind the dam or breakwater, leads to a lesser spreading of the wave energy outside of the shadow zone. This leads to the conclusion that higher waves would be found outside of the shadow zone when transmission over the dam or breakwater would occur. This increase of the wave height is not expressed in the formula. A sketch of the explained situation is found below in Figure 4.9.

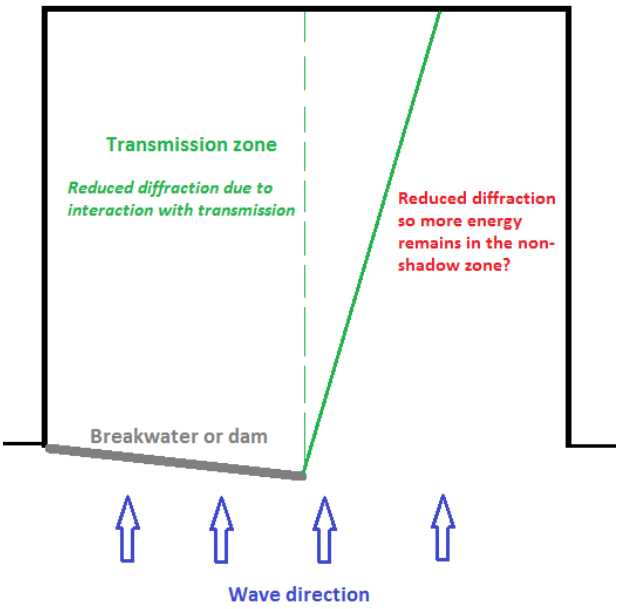

Figure 4.9: Sketch to illustrate the surmise that the application of the formula for the interaction between diffraction and transmission might lead to an underestimation of the wave height in the non-shadow zone.

4.3.5. Wave overtopping

Main elements of the model component '*Wave overtopping*:

- The EurOtop formula for vertical walls is applied (EurOtop, 2016)
- The relevant parameters are the local freeboard, wave height and incoming wave angle
- The considered wave height is the combined wave height from the previous steps
- The considered angle of incidence is taken from the individual wave component which has the smallest angle of incidence

The element of wave overtopping is the final step in the model. The input for this model element are the wave conditions from the previous steps. Furthermore input for the wave direction is required. Obliqueness of waves reduces the amount of wave overtopping. In this model only overtopping of vertical (quay) walls are considered. For specific cases where overtopping of non-vertical structures are relevant the model can be adapted to these conditions by applying different overtopping formulas (EurOtop, 2016). The formula that is implemented in the model is the following (copy from Equation 2-19) (EurOtop, 2016):

$$\frac{q}{\sqrt{g \cdot H_{m0}^3}} = 0.047 \cdot \exp\left[-\left(\frac{2.35}{\gamma_\beta}\frac{R_C}{H_{m0}}\right)^{1.3}\right]$$

The variables in this formula are:

q	=	Specific overtopping discharge (in cubic meters per second per meter width)
g	=	Gravitational acceleration (in meters per second squared)
H_{m0}	=	Spectral significant wave height ($\approx H_s$ in deep water (EurOtop, 2016), in meters)
γ_β	=	Influencing factor for oblique wave attack; beta is the incoming wave angle
R_C	=	Freeboard measured from the still water level (in meters)

As can be seen no dependency on the wave period is present in the EurOtop formula. The reason for this is the very little or non-existent influence it has on the wave overtopping (EurOtop, 2016) (Van der Meer & Bruce, 2014). The negligible effect of the wave period on the wave overtopping discharge is only valid for very steep and vertical structures without wave breaking. For sloping structures wave breaking is likely to occur on the slope. The type of breaking and the amount of wave overtopping then depends on the breaker parameter which has a dependency on the wave period via the wave length:

$$\xi_{m-1,0} = \frac{\tan(slope\ angle)}{\sqrt{H_{m0}/L}}$$

For vertical walls an increasing obliqueness of the angle of incidence decreases the overtopping discharge. In the EurOtop formula this is expressed as the influence factor for oblique wave attack and can be described by (EurOtop, 2016):

$$\gamma_\beta = 1 - 0.0033|\beta| \quad for\ 0° \leq \beta \leq 80°$$

$$\gamma_\beta = 0.736 \quad for\ \beta > 80°$$

For a range of incoming wave angles the EurOtop formula has been plotted in Figure 4.10. It can be seen that an increasing wave angle has a significant influence on the overtopping discharge. This effect relatively increases for larger relative freeboards.

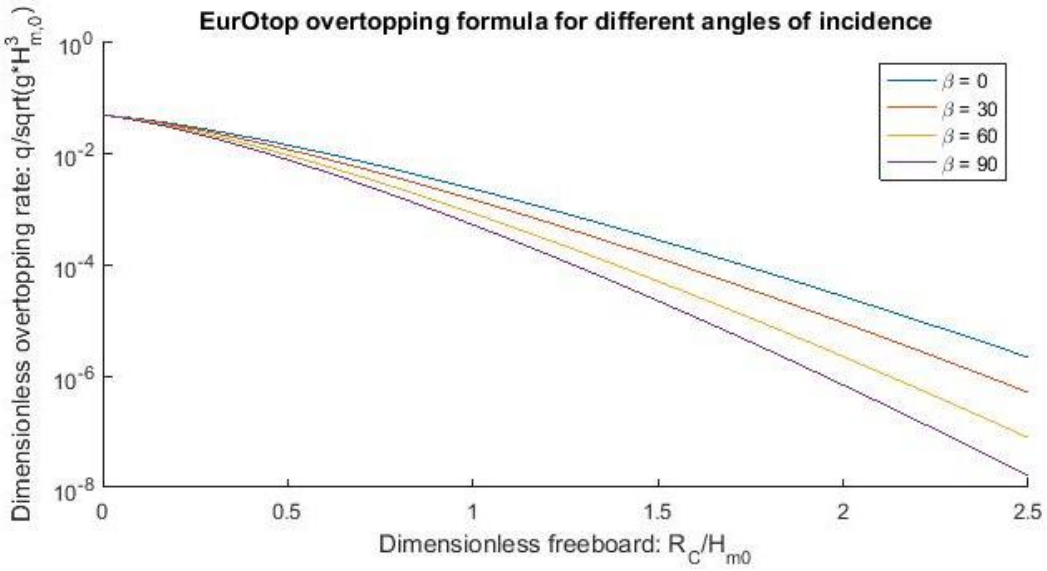

Figure 4.10: EurOtop overtopping formula for four values of the angle of incidence (water depth =15 meters). The formula is plotted for the dimensionless freeboard on the horizontal axis and the dimensionless specific overtopping discharge on the vertical axis

Angle of incidence β

The angle of incidence incorporated in the overtopping formula via the reduction factor γ_β is the only unknown variable left before being able to calculate the specific overtopping discharge. Due to the various wave components no single angle of incidence can be distinguished. To date no research has been undertaken for wave overtopping from a wave field with components in different directions (Van der Meer J. , Personal correspondence on the topic of varying angles of incidence, 2016). Van der Meer suggested a pragmatic approach in which the incident wave angle is interpolated based on the amount of wave energy from the different directions. This approach can be described by the following formula:

$$\beta_{comb} = \frac{\beta_{wind} * E_{wind}}{E_{wind} + E_{trans} + E_{diff}} + \frac{\beta_{trans} * E_{trans}}{E_{wind} + E_{trans} + E_{diff}} + \frac{\beta_{diff} * E_{diff}}{E_{wind} + E_{trans} + E_{diff}}$$

As mentioned by Van der Meer (2016) this approach has never been tested and validated. Therefore it was chosen not to implement the averaging of the angle. Instead, for the sake of a conservative approach, the smallest angle of incidence from the three wave components is taken as the governing angle of incidence for the combined wave field, see Figure 4.11.

The wave directions of these three components are estimated as follows:

- The direction of the wind-generated waves equals the principal wind direction
- The direction of the diffracted waves in the shadow zone equals the angle of the line from the location under consideration towards the origin of the diffraction pattern, see Figure 4.11 for an example.
- The direction of the transmitted waves equals the angle of the outside waves. In the area outside the direct transmission zone (the 15 degree sector on both sides) the actual angle is taken with respect to the edges of the breakwater or dam.

Neither of these determinations of the wave direction for the three components is outright conservative; e.g. waves are also generated in a sector around the principle wind direction. However for the sake of the implementation in the wave overtopping formula it is considered sufficient. As the smallest angle of incidence of the three components is taken as governing for the entire wave field, the conservativeness will be guaranteed as long as one of the components is not dominant over the other two.

The approach in the WGPO model with regards to the angle of incidence β is schematized in an example in Figure 4.11 below.

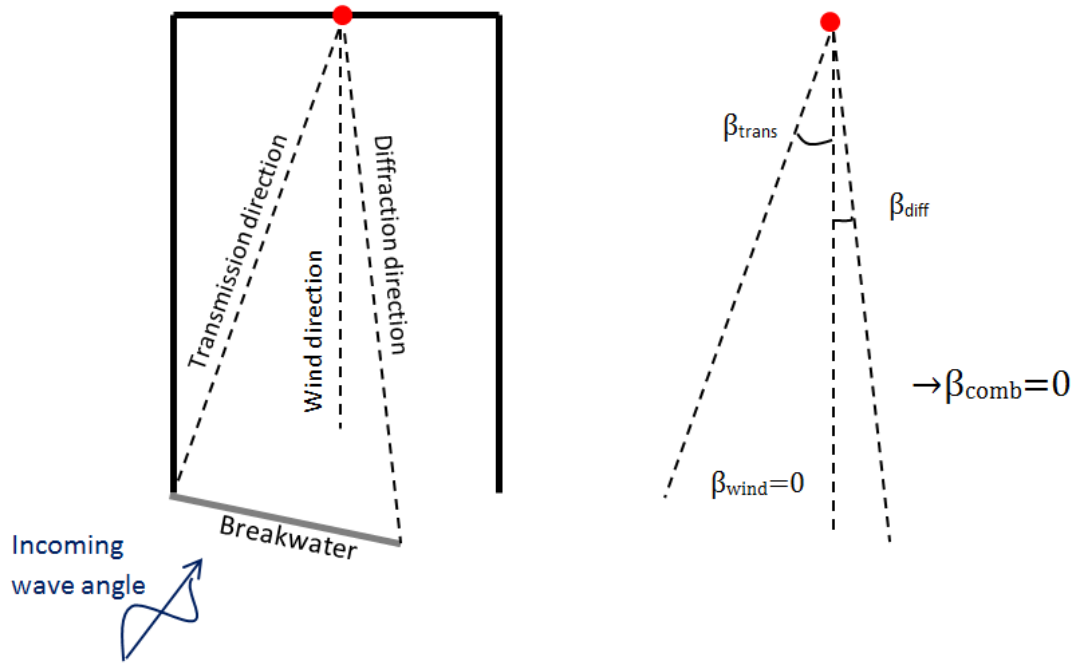

Figure 4.11: Example showing the approach with respect to the angle of incidence in the EurOtop formula. In this example the angle of incidence of the wave field at the red location would be set to 0 degrees.

4.4. Verification of the WGPO model

The continuous 'semi-empirical' to estimate the wave heights inside a harbour area and the subsequent wave overtopping has been described in the previous paragraphs. This section will deal with the verification of the model outcomes.

Roughly the point-based methodology described in the 'RIKZ' manual (Rijkswaterstaat, 2014) has been adopted in the WGPO model. For the method of Rijkswaterstaat the validity has been tested for two test cases (Reijmerink, 2012), see Figure 4.12. These test cases concern examples of harbours in which reflection and multiple diffraction may occur. It appears that the methodology (nearly) always gives conservative estimations of the wave height. The overestimation is generally in the order of a few decimetres (Reijmerink, 2012). It is concluded that the model is applicable for assessment purposes.

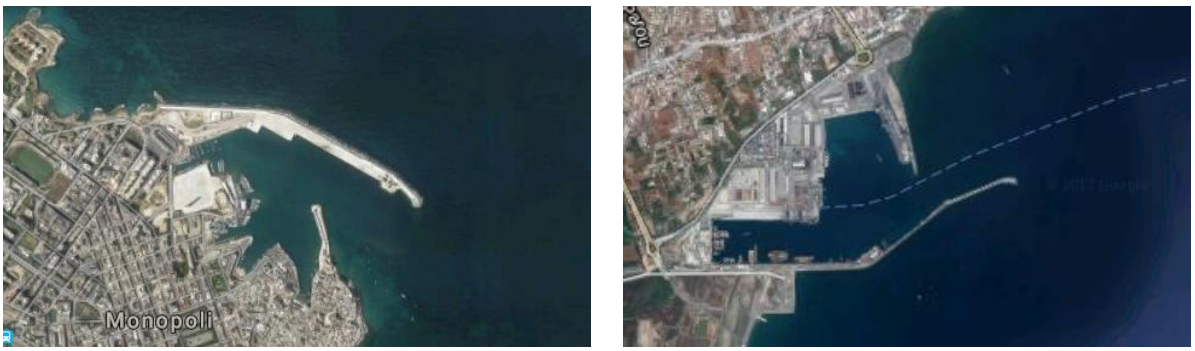

Figure 4.12: Test cases of Reijmerink (2012) for which the performance of the 'RIKZ' method has been validated. *Left*: Harbour of Monopoli, Italy. *Right*: Harbour of Limassol, Cyprus. *Source: Google Maps* (2016)

Such assessment purposes are also the main relevance of the wave overtopping estimation in the light of possible increasing flood risk due to wave overtopping (Chapter 1). Therefore the method of Rijkswaterstaat (Golfbelasting in havens en afgeschermde gebieden: een eenvoudige methode voor het bepalen van golfbelastingen voor het toetsen van waterkeringen, 2014) is likely to be applicable to find the wave heights. What now has to be checked, is if the WGPO model gives similar results compared to the method described by Rijkswaterstaat. This check is performed for the case of the '*Vlissingen Buitenhaven*', see Figure 4.13.

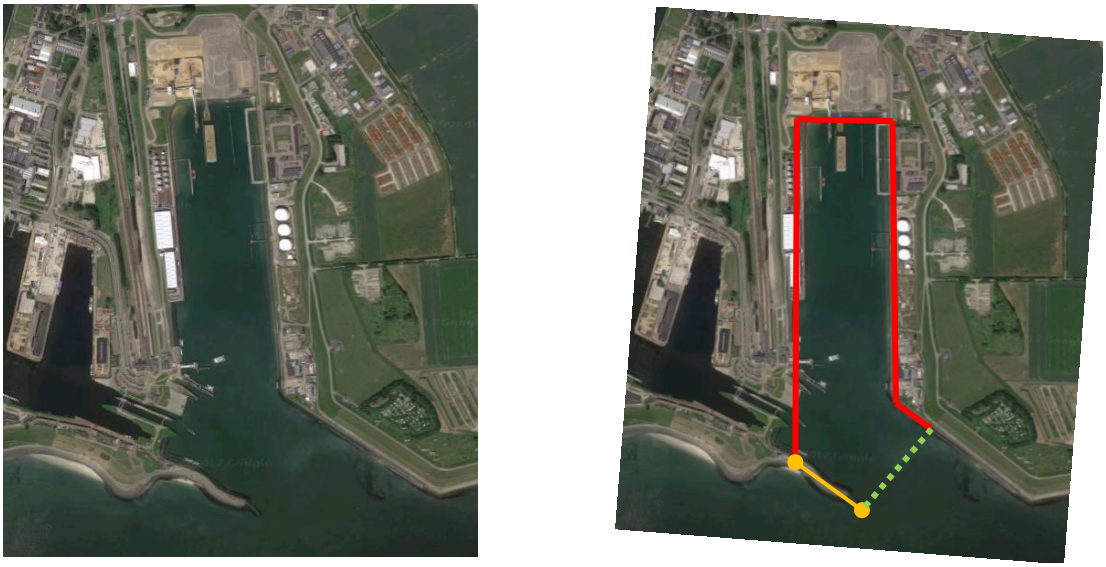

Figure 4.13: Left: aerial picture of the 'Vlissingen Buitenhaven'; right: schematization of the geometry in the empirical model (red = quay walls, orange = closure dam, green dotted = harbour entrance, rotation of the geometry of 5 degrees for practicality reasons

The right figure in Figure 4.13 shows the schematization of the harbour in the WGPO model with respect to the aerial picture. For the sake of simplicity and conservativeness, wave height reducing obstructions have been neglected.

Rijkswaterstaat (2014) chose six output locations for their validity check in the Vlissingen outer harbour case. The coordinates of these six locations have been copied to the WGPO model, shown in Figure 4.14. The report (Rijkswaterstaat, 2014) shows the example calculation for the design conditions. These conditions are (generally, for location 02 the wave height is larger for another wind direction) as follows:

Table 4.2: Boundary conditions for the WGPO model

Design conditions (outside the harbour)	Rijkswaterstaat (2014)	WGPO model
Design water level [m +NAP]	5.3	5.3
Representative bottom level in the basin [m+NAP]	-20.0	-20.0
Representative harbour area elevation [m+NAP]	4.50	4.50
H_s [m]	2.4	2.4
$T_{m-1,0}$ [s]	7.14	7.14
Wind direction [°N]	240	245[1]
Wind speed [m/s]	33	33
Wave direction [°N]	235	240[1]
Representative wave length [m]	77	77.1[2]

[1]Five degrees is added in the WGPO model as a consequence of the rotation of the geometry (Figure 4.13)
[2]The wave length is determined using an iterative approach instead of an explicit approximation

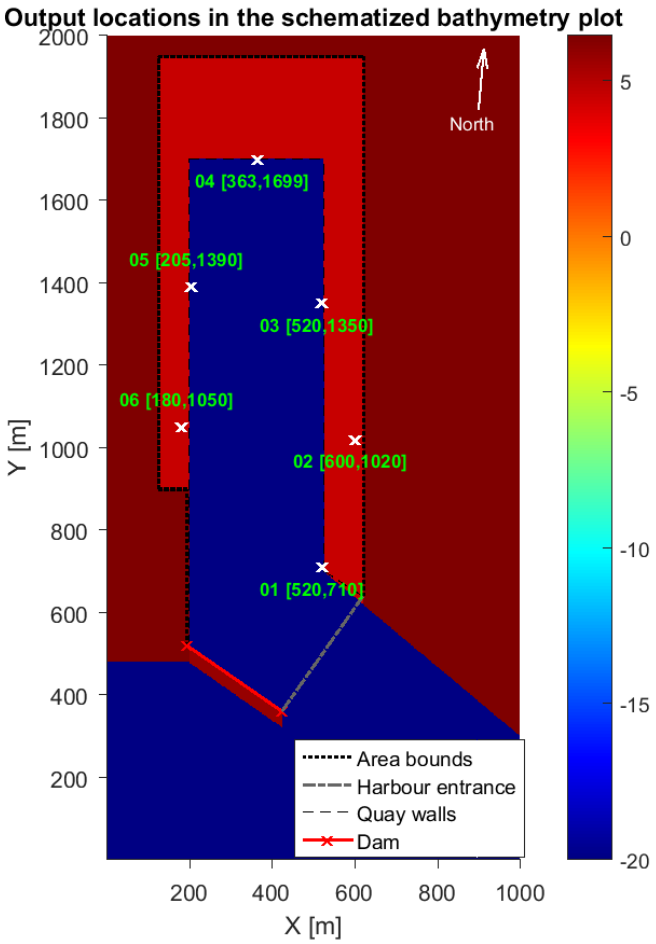

Figure 4.14: Output locations in the WGPO model; four of the locations lie at the edge of the main basin and the other two lie on top of the harbour areas (submerged during design conditions)

For these locations the wave heights found with the WGPO model have been given in Table 4.3 along with the wave heights found by the 'RIKZ' method. Furthermore also the wave heights are given which originate from two other sources, also shown by Rijkswaterstaat (2014). Alkyon performed a numerical study with the use of SWAN (SWAN Team, 2016) on the 'Vlissingen Buitenhaven' case in 2001. At this moment in time the prevailing hydraulic conditions were given in '*Randvoorwaardenboek 1996*' (RVB96, English: '*Hydraulic boundary conditions for primary flood defences 1996'*) (Rijkswaterstaat, 1996). RVB96 gives the wave conditions for the locations inside the harbour as determined via empirical and analytical calculations.

Table 4.3: Comparison of the WGPO model with the RIKZ method (Rijkswaterstaat, 2014) and the values from the RVB96 and the SWAN calculation by Alkyon (Rijkswaterstaat, 2014)

Significant wave height at location:	01 [m]	02 [m]	03 [m]	04 [m]	05 [m]	06 [m]
WGPO model	1.20	1.05	0.90	0.83	0.55	0.56[1]
RIKZ method	1.19	1.18[2]	0.86	0.77	0.55	0.56
RVB 96	1.35	0.85	1.00	0.60	0.60	0.60
Alkyon	1.13	0.67	0.71	0.72	0.41	0.52

Remarks:
[1] For location 06 the wave height has been reduced as the location lies on a submerged harbour area for which significant wave breaking can be expected (Rijkswaterstaat, 2014)
[2] The significant wave height at location 2 is larger for another wind direction, see Appendix F

For five of the six locations the found results match up well with the other methodologies. To first order this proves the validity of the WGPO model with regard to the computation of the wave height. The location for which differences can be observed is location 02. This can readily be explained by the underlying assumptions of the methods. The SWAN model takes into account the wave breaking on the shallow area on which location 02 lies. The RIKZ method does not as its location is too close to the deeper area. In the WGPO model wave breaking is not accounted for at this location. The mismatch with the RIKZ method can be explained by the slight difference in the transmission zone; RIKZ calculated a transmission coefficient of 0.31 while in the model schematization in the WGPO model the location falls just outside of the transmission zone.

In Appendix F: *Analysis of 'Vlissingen Buitenhaven' case in the WGPO model,* the validity of the individual components is proven with respect to the RIKZ method. It includes plots of the wave heights and coefficients concerned with the individual processes. This appendix also shows the applicability of the model for overtopping scenarios (when the harbour areas are not submerged). This case can however only be seen as a supplementary case study. Too little data is available and it is not certain if it falls within the applicability range of the model as significant reflection could be expected.

4.5. Applicability of the model

The applicability ranges of the model can be summarized as follows; a more detailed explanation is found below the box:

Applicability ranges of the WGPO model:

- The applicability of the WGPO model is at least comparable to that described in the method of RIKZ (Rijkswaterstaat, 2014) in which:
  - Multiple wave diffraction is not accounted for
  - Multiple wave transmission is not accounted for
  - Significant wave reflection is not accounted for
- If the model is applicable for a certain geometry it is expected to give conservative, larger, estimations of the wave height distribution in the harbour, generally in the order of a few decimetres (Reijmerink, 2012)
- Similar to the method of RIKZ the model is likely to also be applicable for more complex harbour areas (Reijmerink, 2012)
- The WGPO model can be applied as a first estimation tool after which the results should be judged by experts. The continuous results might give more insight in the accuracy of the estimations.
- The estimation of the wave overtopping discharges is valid in a harbour basin with significant reflection as long as the reflected component is rather insignificant at the opposing quay wall

The WGPO model can only be applied within the ranges of its validity. The limits to the validity of the model are determined by the underlying assumptions and neglected processes within the model. The validity of this model is in line with the methodology of the RIKZ (Rijkswaterstaat, 2014).

The WGPO is unable to model the combination of reflections and multiple diffraction patterns. These inabilities set a restriction on the complexity of the harbour geometry. In cases where multiple diffraction and reflection occurs the wave field becomes too complex. However, Reijmerink (2012) showed the possibilities of using the RIZK method in such cases anyway. An extended validity applies

in cases where reflections are still fairly significant. The reason for this is the conservativeness in the remainder of the model.

This extended validity is also likely to hold in the case of the WGPO model, although this has not been verified. In the case where wave overtopping is the main purpose of the application of the model, the restriction might be even less. This can be explained as follows: the significant wave height at the location of the quay wall nearly doubles due to reflection. However, the overtopping rate is only determined by the wave height of the incoming wave component (EurOtop, 2016). The amount of reflection is then not relevant for the estimation of the overtopping discharge. This validity will only hold up to the location of the 'first reflection'. For relatively narrow basins the reflected wave component will increase the amount of wave energy at an opposing location. Here the amount of wave overtopping increases due to the reflected component. For wider basins the reflected component will have been damped to a large extent such that the effect on the wave overtopping discharge is minor.

5. Case study '*Brittaniëhaven*'

This chapter will discuss the case study on the '*Brittaniëhaven*' in the Botlek area. Prior to this thesis, the flood risk in this harbour was already analysed both including and excluding the flood risk increasing effect of wave overtopping. The availability of these results allows for a simple comparison of the methods. The first paragraph (5.1) of this chapter describes the case and the prior analyses. This includes a description of the location and the land use of the *Brittaniëhaven*. Subsequently (paragraph 5.2) the set-up of this case in the WGPO model is discussed (see Chapter 4 for a description of this model). Paragraph 5.3 will deal with a flood risk analysis in which the WGPO model is used to model the overtopping discharges given the conditions. Finally paragraph 5.4 will show the results of a sensitivity analysis. In this analysis the sensitivities of the model outcomes to single variables are shown, e.g. the water level or the wind speed. Furthermore it will also deal with the uncertainty in the model outcomes originating from the modelling choices, e.g. the choice of a wind-wave growth formula.

5.1. Case description

The *Brittaniëhaven* is located in the Rotterdam harbour area, see Figure 5.1 or Appendix H for a larger and more detailed version. Within the divisions of the Rotterdam harbour area it falls inside the *Europoortgebied*. The *Europoort* is the part of the Rotterdam harbour south of the *Nieuwe Waterweg* and east of the *Maasvlakte* areas. Sometimes the *Brittaniëhaven* and the more southern *Seinehaven* are considered to be part of the Botlek area located to the east.

Figure 5.1: Location of the Brittaniëhaven inside the Rotterdam harbour area. Source: Google Maps (2016). See Appendix H for a larger and more detailed version.

The largest part of the *Brittaniëhaven* consists of a transhipment area for cars, see Figure 5.2. To facilitate this area the northern quay wall of the Brittaniëhaven contains four Ro-ro berths. The southeastern part of the *Brittaniëhaven* consists of chemical industry. The final part is used for steel transhipment containing sheltered loading and unloading facilities.

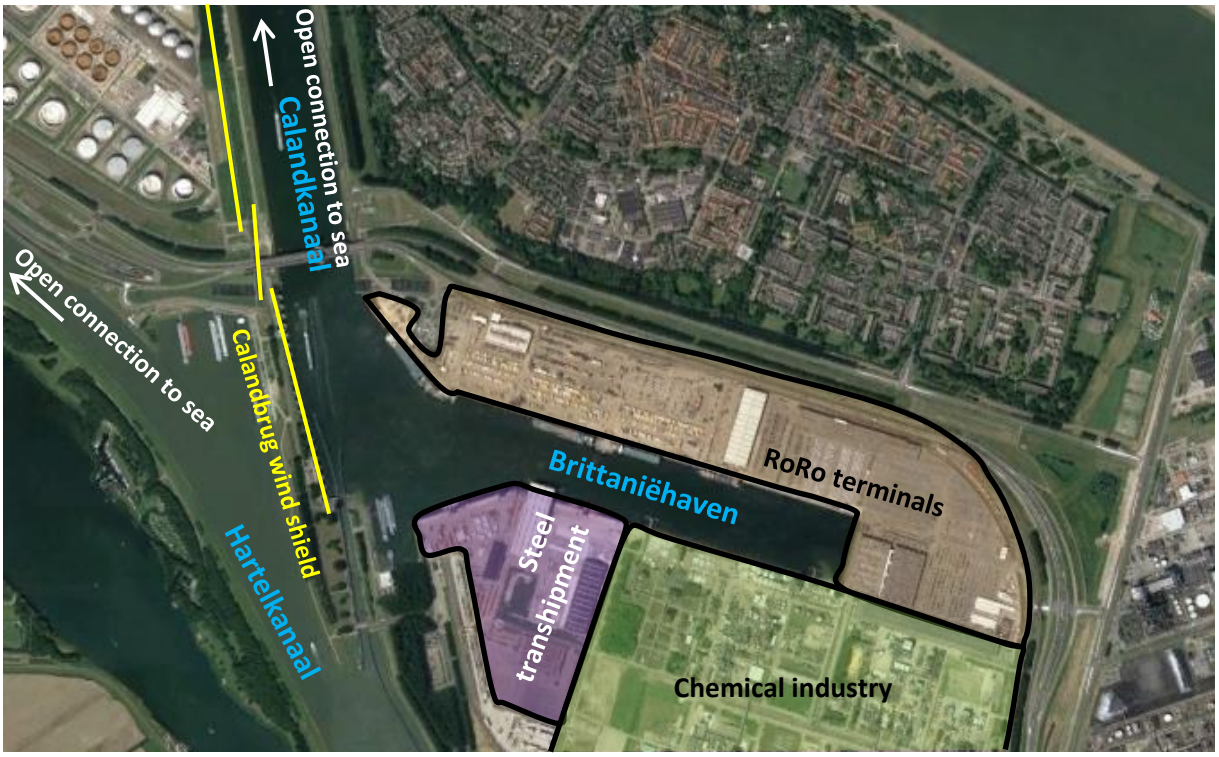

Figure 5.2: Aerial picture of the *Brittaniëhaven* in which the land use is indicated. The location of the Calandbrug wind shield is indicated by the yellow lines. Source: Google Maps (2016). Appendix H gives a larger image which also shows the surroundings of the Brittaniëhaven and indicates more locations of interest.

As a contribution to the '*Strategic adaptation agenda*' (see Chapter 1) and the subsequent '*Pilot Waterveiligheid Botlek'* researches were conducted which analysed the probability of flooding and the flood risk in and around the *Brittaniëhaven.* Slootjes & Wagenaar (2015) focussed on the flooding of the Botlek area from the *Hartelkanaal*, but also included an estimation of the frequency of flooding for the *Brittaniëhaven* only, see Figure 5.3. The presented probabilities were derived statistically from records of high water levels in the *Brittaniëhaven, t*hereby disregarding the influence of wave overtopping and possible flooding of the areas around the *Brittaniëhaven* via the *Hartelkanaal*.

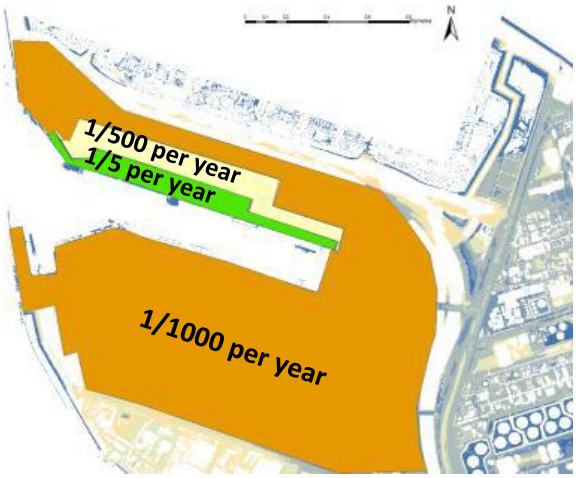

Figure 5.3: Frequency of flooding in 2015 for the Brittaniëhaven excluding the influence of wave overtopping. Source: Slootjes & Wagenaar (2015)

Without a further calculation it was mentioned that the probability of flooding would increase with the effect of wave overtopping; e.g. up to once every year for the low-lying Roro quays in the northern part. Furthermore Slootjes & Wagenaar (2015) concluded a dominant influence of flooding from the *Hartelkanaal* on the flood risk in the southern part of the *Brittaniëhaven* for scenarios with return periods of 1000 years and larger.

In the context of the *'Pilot Waterveiligheid Botlek'* the frequency of flooding and the flood risk were quantified for the entire Botlek area including the *Brittaniëhaven* and the *Seinehaven* (Nicolai, et al., 2016). The influence of wave overtopping was taken into account via an addition to the water level of 0.3 meters for the entire Botlek area, except for the northern parts of the *Brittaniëhaven*. Again the dominant influence of flooding from the *Hartelkanaal* was found (and later assumed). It was recommended to further analyse the probability of flooding of the southern *Brittaniëhaven* from the *Calandknaal*. For illustrations of the described results reference is made to Nicolai et al. (2016).

With the use of the WGPO model discussed in Chapter 4 the isolated case of the *Brittaniëhaven* is analysed in which the role of wave overtopping will be quantified. This case study will include the flooding of both the northern and the southern *Brittaniëhaven*. The set-up of the *Brittaniëhaven* case in the WGPO model is discussed in the next section.

5.2. Model set-up

The description of the model set-up is split into three parts. The first paragraph of this section (5.2.1) deals with the applicability of the model for the *Brittaniëhaven* case. The second paragraph gives the spatial schematization of the *Brittaniëhaven* case. This includes the (simplification of the) bathymetry and the removal of objects. The third part of the model set-up, given in section 5.2.3, are the boundary conditions such as the still water level and wind conditions.

5.2.1. Applicability of the model for the *Brittaniëhaven* case

The application of the WGPO model is only allowed if a case meets the requirements set in section 0. Outside the applicability range the accuracy of the model is uncertain and it may underestimate the wave conditions and wave overtopping discharges. Below the applicability of the model for the *Brittaniëhaven* case is evaluated:

- Multiple wave diffraction is not accounted for: Multiple wave diffraction does not occur inside the *Brittaniëhaven* with the exception of some minor diffraction around berthing facilities and other obstacles.
- Multiple wave transmission is not accounted for: Major transmission does not occur due to the absence of a dam or breakwater at the harbour entrance.
- Significant reflection is not accounted for: It is unknown whether significant reflection will occur. For the dominant western winds (from NW to SW) the primary wave direction will be towards the east such that the likeliness of significant reflection reduces. Still, reflection of wave energy at the sloping eastern boundary of the harbour may cause an increase in the wave energy inside the harbour basin. However it could be expected that this effect is insignificant in relation to the conservativeness of the approach. The amount of reflection is expected to decrease significantly when the northern harbour areas become inundated when the water level exceeds 3.4 meters above NAP.

- Data availability: the required data (water level, waves and wind variables) is available via the database '*CR2011_BenR_Rijndombuiten_oever_a_19_v01*' which can be accessed through Hydra-NL (Duits M. , 2017).

5.2.2. Harbour schematization

In order to be able to implement the *Brittaniëhaven* case into the model a few assumptions and simplifications have to be made. These simplifications are largely in line with the RIKZ method (Rijkswaterstaat, 2014). The schematization of the harbour includes, amongst other aspects, the following simplifications:

- The entrance of the harbour is located just south of the *Calandbrug*
- Only the quays and slopes along the main harbour basin are considered to be overtoppable (red and orange lines in Figure 5.4)
- The elevated harbour terrains have been divided into four distinct elevations; from 3.4 m+NAP along the northern quay walls up to 5.8 m+NAP along the eastern quay wall
- The bottom level of the harbour is assumed to be constant with an elevation of -15.0 m+NAP
- The navigation facilities in front of the *Rozenburgse sluis* are disregarded
- Berthing facilities are disregarded
- The quays are schematized as vertical or as a 1:1 slope

The schematization of the harbour is shown in Figure 5.4. For practicality reasons the geometry is rotated by 15 degrees in anti-clockwise direction. The schematized bathymetry which is an input for the WGPO model is shown in Figure 5.5.

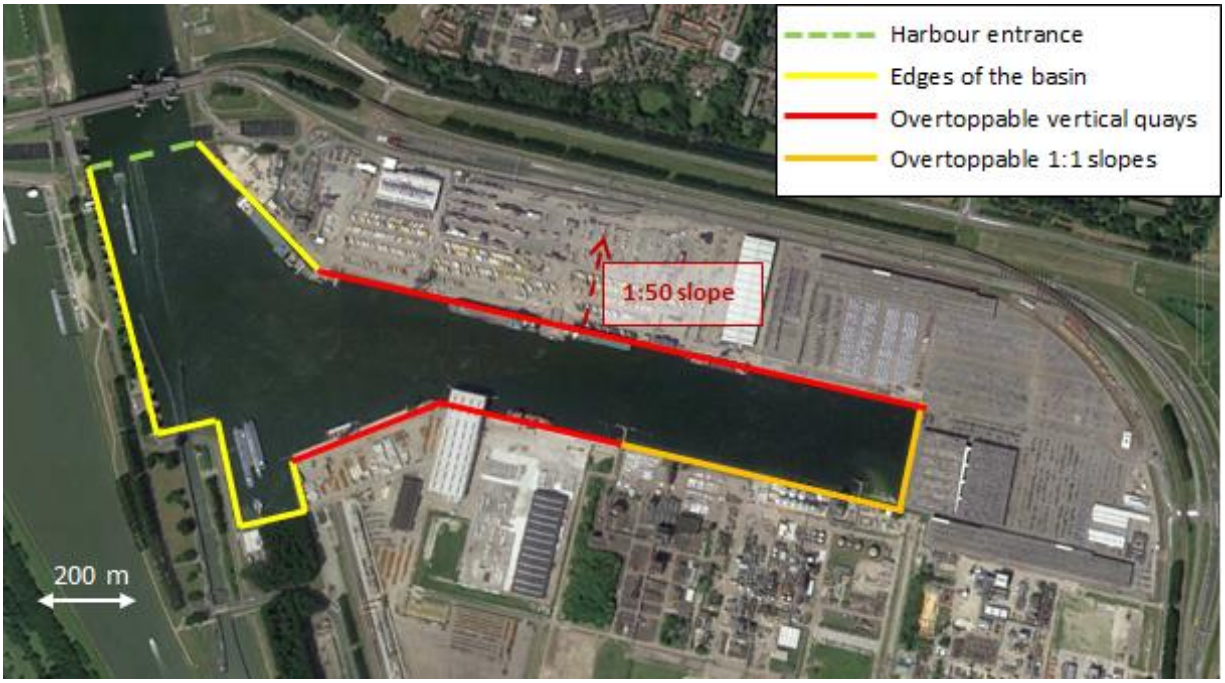

Figure 5.4: Schematization of the *Brittaniëhaven* with a background of an aerial picture of the area.

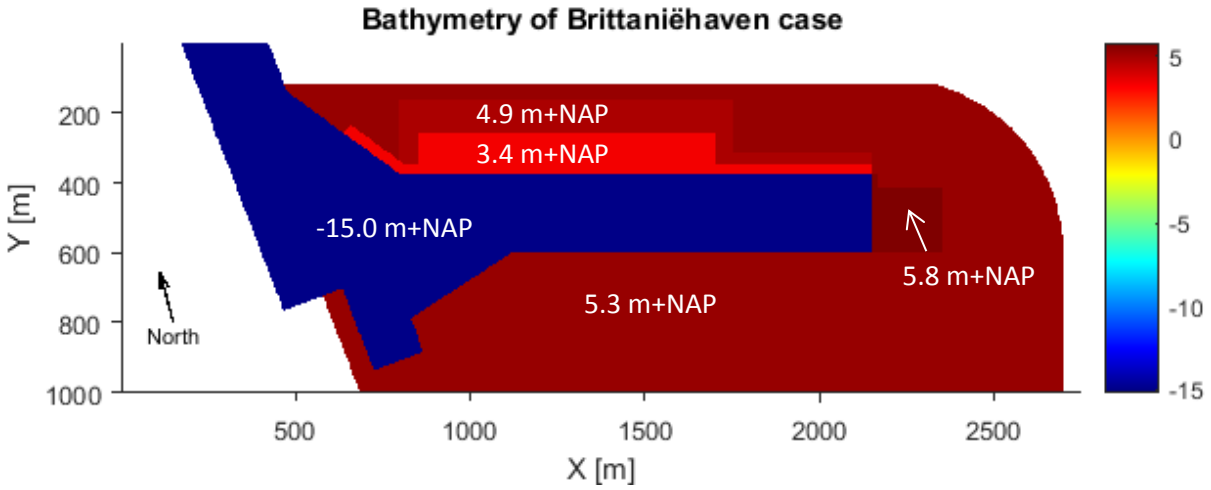

Figure 5.5: Bathymetry of the *Brittaniëhaven* case

5.2.3. Boundary conditions

As mentioned in paragraph 5.2.1 probabilistic data is available from the database '*CR2011_BenR_Rijndombuiten_oever_a_19_v01*'. In this database water levels, wind data and wave conditions are given for return periods ranging from 10 years up to 20,000 years. The data primarily originates from the large SWAN model of the Rhine and Meuse river mouths (Chbab, 2012). The model Hydra-NL (Duits M. , 2017) determines the hydraulic conditions given a certain exceedance probability. These hydraulic conditions (may) concern the still water level and the wave conditions. The main philosophy of the model is taking into account the possibility of extreme conditions not taking place at the same moment; e.g. the highest wind waves are not necessarily found at the same time as the once in a thousand year water level. This means that many different combinations of hydraulic loads (wind directions, water levels, discharges, etc.) lead to the same flood event. This reduces the conservativeness in the hydraulic boundary conditions.

Using Hydra the still water levels for various return periods are found; these are tabulated in

Table 5.1. Although the water levels and the amplitude of the seiches vary slightly (+/- 5 cm) throughout the basin, constant values have been assumed. The variation of the still water level for the dominant western wind directions when considering inundation by both overflow and overtopping (+/- 5 cm), is assumed negligible (return period of a certain water level may differ when considering overtopping besides overflow; this introduces variability in the water level for different wind directions). Appendix G shows the breakdown of the Hydra results for the different wind directions including this minor dependency on the water level. Finally it can be noted that the failure to close the Maeslant barrier has no influence on the boundary conditions in the *Brittaniëhaven* as the *Brittaniëhaven* lies on the seaside of the *Europoortkering.* In contrast, the failure to close the barrier (once every 100 closures) is a dominant factor for the flood risk for locations behind the barrier.

Table 5.1: Still water levels in the *Brittaniëhaven* for various return periods excluding and including the effect of seiches

Return period T [years]	SWL [m+NAP]	SWL + nett seiche effect[1] [m+NAP]
1	2.55	2.93
2	2.75	3.21
5	3.11	3.69
10	3.33	4.00
20	3.54	4.40
50	3.84	4.72
100	4.07	5.03
200	4.30	5.45 [2]
500	4.60	5.76 [2]
1000	4.78	6.04 [2]
2000	4.97	6.32 [2]
4000	5.16	6.61 [2]
10000	5.43 [2]	6.99 [2]

Remarks:
[1]Nett seiche effect is an addition to the still water level, but the amplitude of the seiches is corrected for the possible non-coincidence with the peak water level, see for instance Slootjes & Wagenaar (2015)
[2]Flooding due to the exceedance of the crest heights by the still water level

The wave conditions are far more variable as many different combinations of wind speed, wind direction and water level lead to an event with a certain return period. In the SWAN model (Chbab, 2012), at the basis of the applied database, no long wave penetration was modelled at the end of the *Calandkanaal* near the *Brittaniëhaven.* That means that for the *Brittaniëhaven w*ave penetration from the *Calandkanaal* into the *Brittaniëhaven* is limited to the redirection of wind waves generated on the *Calandkanaal*. Therefore the waves at the model boundary will have a low wave period. As short waves diffract less, wave penetration is likely to be minor compared to locally generated waves inside the harbour basin. Nonetheless the wave conditions at location '*HRextra Europoort63*', see Appendix G, are given in Table 5.2. These conditions relate to the most probable overtopping event being an event with a western wind direction.

Table 5.2: Wave conditions for the western wind direction at location 'HRextra Europoort63'

Return period T [years]	H_s [m]	$T_{m-1,0}$ [s]	Wind speed[1] [m/s]
1	0.26 [2]	1.5	18.0
2	0.24 [2]	1.5	16.7
5	0.31 [2]	1.6	20.6
10	0.35	1.7	22.4
20	0.39	1.8	24.5
50	0.44	1.9	27.0
100	0.48	2.0	29.0
200	0.52	2.0	30.7
500	0.56	2.1	32.5
1000	0.61	2.2	34.3
2000	0.64	2.2	35.5
4000	0.68	2.3	37.4

Remarks:
[1] The wind speed reducing effect of the *Calandbrug* wind shield of which the location is shown in Figure 5.2, is disregarded. This leads to an overestimation of the wave heights in the basin.
[2] Especially for low return periods many different combinations of variables can lead to a flood event with the same return period.

5.3. Flood risk analysis

Using the model set-up from the previous paragraph (5.2) a flood risk analysis is undertaken for the *Brittaniëhaven* case. It must be stressed that the influence of flooding from the *Hartelkanaal* is not taken into consideration. Especially for return periods larger than 1000 years this origin of flooding becomes dominant. In this analysis the influence of seiches has been disregarded. The occurrence of seiches is uncertain and their duration is small, such that their influence on the flood risk may be low (Botterhuis, Nicolai, & Stijnen, 2015). Paragraph 5.4.2 shows the influence of the occurrence of seiches on the flood risk in the *Brittaniëhaven*. It is shown that the flood risk may increase significantly if seiches occur. Further research on the occurrence of seiches and their influence on flood risk is therefore recommended.

For the western wind direction the results of the model analysis are shown in Figure 5.7 and Figure 5.8. Figure 5.7 shows the mean specific overtopping discharge (per unit width)(**MSOD**) for the considered quays which have been divided into four segments: segment 1 is the northern quay wall with an elevation of 3.4 m+NAP, the second segment contains the imaginary quays towards the higher elevation areas in the north, the third segment is the eastern slope and the final segment is the entire southern quay wall. Those segments are shown in Figure 5.6 below.

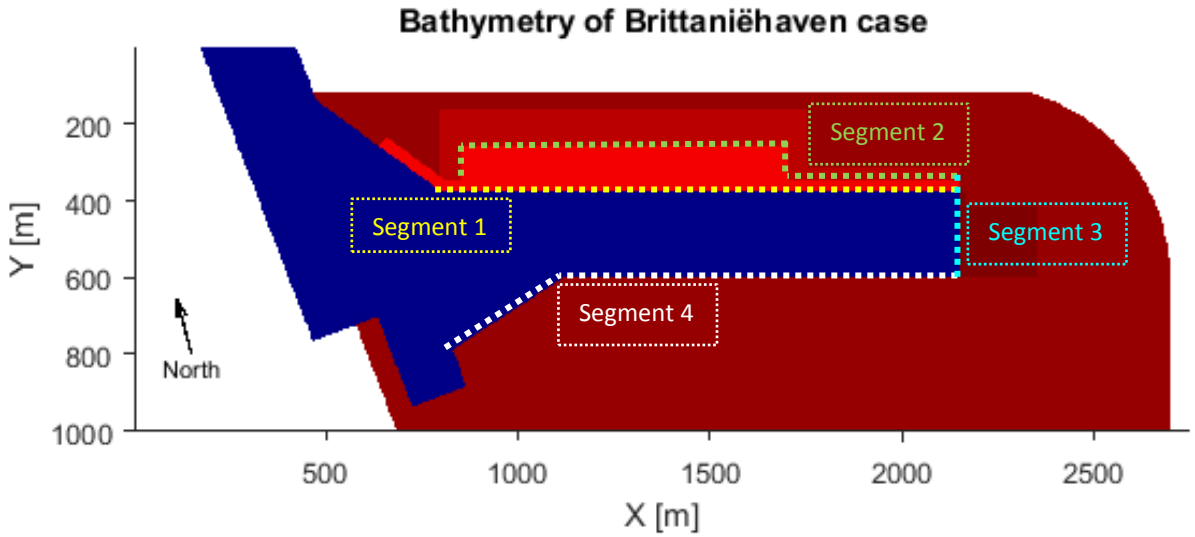

Figure 5.6: Quay wall segments of the *Brittaniëhaven*. The segments correspond to the segments of Figure 5.7

In Figure 5.8 the probabilities are approximated at which wave overtopping occurs and at which the MSOD exceeds the safety limit of 0.42 l/s/m and an arbitrary threshold level of 5 l/s/m^2. Those probabilities are equal to the intersections of the MSOD-lines with the horizontal lines in Figure 5.8. Comparing these figures with the figure from Slootjes & Wagenaar (2015), also shown in Figure 5.8, it appears that probabilities increase significantly when considering wave overtopping. Generally the probability of exceeding the safety level of 0.43 l/s/m is at least twice as large as the probability of 'inundation' as considered by Slootjes & Wagenaar (2015). The largest portion of the *Brittaniëhaven*

[2] The threshold level should be chosen with respect to the extent of flooding as a consequence of a certain overtopping discharge. In the context of this thesis it does not have a significant meaning. It is solely used as an indicative line to show the return period of an arbitrary, but significant overtopping discharge.

has an elevation of 5.3 m+NAP. When considering the influence of wave overtopping the probability of flooding of these areas might increase by a factor of 2.5 (>5.0 l/s/m) up to 5 (>0.43 l/s/m).

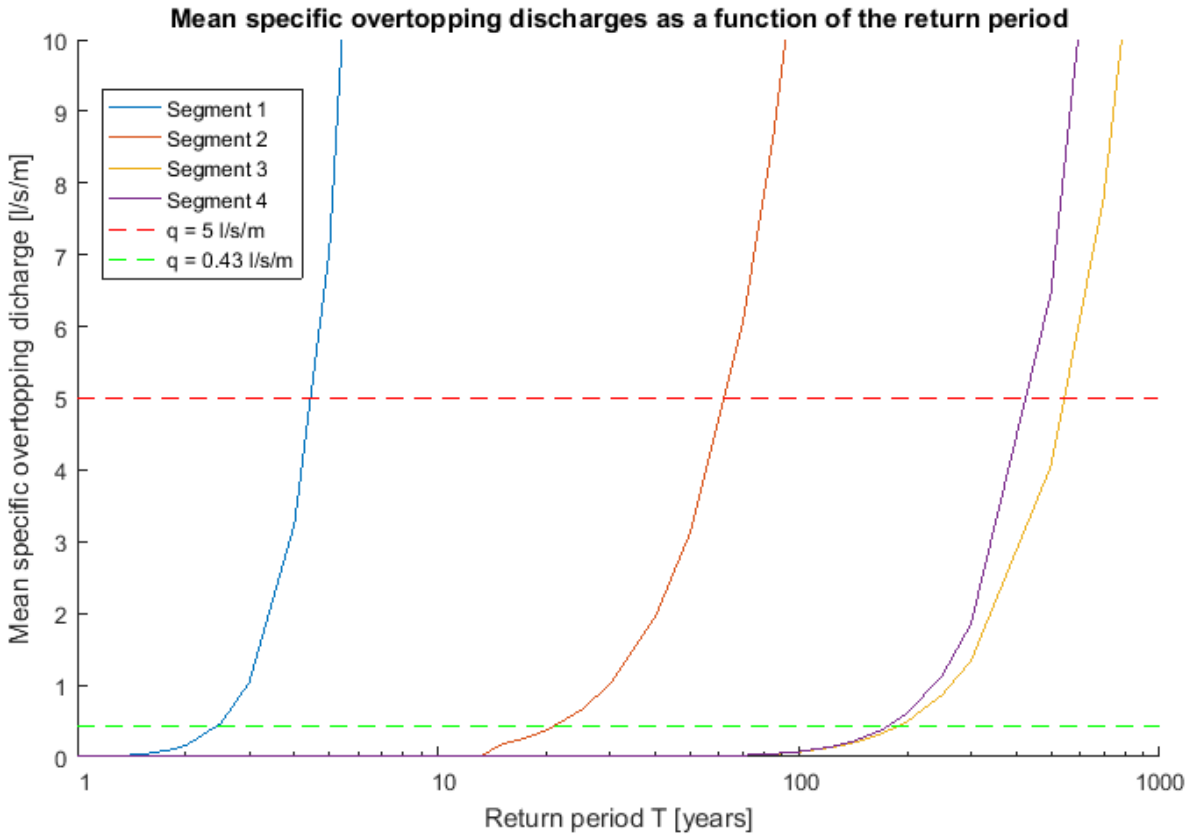

Figure 5.7: Mean specific overtopping discharge (MSOD) for the considered quay segments defined in Figure 5.6. The specific overtopping discharges along these segments have averaged to find the MSOD. Two safety levels have been plotted along the MSOD's: the safety limit of 0.42 l/s/m (De Gijt & Broeken, 2005) and a threshold level of 5 l/s/m.

However, these probabilities of flooding remain rough approximations. As mentioned the influence of flooding from the *Hartelkanaal* is disregarded. Furthermore uncertainties apply to the modelling approach itself and also to the input variables. An example of uncertainty in the input variables is the effect of the *Calandbrug wind shield* of which the location is indicated in Figure 5.2. This wind shield reduces the wind speeds occurring at certain return periods, thereby also decreasing the effect of wave overtopping on the probability of flooding.

Finally, it should be mentioned that the extent of flooding and inundation is not considered in this thesis. To be able to model this as well, another model or calculation is required in which the inflow volumes (overtopping discharges integrated over time) are translated to flooded area and inundation depths.

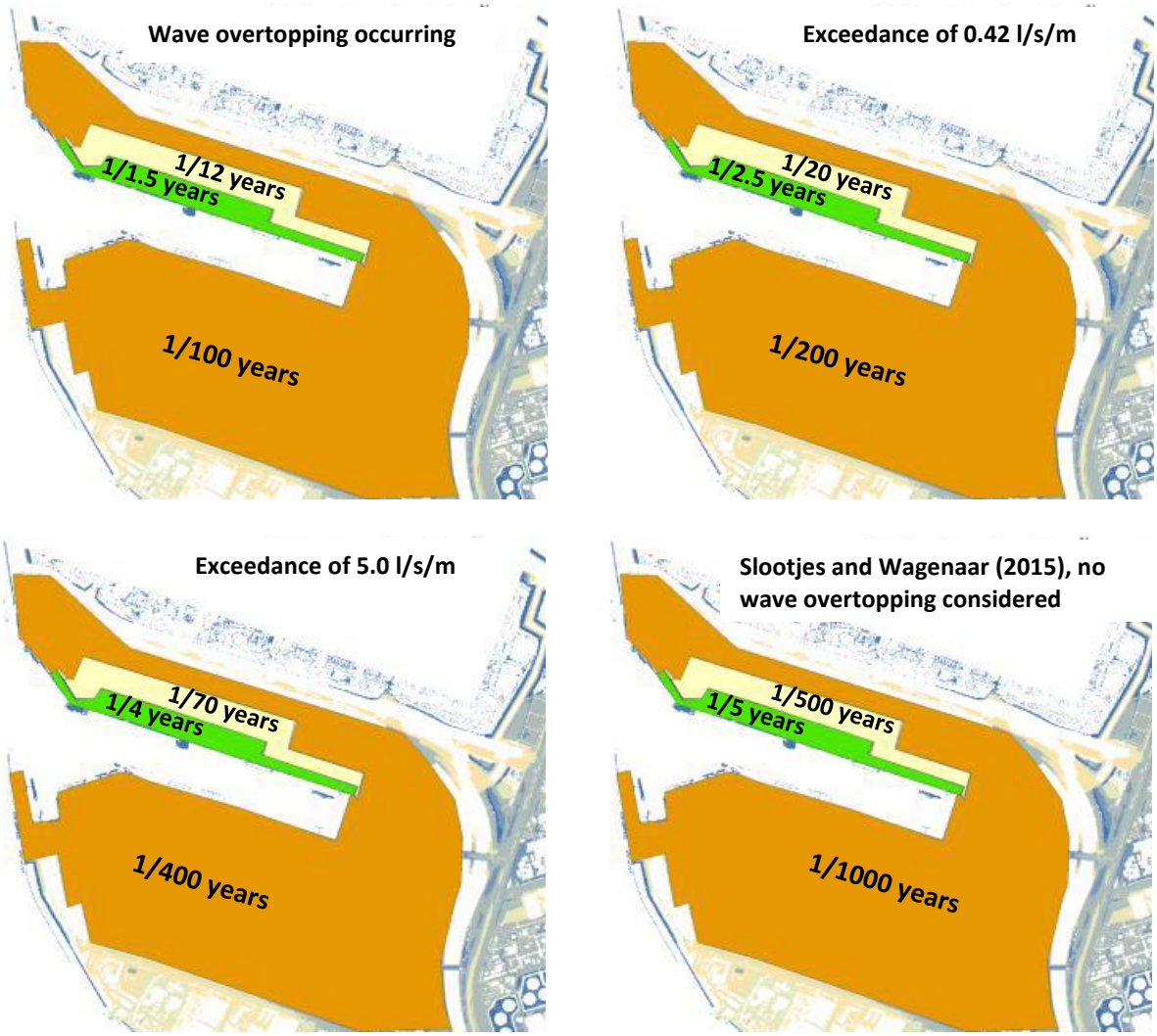

Figure 5.8: Approximated probability of wave overtopping occurring (top left figure) and of the MSOD exceeding the safety limit of 0.42 l/s/m (top right figure) and the threshold level of 5.0 l/s/m (bottom left figure). The bottom right figure is given by Slootjes and Wagenaar (2015) in which wave overtopping has been disregarded (see Figure 5.3)

5.4. Sensitivity analysis

In this section the sensitivity of the model is analysed with respect to model and input uncertainty. In the first paragraph (5.4.1) the outcomes are shown for cases where a different approach is undertaken. This may for instance concern the choice for a different empirical wave growth formula. The second paragraph (5.4.2) looks at the uncertainty concerned with the input variables. An example of this type of uncertainty is an increase or decrease of the wind speed by a certain factor.

5.4.1. Model uncertainty

This paragraph will analyse and discuss the uncertainty concerned with some aspects of the modelling approach. The following sources of uncertainty are analysed:

- Choice for a certain wave growth formula
- Uncertainty revolved around the EurOtop overtopping formula
- The approach at which the angle of incidence is applied in the overtopping formula
- Choice between the maximum fetch in a certain range and the effective fetch

All figures in this paragraph show the original MSOD (mean specific overtopping discharge) lines, see Figure 5.7, for the segments defined in Figure 5.6. The same calculation was performed but with the different modelling approach. The results of these calculations are illustrated by the dash-dotted lines. A graphical comparison between the two lines can both be done vertically or horizontally: a vertical comparison shows the difference in overtopping rates for a certain return period, while a horizontal comparison gives the difference in return periods for a specific MSOD. When the dash-dotted line is left of the original MSOD-line the flood risk is increased and vice-versa. The results of the model uncertainty analysis are summarized in Table 5.3 and Table 5.4 below. It can be seen that the uncertainty due to the methodology of the calculation of the wind waves is large for this specific case. By applying the method of the effective fetch instead of the maximum fetch the modelled return periods increase up to a factor 2.

Table 5.3: Return periods in years for the MSOD being larger than the safety limit of 0.42 l/s/m for the variation of modelling choices.

Return periods MSOD>0.42 l/s/m [years]		Segment 1	Segment 2	Segment 3	Segment 4
Wave growth formula	Bretschneider	2.5	20	200	200
	Young & Verhagen	3	40	300	400
Fetch	Maximum	2.5	20	200	200
	Effective	3	40	400	700
Overtopping formula	Original	2.5	20	200	200
	Design	2	12	120	120
Angle of incidence	Minimum	2.5	20	200	200
	Averaged	2.5	20	200	350

Table 5.4: Return periods in years for the MSOD being larger than the (arbitrary) threshold of 5.0 l/s/m for the variation of modelling choices.

Return periods MSOD>5.0 l/s/m [years]		Segment 1	Segment 2	Segment 3	Segment 4
Wave growth formula	Bretschneider	4	70	500	400
	Young & Verhagen	4	110	800	700
Fetch	Maximum	4	70	500	400
	Effective	5	110	>1000	>1000
Overtopping formula	Original	4	70	500	400
	Design	3	40	300	300
Angle of incidence	Minimum	4	70	500	400
	Averaged	4	70	500	>1000

Wave growth formula

To determine the significant wave height at a certain location use is made of the Bretschneider formula for wave growth (U.S. Army Coastal Engineering Research Center, 1975). This choice was made on the basis of conservativeness and as it is most often used in practice, see paragraph 4.3.1. Figure 4.2 in Paragraph 4.3.1 showed a model comparison between different wave growth formulas, in which it was shown that the Young & Verhagen formula (Young & Verhagen, 1996) deviates most from the other formulas in relatively deep water and for short fetches. To show the impact of the

choice for a certain formula, Figure 5.9 shows the results when the Young & Verhagen formula is applied. A lateral displacement of the MSOD lines can be seen, indicating a decrease in the overtopping discharges when the Young & Verhagen formula is applied. The Bretschneider is thus a conservative formula for this case, but the uncertainty is significant. Additional research on this topic may therefore be valuable as the flood risk could be lower when a different formula fits the local situation better.

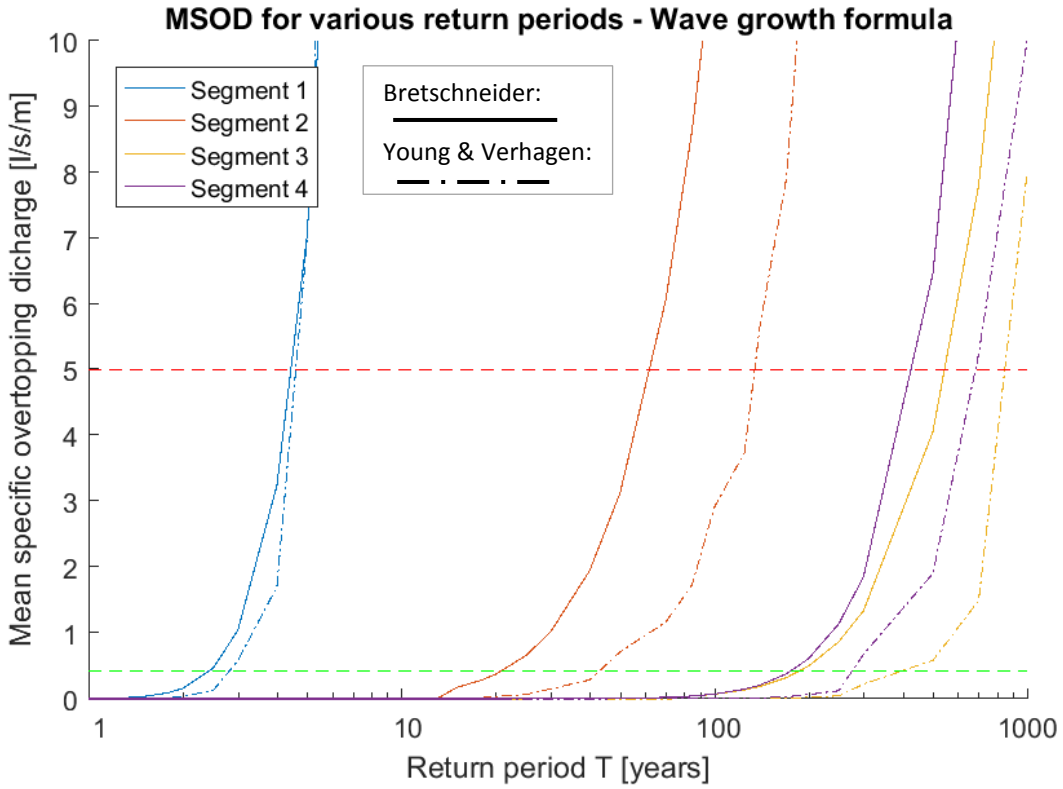

Figure 5.9: Uncertainty due to the choice for a wave growth formula. The dash-dotted lines show the MSOD-lines when the Young & Verhagen formula (see Equation 2-8 and Figure 4.2) is applied.

Maximum fetch vs. effective fetch

Figure 5.10 illustrates the differences between applying the effective fetch approach versus the maximum fetch approach. In Appendix G the fetches are illustrated for both approaches. The default option in the WGPO model is the maximum fetch in a 60 degree range around the principle wave direction (see section 4.3.1). The effective fetch is a weighted average of the fetches in the same 60 degree range. By definition the effective fetch is smaller than the maximum fetch. When applying the effective fetch lower wave heights will be found, which results in lower wave overtopping discharges. It can be seen that this effect is significant for larger waves which occur at larger return periods. By applying the maximum fetch instead of the effective fetch the conservativeness is guaranteed, but a possibly large overestimation of the flood risk is also evident (possibly by a factor 1.5 for segments 2, 3 and 4).

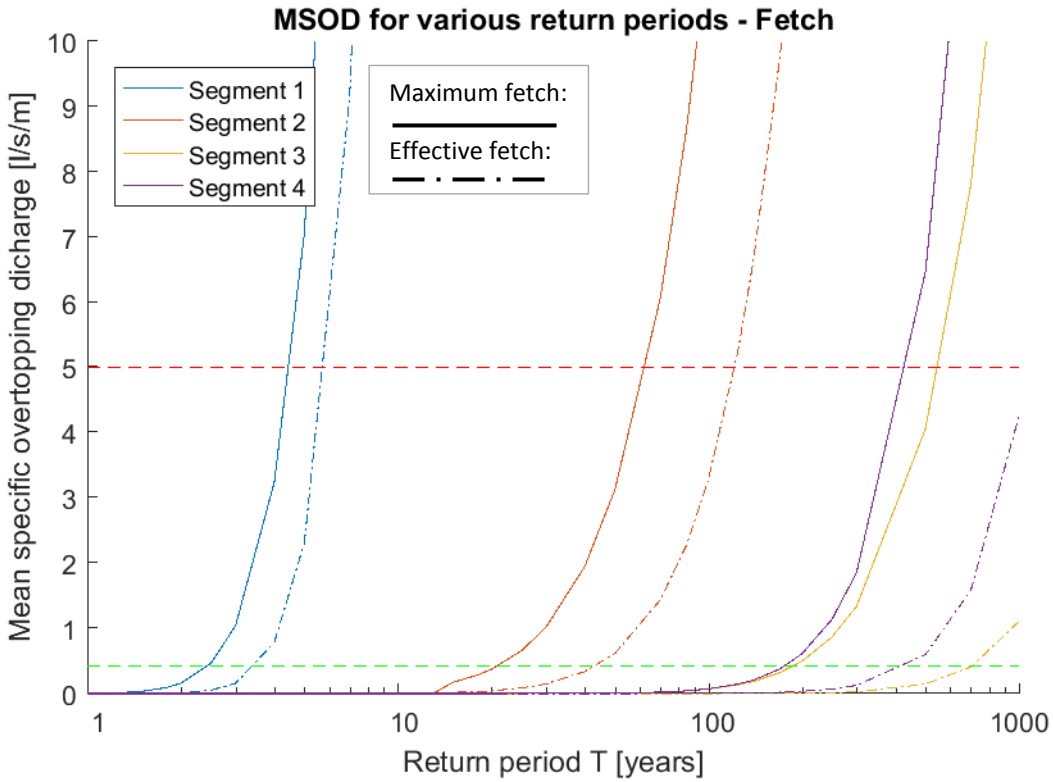

Figure 5.10: The uncertainty due to the choice for the effective fetch or the maximum fetch in a range of 60 degrees around the principle wind direction.

EurOtop overtopping formula

The EurOtop manual gives various overtopping formulae. In the second edition of the manual (EurOtop, 2016) one formula (see Equation 2-19) is valid for the entire range of conditions of overtopping over a vertical wall. However, this formula also deals with uncertainty. For design purposes EurOtop advises to use a formula in which the parameters have been changed by one standard deviation such that for the same conditions a larger overtopping discharge is found. Figure 5.11 shows the effect of this design formula on the final outcomes. Obviously the return periods become lower for a same value of the overtopping discharge. It can be seen that this effect slightly increases for larger waves and larger return periods (sector 3 and 4). This leads to the conclusion that under design conditions (often a large return period) the use of the design formula instead of the original formula is required.

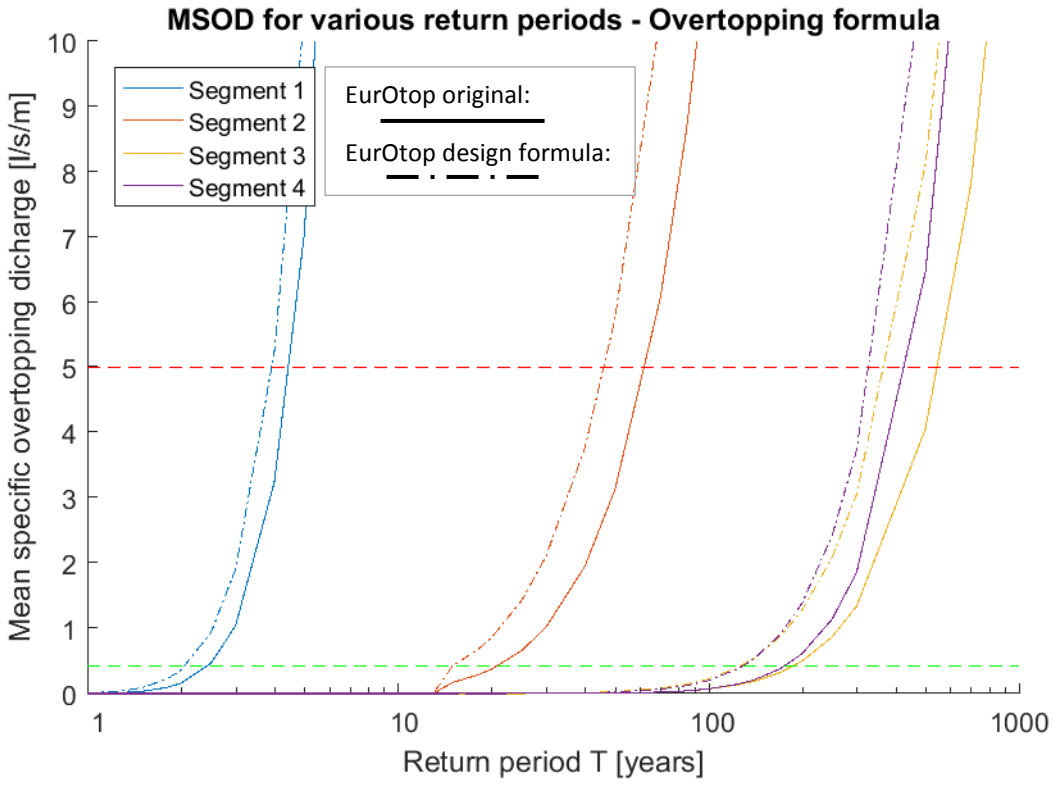

Figure 5.11: Uncertainty due to the wave overtopping formula in the EurOtop formulas (EurOtop, 2016). The manual gives formulas for design purposes in which the value of the parameters is increased by one standard deviation, see section 2.4 and Equation 2-19.

Method to determine the angle of incidence

As discussed in section 4.3.5 the smallest angle of incidence with respect to the quay wall of any wave component is taken. This angle β is independent of the angle of incidence of any other component. This choice was made as no research was undertaken on this specific topic. A form of averaging of the angles from different components was also opted (Van der Meer J. , Personal correspondence on the topic of varying angles of incidence, 2016). The weighted averaging, see paragraph 4.3.5, follows from the wave energy per component such that the largest component has the largest influence on the combined angle of incidence. The consequence of this alternative approach can be seen in Figure 5.12.

For the first three segments no large differences can be distinguished between the two approaches. This is because the local waves dominate over the penetrated waves and the wind direction has the smallest angle of incidence with the quays. The weighted angle of incidence is therefore close to the smallest angle of incidence. However, for segment 4 a large difference is found. The smallest angle of incidence is found for the penetrated waves. Averaging the angle with the wind component results in a much larger angle of incidence and subsequently lower overtopping rates. This leads to the conclusion that if one of the wave components (local waves, diffracted or transmitted waves) dominates over the other components a large overestimation of the wave overtopping discharges is made when applying the 'smallest angle approach'. However, due to the lack of research on the topic no conclusive recommendation can be done on which approach should be followed.

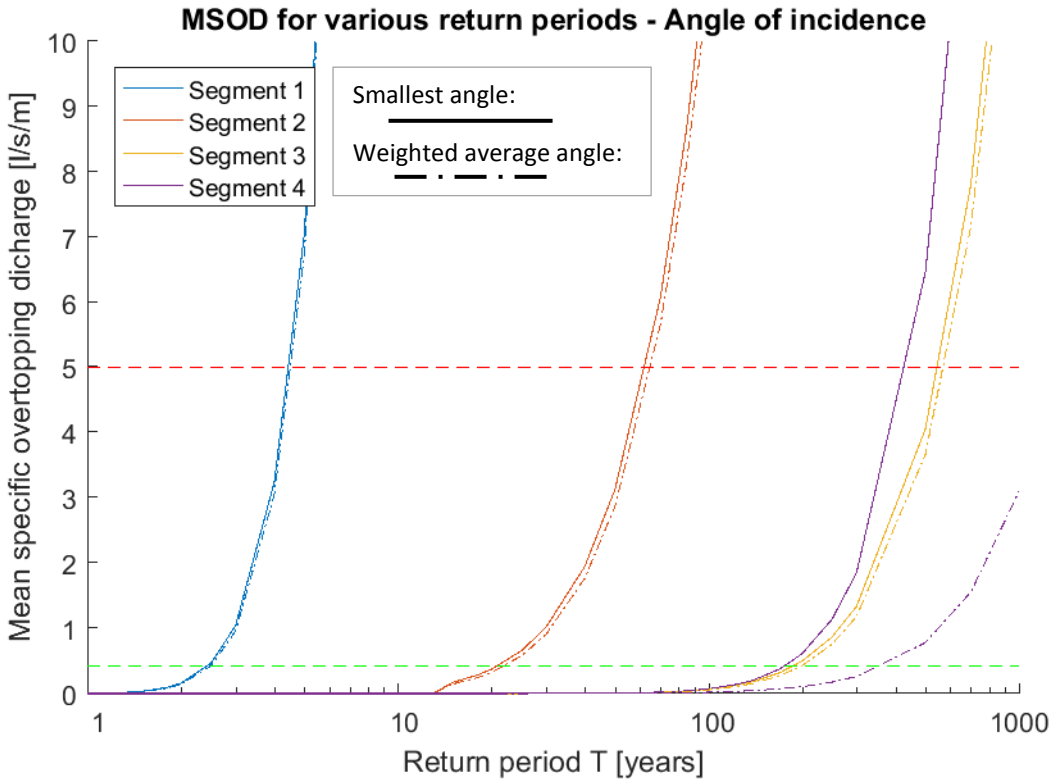

Figure 5.12: Uncertainty due to the lack of knowledge on the angle of incidence in the wave overtopping formula when the wave field contains multi-directional components.

5.4.2. Input uncertainty

Uncertainty in the input parameters will have a certain degree of influence on the flood risk of the harbour areas. This will give insight in the sensitivity of the model towards the input parameters. This may help evaluate the real flood risk in the harbour areas. An example is the influence of the *Calandbrug* wind shield of which the location is indicated in Figure 5.2. It Is unknown what the quantitative effect of the wind shield is on the local extreme wind conditions. But with this analysis it can be concluded whether the effect on the flood risk might be significant or not and would therefore be worthy of a more comprehensive analysis. The results for segment 3 are not included in the figures as these lines are fairly similar to the results for segment 4.

The sensitivity of the overtopping discharges to the following variables are tested:

- Local freeboard (structure height minus the still water level)
- Occurrence of seiches
- Wind speed
- Wind direction

The results of the uncertainty analysis are summarized in Table 5.5 and Table 5.6 below. It can be seen that the change in the return periods due to the possible occurrence of seiches may be the largest contributor to the uncertainty of the model outcomes.

Table 5.5: Return periods in years for the MSOD being larger than the safety limit of 0.42 l/s/m for the variation of the model parameters.

Return periods MSOD>0.42 l/s/m [years]		Segment 1	Segment 2	Segment 4
Local freeboard	-25%	1.5	12	80
	Default	2.5	20	200
	+25%	3	40	300
Occurrence of seiches	No seiches (default)	2.5	20	200
	Seiches	1.2	12	40
Wind speed	-25%	4	40	320
	Default	2.5	20	200
	+25%	1.5	12	80
Wind direction	225°N (SW)	3	30	900
	270°N (W, default)	2.5	20	200
	315°N (NW)	10	50	150

Table 5.6: Return periods in years for the MSOD being larger than the (arbitrary) threshold of 5.0 l/s/m for the variation of model parameters.

Return periods MSOD>5.0 l/s/m [years]		Segment 1	Segment 2	Segment 4
Local freeboard	-25%	3	30	200
	Default	4	70	400
	+25%	5	100	600
Occurrence of seiches	No seiches (default)	4	70	400
	Seiches	2	25	80
Wind speed	-25%	6	120	700
	Default	4	70	400
	+25%	3	30	200
Wind direction	225°N (SW)	5	80	>1000
	270°N (W, default)	4	70	400
	315°N (NW)	11	150	300

Local freeboard

It can be expected that a change in the freeboard has a fairly significant influence on the overtopping discharge and the corresponding MSOD lines. Figure 5.13 shows the influence the freeboard has on the MSOD lines. In this figure the local freeboard is increased and decreased by 25% (thus not by a standard value).

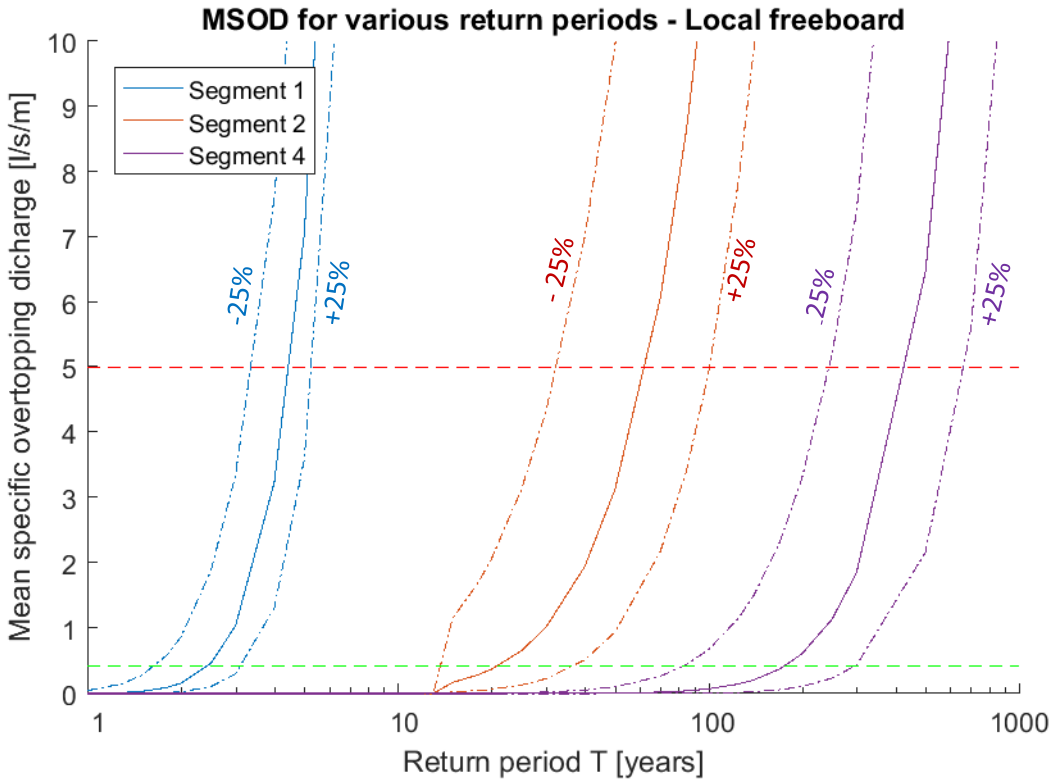

Figure 5.13: Variability of the MSOD lines as a consequence of a variation in the freeboard (structure height minus SWL). This variability in the freeboard may occur due to a change in the still water level as well as an uncertainty in the height of the quay walls. The '+25%' thus indicates a 25 percent increase of the local freeboard and not a 25% increase of the structure height or the SWL with respect to 0 m+NAP.

Occurrence of seiches

As mentioned in the paragraph on the flood risk analysis (5.3) the occurrence of seiches is uncertain as well as their influence on the flood risk. Due to their little duration they are sometimes neglected. However, Figure 5.14 and Figure 5.15 show that as a consequence of neglecting seiches, flood risk may be underestimated. Figure 5.14 shows the MSOD (mean of all segments) as a function of time if a seiche is imposed with a period of 20 minutes and an amplitude of 0.46 meters (conditions at T=2 years). It shows that the time-averaged overtopping discharge is dominated by the high peak at the top of the seiche signal. This peak is caused by the nonlinear relation between the freeboard and the overtopping discharge.

The MSOD-lines in Figure 5.15 have been constructed using the (nett) seiche amplitudes which can be derived from

Table 5.1. Looking at these MSOD-lines it can be concluded that the overtopping discharges increase significantly when seiches would occur. The decrease in return periods is of a factor 2 to up to a factor 5. The results from this analysis show the importance of further research on the topic of seiches.

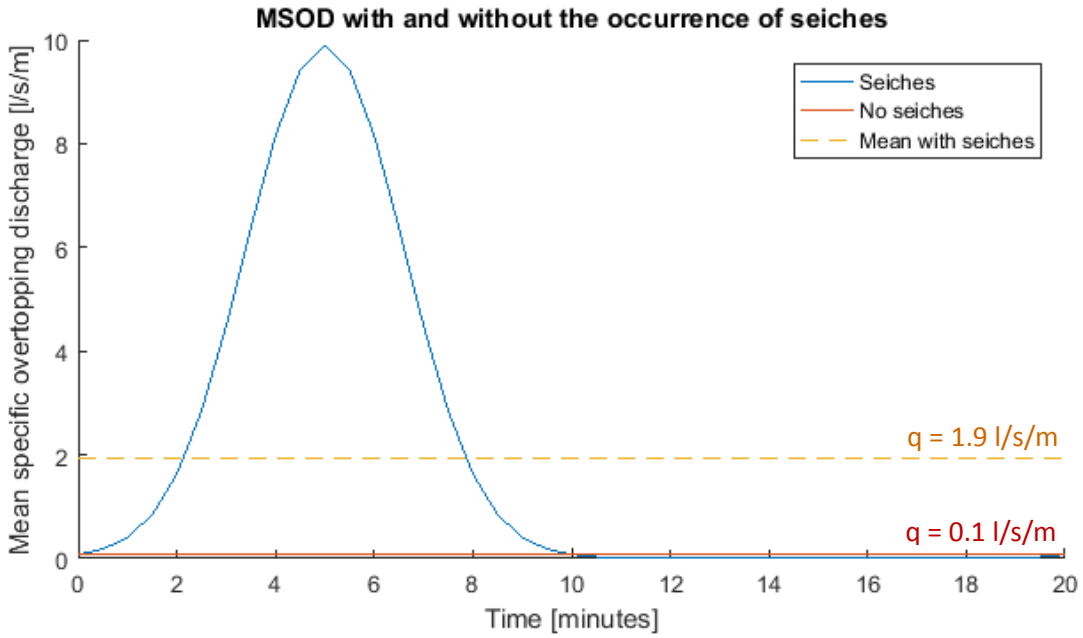

Figure 5.14: The mean specific overtopping discharge in time for the entire basin based on the parameter settings at return period T = 2 years, see

Table 5.1 and Table 5.2. A sinusoidal seiche signal with a period of 20 minutes and an amplitude of 0.46 meters is imposed.

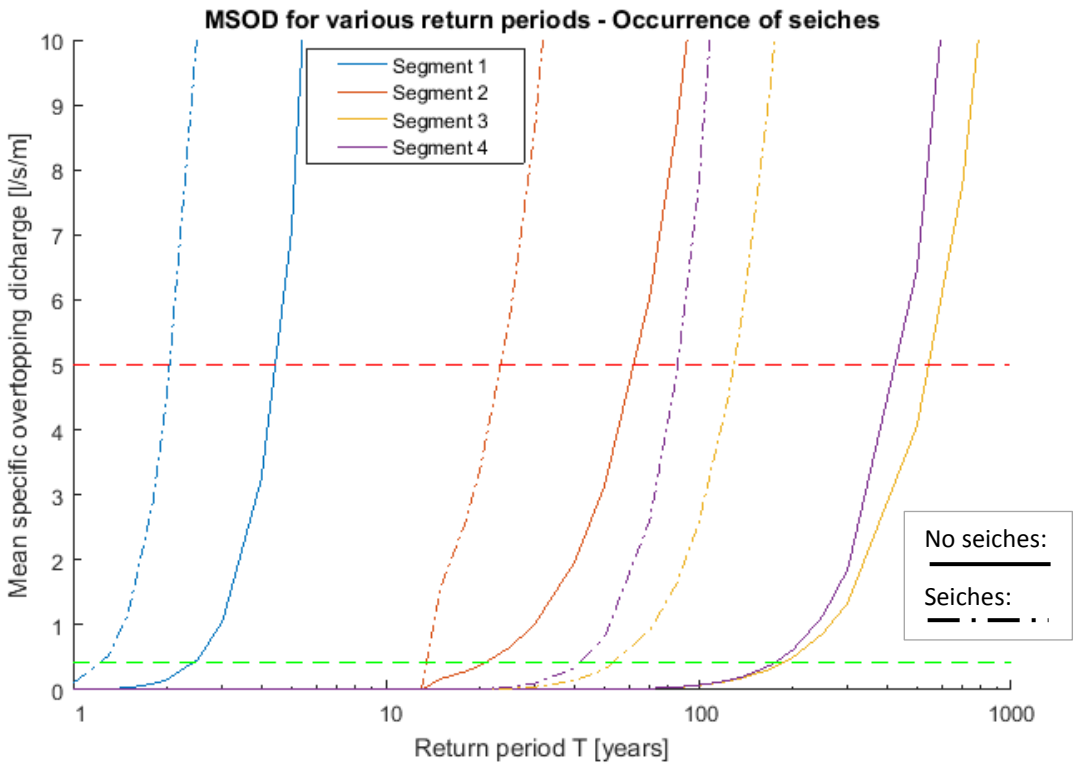

Figure 5.15: MSOD lines for the occurrence and non-occurrence of seiches. For the model runs in which seiches occur, the MSOD has also been time-averaged over one period of the seiche.

Wind speed

The sensitivity of the overtopping discharges towards the wind speed is due to the increasing height of the locally generated waves. This sensitiveness is illustrated in Figure 5.16. This figure shows a large spread in the return periods for a certain overtopping discharge, e.g. for segment 2 the return period of a MSOD of 5 l/s/m varies between 30 and 110 years. A cause of this large spread is the highly nonlinear relation between the overtopping discharge and the wave height in the EurOtop overtopping formula (see Equation 2-19).

Uncertainty in the wind speed may originate from the probabilistic combination of variables (as is the basis of Table 5.2) as well as the physical situation. In this case of the *Brittaniëhaven* the effect of the *Calandbrug* wind shield on the wind speed is ignored. From Figure 5.16 it can be concluded that this wind shield could have a significant effect on the amount of wave overtopping in the *Brittaniëhaven*.

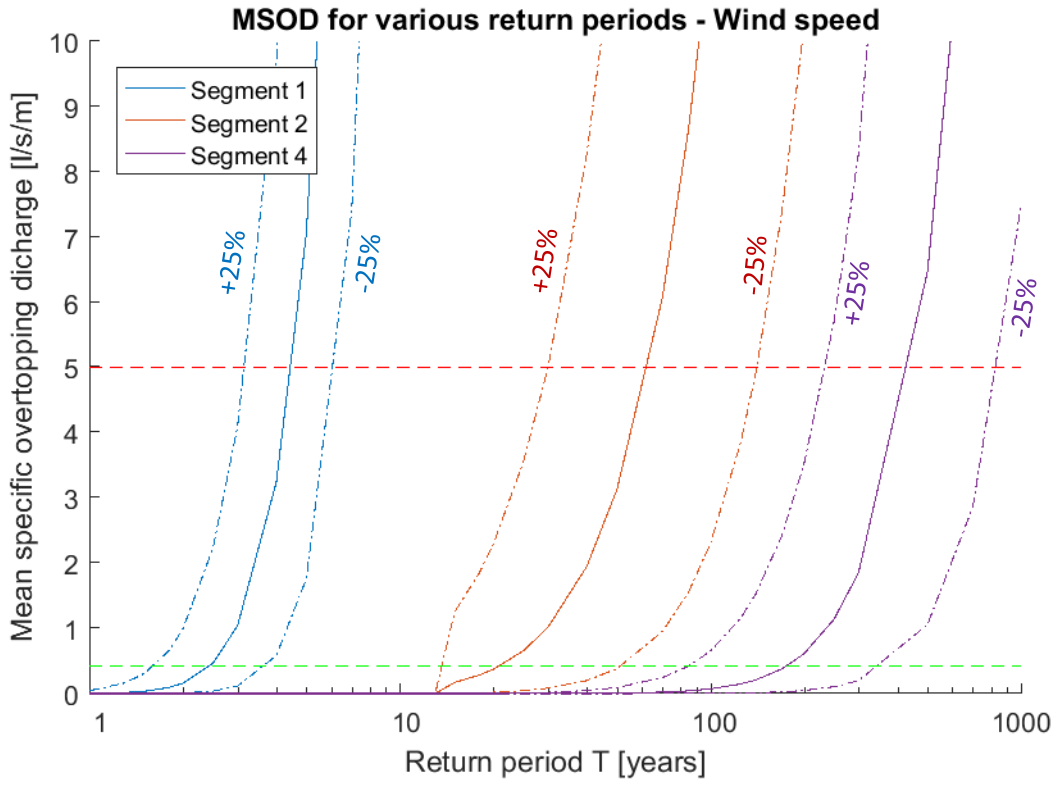

Figure 5.16: Variability of the MSOD lines as a consequence of a variation in the wind speed. The figure shows the results when the wind speeds are 25% lower and higher with respect to the original situation as given in Table 5.2.

Wind direction

The impact of a change in the wind direction on the overtopping discharges is very location dependent. Figure 5.17 at least shows that the wind direction may have a significant influence. To create this figure the parameter settings for the default western wind direction were kept for the calculation with a southwestern and northwestern wind direction. Obviously, these values change in reality. The figure shows that an analysis for a singular (dominant) wind direction may be an inadequate approach to determine the flood risk. Instead multiple wind directions must be accounted for.

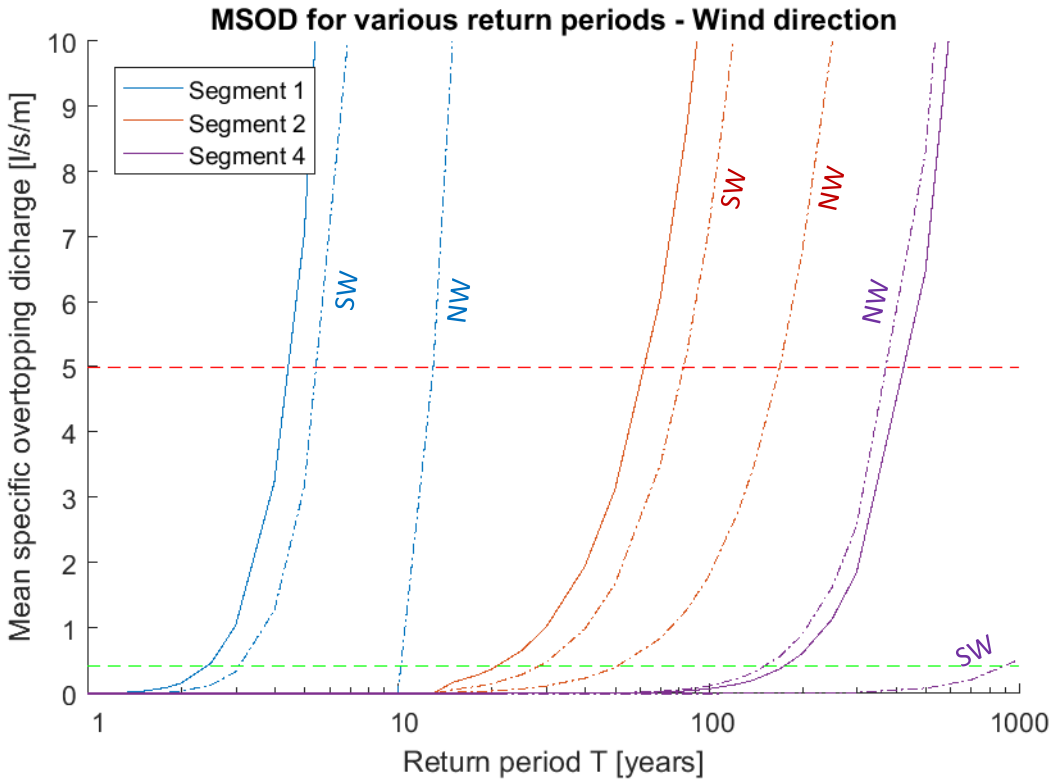

Figure 5.17: Variability of the MSOD lines as a consequence of a variation in the wind direction. In this analysis the change in values of the boundary conditions is disregarded (e.g. no change in the wind speed).

6. Discussion, conclusion and recommendations

This chapter consists of a discussion, a conclusion and a set of recommendation with regards to the methodology by which wave overtopping can be modelled in a harbour area. Thereby a conclusion will be drawn with respect to the main research of this model:

What is the best approach to model wave overtopping in a harbour area under the influence of wave penetration and local wave generation and how does it affect flood risk?

The analysis of the subject and the gathered results will be discussed and reflected. This will lead to a set of recommendations on how to deal with wave overtopping in harbour areas in future research.

6.1. Discussion

In this thesis a method has been developed with which wave overtopping in harbour areas can be modelled: the **W**ave **G**eneration **P**enetration **O**vertopping model. However, many assumptions stood at the base of this model. Many of these assumptions are up for discussion.

The choice was made to develop a new semi-empirical and deterministic model (Chapter 3). This choice was mainly based on the current limitations of numerical models. On the one hand some numerical models are not (sufficiently) capable of modelling the most essential processes, such as wave overtopping (e.g. SWASH). On the other hand the numerical models which can actually model the most relevant processes require too much computational effort (a SPH solver for example). In the ongoing improvements of models and computer power these limitations might vanish. Therefore it must be stressed that a reconsideration of the assessment criteria is likely to be necessary in the future.

The developed WGPO model is currently only applicable for relatively simple harbour geometries. Improvements to the WGPO model or the development of a new method are required to deal with complex geometries. An example of such a geometry is the harbour of IJmuiden (see Figure 6.1). It is expected that wave overtopping may also have a significant influence on the flood risk in this harbour.

Figure 6.1: Sea harbour of IJmuiden where wave overtopping might also have a significant influence on flood risk (Google Maps, 2016)

With regards to the model itself, the assumptions which stand at the base of the model might lead to inaccuracies in the results. Several processes are neglected or simplified. Many of these simplifications are suspected to lead to more conservative approximations. The main exception is the process of wave reflection. By disregarding the effect of wave reflection inside the harbour areas an overall underestimation of the wave heights and the wave overtopping is possible.

6.2. Conclusion

A theoretical study on wave propagation, wave transformation, wave energy dissipation and structure-induced wave processes showed the large amount of phenomena that should be accounted for. The most influencing processes for the wave field inside the harbour are wave diffraction, local wind-wave generation, wave transmission and wave reflection. With the purpose of this thesis to quantify wave overtopping discharges, this process is obviously the most relevant process.

It appeared that no single modelling approach was able to account for every process within the limits of practicality. These practicality limits include the easiness to use the approach and the interpretability of the results. Within these practical limits the nonlinear and non-hydrostatic numerical wave model SWASH had the most potential. It has been successfully applied for studies on wave penetration into harbours prior to this thesis. However, a clear limitation to SWASH within the scope of this thesis is the current inability to model wind-wave generation. Furthermore it appeared that SWASH had difficulties to model wave overtopping accurately: amongst others, instabilities arose for cases of relatively large waves or relatively large freeboards. More complex and comprehensive numerical models should be able to model all the processes well. However, such models have never been applied on the scale of a harbour. Therefore they were not considered to be suitable.

Instead a non-numerical method is employed. This method is developed in line with the manual *'Golfbelasting in havens en afgeschermde gebieden: een eenvoudige methode voor het bepalen van golfbelastingen voor het toetsen van waterkeringen'* (Rijkswaterstaat, 2014). A critical review of this method lead to some different modelling choices. The considered processes in the model are local wave generation, wave diffraction and transmission and wave overtopping. Other processes were concluded to be irrelevant for a simple, conservative analysis in the considered harbour cases. The modelling of these processes all followed an analytical or empirical approach. Where necessary, conservative assumptions were taken.

Wave overtopping was quantified via an empirical formula with input of the wave height, freeboard and angle of incidence. No prior research on wave overtopping from wave components with different spatial directions has been undertaken. It is therefore unknown how the overtopping rate depends on the various directions in the combined wave field. For the sake of conservativeness the smallest occurring angle of incidence of any wave component is applied in the model.

The developed WGPO model is able to model the wave field and wave overtopping discharges in any harbour with a relatively simple geometry. In principal no reflection and multiple diffraction may occur. It is expected that the wave overtopping rate estimations are valid even in cases of reflection, as long as the reflection does not lead to an increase of wave energy at an opposing quay wall. However, this surmise is not verified within the scope of this thesis.

The proposed method can be a supportive and simple tool. Its results may help in the assessment of the flood risk of harbour areas. Expert judgement will however always be required to verify the results. Future improvements to the method could be found in the handling of the individual processes and the interaction between the processes. Such improvements could also be reached by

the partly application of a numerical model, see the recommendations. However, while this would likely increase the accuracy of the results, it will also increase the complexity of the model.

For the case of the *Brittaniëhaven* it was shown that wave overtopping is likely to have a significant influence on the probabilities of flooding. The modelled probabilities of flooding are (at least) a factor two higher than the case in which wave overtopping is disregarded. With increasing probabilities of flooding, flood risk rises as well. This case study shows the necessity of taking into account wave overtopping in a flood risk analysis.

Under the influence of future sea level rise the topic of wave overtopping becomes even more relevant. As water levels approach elevation levels of unembanked areas the frequency of wave overtopping events will see a large increase. This increases the relevance to be able to predict overtopping discharges (more) accurately. Future research on this topic is therefore strongly recommended.

6.3. Recommendations

This paragraph will give recommendations for updates of the WGPO model and for future developments of a new method. Whether the preference is given to improvements of current methods or the development of a new method mainly depends on the future capabilities of numerical models, as was discussed in paragraph 6.1. Furthermore additional research is recommended on some specific topics.

One of the most important recommendations is to gather more wave data for port applications. This would require the organization of extensive measurement campaigns. Currently a lot of wave measurements in harbour areas are not openly available. The availability of the measurements is relevant for future research on the topic of flood risk in harbour areas, because it enables improvements and developments of models.

The list below gives the recommendations on possible improvements and developments of the WGPO model:

- Carry out additional case studies to gain practical knowledge on the topic of wave overtopping in harbours. It can be expected that wave overtopping has a different contribution to flood risk for different harbour areas; e.g. where the occurrence of high wave heights is possible, the contribution of wave overtopping is large. Furthermore this will also help validating the model.
- Perform a study in which the wave height distribution of the WGPO model is compared to a numerical model simulation of wave penetration for several harbour geometries. This allows for a clearer formulation of the accuracy and the applicability range of the WGPO model.
- The current WGPO model does not include time-dependency of the input parameters. If this time-dependency is added more insight is gained into the total contribution of wave overtopping to the flooding of the harbour areas. This also allows for modelling the inundation of the harbour areas using another model (e.g. SOBEK), as the overtopping rate in time is a boundary condition for the model.
- Investigate whether it is possible to use the model for more complex geometries. Reijmerink (2012) has shown that the 'RIKZ method' is still able to give a rough prediction of the wave heights in such complex geometries, see paragraph 4.4 and 0. Reijmerink used a 'train-like'

approach in which a harbour is divided into sub-sections. The method is then applied to find the wave conditions in every sub-section. This approach may also be useful for the WGPO model.

The list below gives recommendations with regards to the development of a new (numerical) approach to model wave overtopping in harbour areas:

- Investigate the advantages of using a numerical model to determine the wave heights inside the basin. Depending on the gained accuracy compared to the WGPO model (or any other non-numerical method), it could be opted to focus on the development of a new numerical method.
- Specifically on the nonlinear and non-hydrostatic model SWASH:
  - Further explore the abilities and inabilities of SWASH with regards to wave overtopping over vertical structure. Appendix C showed the results of an initial study on the validity of SWASH for overtopping scenarios. It appeared that instabilities arose for several sets of conditions. It appeared difficult to find the exact source of the instabilities and when they would actually appear. In future developments of SWASH it could then be possible to extend the stability limits of SWASH.
  - Currently a rectilinear or a curvilinear grid (or a combination of the two) are the only possible grid lay-outs in SWASH. Specifically for a harbour case it would be worthwhile if a more flexible grid could also be applied. However, in a broader context it is difficult to assess the value of this comprehensive update.

Finally, in the list below gives some general recommendations and suggestions for future research on topics that were dealt with in this thesis, but may require additional research.

- Currently, no numerical model is available which can model all relevant processes within the limits of computational capabilities. This means that at least two models are required to model both the amount of wave overtopping and the subsequent flooding and inundation (which can be modelled by SOBEK 2D for example). Boundary conditions are required at the intersection of the two models which describe the ingoing (into the hinterland) and outgoing (back into the harbour) discharges. Little is known about the outgoing discharge or in other words the flow back fraction. To a large extent this flow back fraction determines the degree of inundation of the hinterland. Therefore it is strongly recommended to gain insight in this mechanism.
- In a personal surmise of the author of the thesis it was stated that the interaction between wave diffraction and wave transmission is taken into account incorrectly in the RIKZ method (see 4.3.4). In the current method an underestimation of the wave energy in the non-shadow zone of a harbour might be possible. It is suggested to investigate this interaction between the wave diffraction and transmission analytically (linearized components) and numerically.
- The EurOtop formulas used in this thesis currently do not have a straight-forward procedure of taking into account the varying directions of a multi-directional wave field when determining the overtopping rates (see 4.3.5). It is suggested to study the associated influence factor γ_β for such a multi-directional wave field.
- In the case study it was shown that seiches could have a significant influence on the flood risk. Therefore, their limited duration should not be a reason to exclude them from a flood risk analysis in advance. It is recommended to analyse the flood risk in a harbour area including the effect of wave overtopping as well as the possible occurrence of seiches.

Bibliography

Alabart, J., Sánchez-Arcilla, A., & Van Vledder, G. (2014). Analysis of the performance of SWASH in harbour domains. *3rd IAHR Europe Congress.* Porto, Portugal.

ANP. (2016). Het Noordereiland in Rotterdam. Retrieved January 12, 2017, from http://www.ad.nl/rotterdam/zandzakken-voor-bewoners-van-noordereiland~a4652703/

ANP. (N.D.). Botlekgebied. Retrieved May 24, 2016, from http://www.ad.nl/ad/nl/1038/Rotterdam/article/detail/3674039/2014/06/17/Stank-in-Spijkenisse-na-stroomstoring-Botlek.dhtml

Benítez, J., & Mercado-Irizarry, A. (2015). *Storm surges in Puerto Rico*. (University of Puerto Rico) Retrieved from Coastal hazards: http://coastalhazards.uprm.edu/?Puerto_Rico_Maps:P.R._Storm_Surge_KMZ_2015

Boeyinga, J. (2010). *Boussinesq-type wave modelling in port applications.* TUDelft.

Bottema, M., & Van Vledder, G. (2008). Effective fetch and non-linear four-wave interactions during wave growth in slanting fetch conditions. *Coastal Engineering, 55*, pp. 261-275.

Botterhuis, T., Nicolai, R., & Stijnen, J. (2015, October 16). Methode combineren inundatiekaarten Botlek als gevolg van hoogwater op Nieuwe Waterweg, Calandkanaal en Hartelkanaal. HKV lijn in water.

Breugem, W., & Holthuijsen, L. (2007, May 1). Generalized Shallow Water Wave Growth from Lake George. *Journal of Waterway, Port, Coastal and Ocean engineering, 133*(3), 173-182.

Chbab, H. (2012). *Achtergrondrapportage hydraulische belasting voor de Benedenrivieren.* Deltares. Rijkswaterstaat.

De Gijt, J., & Broeken, M. (2005). *Handbook of quay walls* (First edition ed.). Rotterdam: Centre for Civil Engineering Research and Codes (CUR).

Deltacommissaris. (2016). *Waterveiligheid in buitendijks gebied.* Deltaprogramma 2017. Retrieved from https://www.deltacommissaris.nl/deltaprogramma/documenten/publicaties/2016/06/13/waterveiligheid-in-buitendijks-gebied

Deltares. (2008). *Triton 1.0 - User and technical manual.* Delft: Deltares.

Deltares. (2010). *Overtopping Neural Network*. Retrieved from http://v-das001.deltares.nl/Overtopping/disclaimer.aspx

Deltares. (N.D.). *PHAROS*. Retrieved June 1, 2016, from Deltares Software: https://www.deltares.nl/en/software/pharos/

Demirbilek, Z., & Panchang, V. (1998). *CGWAVE: A Coastal Surface Water Wave Model of the Mild Slope Equation.* U.S. Army Corps of Engineers.

DHI Group. (N.D.). *MIKE 21 Wave Modelling: short description.* Hørsholm, Denmark.

Duits, M., & Kuijper, B. (2012). *Gebruikershandleiding Hydra-Zoet.* HKV Lijn in Water.

Dusseljee, D., Klopman, G., Van Vledder, G., & Riezebos, H. (2014). Impact of harbor navigation channels on waves: a numerical modelling guide. *34th International Conference on Coastal Engineering.* Seoul, South Korea.

Elshof, A. (2014). *Basisdocument Deltaprogramma Nieuwbouw en Herstructurering Buitendijkse Gebieden.* Elshof Advies.

Enet, F., Nahon, A., Van Vledder, G., & Hurdle, D. (2006). Evaluation of diffraction behind a semi-infinite breakwater in the SWAN wave model. *9th International Workshop on Wave Hindcasting & Forecasting.* Victoria, B.C. Canada: Alkyon Hydraulic Consultancy & Research.

EurOtop. (2016). *Manual on wave overtopping of sea defences and related structures; An overtopping manual largely based on European research, but for worldwide application.* Van der Meer, J.W., Allsop, N.H.W., Bruce, T., De Rouck, J., Kortenhaus , A., Pullen, T., Schüttrumpf, H., Troch, P., Zanuttigh, B.,. Retrieved from www.overtopping-manual.com

Flow Science. (N.D.). *FLOW-3D.* Retrieved from https://www.flow3d.com/home/products/flow-3d

Gemeente Rotterdam. (2016). *Tussenresultaten Pilot Waterveiligheid Botlek.* Rotterdam. Retrieved from http://www.rotterdam.nl/fase1afgerond

Gesteira, M., Rogers, B., Dalrymple, R., Crespo, A., & Narayanaswamy, M. (2010). *User Guide for the SPHysics code.*

Gingold, R., & Monaghan, J. (1977, November). Smoothed particle hydrodynamics - Theory and application to non-spherical stars. *Monthly Notices of the Royal Astronomical Society, 181*, 375-389.

Goda, Y., Takayama, T., & Suzuki, Y. (1978). Diffraction diagrams for directional random waves. *19th International Conference of Coastal Engineering*, (pp. 628-650). Hamburg.

Goda, Y., Takeda, H., & Moriya, Y. (1967). *Laboratory Inverstigation on Wave Transmission over Breakwaters.* Port an harbour research institute, Hydraulic Engineering Division.

Google Maps. (2016). Retrieved from https://www.google.nl/maps/@51.861189,4.3806248,10.75z

Gruwez, V., Bolle, A., Verwaest, T., & Hassan, W. (2011). Numerical and physical modelling of wave penetration in Oostende Harbour during severe storm conditions. *5th International Short Conference on Applied Coastal Research.* Aachen, Germany.

Guillou, N. (2014, May 15). Wave-energy dissipation by bottom friction in the English Channel. *Ocean Engineering, 82*, pp. 42-51.

Hasselmann, K. (1974, March). On the spectral dissipation of ocean waves due to white capping. *Boundary-Layer Meteorology, 6*(1), pp. 107-127. doi:10.1007/BF00232479

Heuts, R. (2010). *Port Design - Nador.* Arcadis/TUDelft.

Holthuijsen, L. (2007). *Waves in Oceanic and Coastal waters.* Delft: Cambridge University Press.

Honda, T., Wellens, P., & Van Gent, M. (2011). Numerical Simulations for Wave Overtopping by Irregular Waves.

Hughes, S. (1993). *Physical Models and Laboratory Techniques in Coastal Engineering.* Singapore: World Scientific.

IH Cantabria. (N.D.). *IH2VOF*. Retrieved from http://ih2vof.ihcantabria.com/

Kahma, K., & Calkoen, C. (1992, December). Reconciling Discrepancies in the Observed Growth of Wind-generated Waves. *Journal of Physical Oceanography, 22*, pp. 1271-1285.

KNMI. (2015). *KNMI '14, klimaatscenario's voor Nederland.*

Kofoed-Hansen, H., Kerper, D., Sørensen, O., & Kirkegaard, J. (2005). Simulation of long wave agitation in ports and harbours using a time-domain Boussinesq model. *Fifth International Symposium on Ocean Wave Measurement and Analysis.* Madrid, Spain.

Lucy, L. (1977, December). A numerical approach to the testing of the fission hypothesis. *Astronomical Journal, 82*, 1013-1024.

Ma, G., Kirby, J., & Shi, F. (2014). *Non-Hydrostatic Wave Model NHWAVE - Documentation and user's manual.* Center for Applied Coastal Research; University of Delaware.

MathWorks. (2017). *Matlab*. Retrieved from https://mathworks.com/products/matlab.html

Miles, J. (1957, November). On the generation of surface waves by shear flows. *Journal of Fluid Mechanics, 3*(2), 185-204. doi:http://dx.doi.org/10.1017/S0022112057000567

Nederpel, A., & Van Balen, W. (2015). *Bureaustudie ter validatie van golfgroeiformules voor gelimiteerde strijklengte.* HKV Lijn in Water.

Nicolai, R., Van Vuren, S., Pleijter, G., Huizinga, J., Koks, E., & De Moel, H. (2016). *Pilot Waterveiligheid Botlek; Kwantitatieve analyse overstromingsrisico's.* Rotterdam: HKV Lijn in Water & Vrije Universiteit Amsterdam.

Philips, O. (1957). On the generation of waves by turbulent wind. *Journal of fluid mechanics, 2*(5), 417-455.

Pieterse, N., Knoop, J., Nabielek, K., Pols, L., & Tennekes, J. (2009). *Overstromingsrisicozonering in Nederland.* Den Haag: Planbureau voor de Leefomgeving.

Planbureau voor de Leefomgeving. (2009). Overstromingsgevoelig gebied 2005. Retrieved from http://www.pbl.nl/infographic/overstromingsgevoelig-gebied-2005

Reijmerink, S. (2012). *Golfrandvoorwaarden in havens; Bruikbaarheidsgrenzen voor (numerieke) modellen.* Delft: TU Delft.

Rijksoverheid. (2009). *Nationaal Waterplan 2009-2015.* Retrieved May 24, 2016, from https://www.rijksoverheid.nl/documenten/rapporten/2009/12/01/nationaal-waterplan-2009-2015

Rijksoverheid. (2015). *Nationaal Waterplan 2016-2021.* Minisiterie van Infrastructuur en Milieu. Retrieved from http://www.helpdeskwater.nl/onderwerpen/wetgeving-beleid/nationaal/nationaal-waterplan/

Rijkswaterstaat. (1996). *Hydraulische randvoorwaarden voor primaire waterkeringen.* Den Haag: Ministerie van Verkeer en Waterstaat.

Rijkswaterstaat. (2012, July). Waterveiligheid Buitendijks. Retrieved May 23, 2016

Rijkswaterstaat. (2014). *Golfbelasting in havens en afgeschermde gebieden: een eenvoudige methode voor het bepalen van golfbelastingen voor het toetsen van waterkeringen.* Update from RIKZ (2004), version 3, Lelystad.

Rijkswaterstaat. (2015). *Deltaprogramma 2015; Werk aan de delta.*

Rijkswaterstaat. (N.D.). *Seiches verwachtingen*. Retrieved July 18, 2016, from Waterberichtgeving RWS: https://waterberichtgeving.rws.nl/nl/projecten_seiches.htm

Slootjes, N., & Wagenaar, D. (2015). *Potentiële inundatie Botlek.* Delft: Deltares.

Smit, P., Stelling, G., Van Thiel de Vries, J., McCall, R., Van Dongeren, C., Zwinkels, C., & Jacobs, R. (2010). *XBeach: Non-hydrostatic model.* Deltares.

Stratigaki, V., & Troch, P. (2012). *An introduction to the wave propagation model MILDwave, MILDwave manual.* Ghent University.

Suzuki, T., Gruwez, V., Bolle, A., Verwaest, T., & Mostaert, F. (2012). *Numerical modelling of the extreme wave climate in the Belgian harbours: Part 3: Marina of Blankenberge.* Flanders Hydraulics Research & IMDC, Antwerp, Belgium.

Suzuki, T., Verwaest, T., Hassan, W., Veale, W., Reyns, J., Trouw, K., . . . Zijlema, M. (2011). The applicability of SWASH model for wave transformation and wave overtopping: A case study for the Flemish coast. *Fifth International Conference on Advanced Computational Methods in ENgineering.* Liège, Belgium: University of Liège.

SWAN Team. (2016). *SWAN User Manual.* Delft: Delft University of Technology. Retrieved May 31, 2016

SWASH team. (2010). *SWASH User manual.* Delft: Delft University of Technology.

The WAMDI Group. (1988). The WAM model - A third generation ocean prediction model. *Journal of Physical Oceanography, 18*(12). doi:http://dx.doi.org/10.1175/1520-0485(1988)018<1775:TWMTGO>2.0.CO;2

The WISE Group. (2007). Wave modelling - The state of the art. *Progress in Oceanography, 75*, 603-674. doi:doi:10.1016/j.pocean.2007.05.005

Tolman, H. (2009). *User manual and system documentation of WAVEWATCH III.* NOAA. Retrieved from http://nopp.ncep.noaa.gov/mmab/papers/tn276/MMAB_276.pdf

U.S. Army Coastal Engineering Research Center. (1975). *Shore Protection Manual* (2nd ed.). Fort Belvoir, Virginia: U.S. Army Corps of Engineers.

U.S. Army Corps Of Engineers. (2008). *Coastal Engineering Manual* (EM 1110-2-1100 ed.). Washington D.C.: Military bookshop.

Van Barneveld, N. (2013). *Rotterdamse Adaptatiestrategie; themarapport waterveiligheid.* Rotterdam: Rotterdam Climate Initiative.

Van Buuren, A., Eshuis, J., & Van Vliet, M. (2015). *Action Research for Climate Change Adaptation; Developing and applying knowledge for governance.* Abingdon: Routledge.

Van der Meer , J. (2016, October). Personal correspondence on the topic of varying angles of incidence.

Van der Meer, J., & Bruce, T. (2014). New physical insights and design formulas on wave overtopping at sloping and vertical structures. *Journal of Waterway, Port, Coastal & Ocean Engineering, 140*.

Van der Meer, J., Langenberg, J., Breteler, M., Hurdle, D., & Den Heijer, F. (2002). Wave boundary conditions and overtopping in complex areas. *28th International Conference on Coastal Engineering.* Cardiff, Wales.

Van Mierlo, F. (2014). *Numerical modelling of wave penetration in ports.* MSc Thesis, Deltares, National University of Singapore, TUDelft.

Van Veelen, P. (2013). *Adaptive Strategies for the Rotterdam Unembanked Areas.* Knowledge for Climate.

Van Vledder, G., & Zijlema, M. (2014). Non-hydrostatic wave modelling in partly sheltered areas. *34th International Conference on Coastal Engineering.* Seoul, South Korea: Coastal Engineering Research Council.

Vanneste, D., Altomare, C., Suzuki, T., Troch, P., & Verwaest, T. (2014). Comparison of numerical models for wave overtopping and impact on a sea wall. In P. Lynett (Ed.), *34th International Conference on Coastal Engineering*, *34.* Seoul, South Korea. Retrieved from http://dx.doi.org/10.9753/icce.v34.structures.5

Veerbeek, Huizinga, Asselman, Lansen, Jonkman, Van der Meer, & Barneveld. (2010). *Flood risk in unembanked areas.* Rotterdam: Rotterdam Climate Initiative.

Violante-Carvalho, N., Paes-Leme, R., Accetta, D., & Ostritz, F. (2009, December). Diffraction and reflection of irregular waves in a harbor employing a spectral model. *Anais da Academia Brasileira de Ciências, Vol.81*(No.4). Retrieved from http://dx.doi.org/10.1590/S0001-37652009000400019

Wilson, B. (1965, May). Numerical prediction of ocean waves in the North Atlantic for December, 1959. *Deutsche Hydrographische Zeitschrift, 18*(3), pp. 114-130. doi:10.1007/BF02333333

Young, I., & Verhagen, L. (1996, December). The growth of fetch limited waves in water of finite depth. Part 1. Total energy and peak frequency. *Coastal Engineering, 29*(1-2), 47-78.

Yu, X., & Togashi, H. (1996). Combined diffraction and transmission of water waves around a porous breakwater gap. *25th International Conference on Coastal Engineering*, (pp. 2063-2076). Orlando, Florida. doi:10.1061/9780784402429.160

Zijlema, M., Stelling, G., & Smit, P. (2011). Simulating nearshore wave transformation with non-hydrostatic wave-flow modelling. *12th Wave Workshop.* Kohala Coast, Hawaii. Retrieved June 1, 2016, from http://www.waveworkshop.org/12thWaves/papers/Zijlema_12thWaveWorkshop_Nov2011.pdf

Zou, Z. (1999). Higher order Boussinesq equations. *Ocean Engineering, 26*, 767-792.

Appendix A. Relative influence of various wave processes and phenomena

This appendix will clarify the relative influence of the various wave processes and phenomena as they have been mentioned in Table 3.1, which is repeated below. In the subsequent paragraphs the processes will be discussed individually in the order they have discussed in Chapter 2.

Table A.1: The relative influence of the wave

#	Process:	Relative influence
1	Wave overtopping	**+++**
2	Diffraction	**+++**
3	Local wind-wave generation	**+++**
4	Reflection	**++**
5	Transmission	**++**
6	Quadruplet wave-wave interactions	**+**
7	(Bound and free) long waves	**+**
8	Energy dissipation through bottom friction	**+**
9	Whitecapping	**+**
10	Resonance/harbour oscillations	**+**
11	Refraction and shoaling	**+**
12	Frequency dispersion	**+**
13	Depth-induced wave breaking	**-**
14	Triad wave-wave interactions	**-**
+++ = Dominant, ++ = Significant, + = Minor influence, - = Very little influence thus negligible		

A.1. Frequency dispersion

A relative influence of '+' was chosen as the frequency dispersion relation is employed to calculate the wave length, but is not a significant phenomenon once the waves have entered the harbour.

Frequency dispersion is the phenomenon of waves with different frequencies travelling at different speeds. It is described by the following formula:

$$\omega^2 = gk\tanh(kh) \quad or \quad \lambda = \frac{g}{2\pi}T^2\tanh\left(2\pi\frac{h}{\lambda}\right)$$

The phenomenon itself is not relevant inside a small scale model (relative to the wave length) such as a harbour. Especially in a steady state model the relevance of including the phenomenon is absent. One exception holds: the frequency dispersion relation determines the wave length given a certain wave period or vice versa. If only one of the two variables is known the implicit frequency dispersion relation or an explicit form should be applied to find the value of the other variable. This is especially essential for a non-numerical method.

Furthermore it is important to take varying frequencies (width of a wave spectrum) into account in the boundary conditions of the model. The width of the spectrum is of influence on the amount of wave penetration occurring (Alabart, Sánchez-Arcilla, & Van Vledder, 2014).

A.2. Wind-wave generation and wave growth

The maximum relative influence of '+++' was chosen as wind-wave generation will nearly always have a significant if not dominant influence on the wave load at the quay walls.

The effect of wind-wave generation on the significant wave height is obvious: the wind adds energy to the waves. The relative influence of the process is more difficult to assess. This mainly depends on the local conditions. In a sea harbour (with an open connection) such as IJmuiden (Figure 6.1) the relative influence might be small as the penetrated waves are likely to be dominant over the local energy-input by wind. However for more sheltered harbours energy input from wind might be the only source of wave energy present. Therefore in a general sense it can most definitely not be neglected. In practice wind-wave generation can be neglected only if the governing fetch is less than 100 meters and the wind speed is less than 5 meters per second. Normally these conditions will not be met for any harbour.

A.3. Wave shoaling and refraction

A relative influence of '+' was chosen as (linear) shoaling and refraction due to the absence of large bottom gradients in a harbour area, with shoaling and refraction being a depth-gradient induced process.

Wherever there is a gradient in the bottom topography shoaling and refraction will occur. These processes are significant in the nearshore area. Inside a harbour often one will not find large bottom gradients. Only locally shallow areas may be present at which shoaling may increase the wave height. Due to the local effect of shoaling the relative influence on the wave heights in the entire basin is minor. Depending on the specific circumstances refraction may increase or decrease the wave heights inside the basin. It appears that generally speaking refraction reduces the wave energy in the basin if the harbour entrance and the navigation channel are deeper or equally deep as the harbour basin (Rijkswaterstaat, 2014). The relative influence may therefore be considered to be minor.

A.4. Wave diffraction

A relative influence of '+++' was chosen as diffraction is the main process which causes wave penetration into harbours. Also inside the harbour it causes the directional spreading of wave energy to sheltered locations.

Wave diffraction is the main process which allows wave penetration to occur. It causes a spreading of wave energy to the shadow zones inside the wave basin and it allows for waves to travel around corners. Without the process of wave diffraction little to no wave penetration would be found inside the harbour, generally causing a significant underestimation of the wave heights inside the basin.

A.5. Bound and free long waves

A relative influence of '+' was chosen as the presence of long waves in the incoming wave spectrum may increase the amount of wave penetration to occur, but does not play a role on its own.

Bound and free long waves are linked to the existence of wave groups. Their amplitudes become significant in shallow water due to the process of shoaling. Generally the water inside a harbour is too deep for a significant amplitude to develop. However, as the effect of wave diffraction increases

for longer waves, the (possible) presence of these waves is very relevant in the determination of the penetrated wave field. So, it can be said that the process itself does not play a role, but that the long waves must be accounted for in the wave boundary conditions.

A.6. Energy dissipation by bottom friction

A relative influence of '+' was chosen as energy dissipation by bottom friction does have an effect on the wave height for larger harbours, but becomes of very minor importance in relatively deep water.

Bottom friction causes a gradual decline of the wave height over time and space. To get an insight in the relevance in a harbour case a simplified one-dimensional formula is derived:

$$f_c = \frac{H_2}{H_1} = \frac{1}{\sqrt{1 + \frac{\chi}{g^2}\left(\frac{\omega}{\sinh(kd)}\right)^2 * \frac{\Delta n}{\frac{L}{2T}\left(1 + \frac{2kd}{\sinh(2kd)}\right)}}}$$

In which:

f_c = Reduction factor of the wave height between two locations (dimensionless)
H_i = Wave height at a certain location (in meters)
χ = Coefficient for dissipation, χ=0.038 $m^2 s^{-3}$ for a conservative amount of dissipation (Hasselman et al., 1973)
ω = Radian frequency = 2π/T (in s^{-1})
k = Wave number = 2π/L (in m^{-1})
d = Water depth (in meters)
Δn = Travel distance of a wave between location x_1 and x_2

This formula is valid under the following conditions: the water depth is constant, no other dissipative terms are considered and linear wave theory and the quadratic friction law apply. Plotting this equation for relevant parameter settings (with respect to a harbour case), results in Figure A.1.

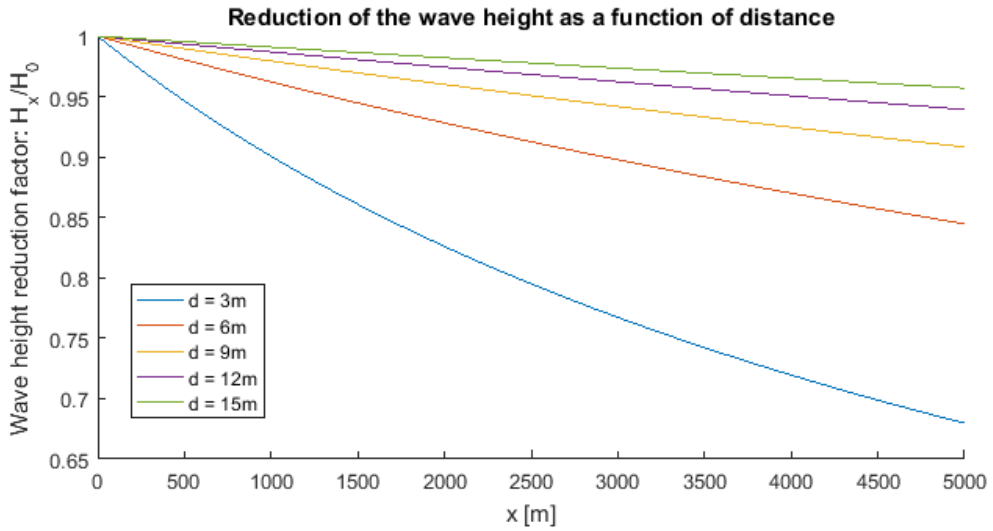

Figure A.1: Wave height reduction factor as a function of the travel distance of the wave (χ=0.038 $m^2 s^{-3}$, T = 10s)

It can be seen that bottom friction plays a very minor role for a harbour case if this harbour is deeper than ten meters. A wave height reduction of at maximum 10% can be recognized. Only for very long and relatively shallow harbours bottom friction will play a role.

A.7. Whitecapping

A relative influence of '+' was chosen for whitecapping as whitecapping influences the formation and evolution of young wind seas. It is irrelevant for longer waves as their steepness is low.

Whitecapping occurs wherever the waves become too steep. The steepest waves in a harbour are the locally generated waves as their wave periods are very low. For this type of waves whitecapping plays a fairly significant role. It dissipates energy from the waves with the highest frequency and thereby increasing the spectral period over time and distance. In principle the process of whitecapping counteracts local wave growth by wind. Therefore, in empirical wave growth formulas whitecapping is taken into account implicitly.

A.8. Depth-induced wave breaking

Depth-induced wave breaking can be neglected (relative influence of '-') as it is very unlikely to occur in a harbour area which is sufficiently deep and has little bottom gradients.

Depth-induced wave breaking occurs when the water depth is too low with respect to the wave height. In a harbour area waves do not tend to become larger except for the locally generated waves. These locally generated waves are influenced by whitecapping instead of depth-induced breaking. In the absence of (very) shallow areas depth-induced breaking will therefore not occur.

A.9. Quadruplet wave-wave interaction

A relative influence of '+' was chosen as quadruplet wave-wave interaction plays a role in the formation and evolution of a locally generated wave field, but it does not influence the penetrated waves.

Quadruplet wave-wave interactions cause a transfer of energy from the high-frequency part of the wave spectrum towards the lower-frequency part of the spectrum. Thereby it is an important process in the initial development of a wave field. For the penetration of waves it is less relevant as for these types of waves the harbour basin will be relatively shallow with respect to the wave length. In empirical wave growth formulas this process is taken into account implicitly.

A.10. Triad wave-wave interaction

Triad wave-wave interaction can be neglected (relative influence of '-') because no interaction between only three components can occur in deep water.

Wave-wave interaction between three components (triad) can only occur in (very) shallow water (Holthuijsen, 2007). Tt will not occur in deep harbour basins and can therefore be neglected.

A.11. Wave reflection

Wave reflection is significant (relative influence of '++') for harbours in which the vertical quay walls reflect nearly all energy, thereby spreading it further through the entire basin. To a first order reflection does not influence the amount of wave overtopping.

Wave reflection has a significant influence on the characteristics of the wave field inside a harbour basin. For vertical quay walls nearly all wave energy will be reflected back into the basin. Depending on the angle of incidence this may cause a significant increase of the wave energy at an opposing quay wall. This may also cause wave energy to penetrate deeper into a harbour. For wave overtopping specifically reflection does not influence the amount of overtopping at the first quay wall a specific wave encounters. Although there is a clear negative correlation (i.e. the more waves overtop a structure, the less wave energy can reflect), they do not influence each other. This is also expressed in the overtopping formulas given by the EurOtop manual as these formulas require the height of the incoming waves only. The main influence reflection thus has on the (total) amount of wave overtopping is the increase of wave energy at an opposing quay wall. This influence may be significant for relatively small harbours (with respect to the wave length), but may be minor for large harbour basins such as the IJmuiden harbour.

A.12. Resonance/harbour oscillations

The process of seiches and harbour oscillations are of minor influence (relative influence of '+'). If such oscillations occur the water level may increase, thereby increasing the amount of wave overtopping. Generally it will be accounted for in the boundary conditions.

The prediction of seiches and harbour oscillations is a fairly difficult process. It depends on the local geometry and the local waves. Only a few wave components would lead to resonance in a basin. If resonance occurs it will cause an oscillation of the (still) water level with a period of 20 minutes up to a few hours. During the 'highs' of the oscillation the amount of wave overtopping is expected to increase significantly. Therefore it is important to take the possible occurrence of the process into account. Generally it will be accounted for via the boundary conditions of a model as it may be difficult to model accurately.

A.13. Wave transmission

Wave transmission can have a significant influence (relative influence of '++') for harbours which have a breakwater or dam at the entrance of the harbour. Generally it causes less wave penetration compared to diffraction, but it can still be significant.

Wave transmission through, but mainly over breakwaters and dams is the second cause of wave penetration into the shadow zones of harbours besides wave diffraction. Obviously it can only occur if a breakwater or dam is present at the entrance of a harbour. Depending on the relative height (compared to water level and the wave heights) and the porosity of the structure it may either have a dominant or lesser, but still significant influence on the wave energy in the shadow zone. Generally structures are sufficiently high to not be submerged or nearly submerged. In these cases often wave diffraction causes more wave energy to enter the harbour compared to wave transmission.

A.14. Wave overtopping

Obviously the process of wave overtopping has a dominant influence: '+++' as it is the main topic of this research.

Appendix B. Numerical wave models

This appendix describes several types of wave models currently available. A quick scan is made of the background and the purpose of the model through either the governing equations or model philosophy. Both advantages and disadvantages of the wave model types in the scope of this thesis will be discussed. Finally examples are given of modelling software which belong in the discussed model type. The following model types will be discussed:

- Shallow water models
- Phase-averaged wave models
- Boussinesq-type models
- Mild slope models
- Non-hydrostatic wave models
- Reynolds averaged wave models
- SPH solvers

B.1 Shallow water models

Shallow water models are those models that are based on the shallow water equations (also called the Saint-Venant equations). The name of the set of equations also describe the most important assumption: shallow water. Shallow water in the sense of this assumption is a small ratio of the water depth over the wave length.

To attain the shallow water equations the three-dimensional Navier-Stokes equations are integrated over depth under certain additional assumptions. The vertical dimension is completely eliminated by neglecting vertical accelerations, thereby assuming hydrostatic conditions. This assumption is only valid for long waves where horizontal dimensions are much larger than the vertical dimensions. Evident now becomes the largest restriction in the scope of this thesis: it cannot model short waves.

To overcome this issue a coupling can be made with a phase-averaged wave model (discussed in the next section). An example of this is Delft3D-Wave. This model calculates the flow conditions in two stages: low-frequency motions with the shallow water equations and wind-generated short waves with the spectral model SWAN. Applicability remains limited though. The hydrostatic assumption is still not overcome. This disables the modelling of frequency-dispersive waves.

Examples in this class of models are: Delft3D, DFLOW-Flexible Mesh and MIKE 11.

B.2 Phase-averaged models

The first numerical model type that will be discussed is the phase-averaged model or the spectral wave model. Such models are designed for modelling surface gravity wave propagation in the nearshore. It can account for several wave processes.

A very important aspect of phase-averaged models is that it does not solve the sea surface elevation in time. In phase-averaged wave models the phase is averaged over the long wave period. As of such long waves are simulated exact in time while short waves are not. Instead short wave statistics can be derived by solving the energy or action balance equation. This type of model is a computationally efficient model. However as the phase is averaged some information gets lost. A very important

limitation of spectral wave models is the inability to model reflection and diffraction as these processes are very phase-dependent.

Often spectral wave models are only applicable in deep water; some examples exist where some shallow water processes have been taken into account. For instance, the spectral wave model SWAN can account for bottom friction, triad wave-wave interaction and wave breaking. SWAN also has a diffraction module built in. This diffraction module can often be applied in cases of absorbing and reflecting coastlines with only occasional obstacles. Under these circumstances the module can lead to accurate results (SWAN Team, 2016) (Enet, Nahon, Van Vledder, & Hurdle, 2006). In harbours reflection and diffraction take place multiple times, making it a dominant process. In this case it is not recommended to use the diffraction module of SWAN (Enet, Nahon, Van Vledder, & Hurdle, 2006) (Violante-Carvalho, Paes-Leme, Accetta, & Ostritz, 2009) (SWAN Team, 2016).

Some examples of phase-averaged models besides SWAN are: WAM (The WAMDI Group, 1988) and WAVEWATCH III (Tolman, 2009). Due to their limitations, phase-averaged models are likely to not be applicable in harbour domains.

B.3 Boussinesq-type wave models

Models of this type are based on the Boussinesq equations. These equations approximate the three-dimensional nonlinear potential flow equations by series expansions. With this approach the vertical structure of the horizontal and vertical velocities can be estimated. Depending on the number of terms in these series expansions the accuracy and the complexity of the equations may vary. Models of the Boussinesq type include different amounts of higher order terms.

When many higher order terms are included this model can estimate nonlinear flow phenomena rather well. In very shallow water depths, where nonlinear effect become more and more dominant, the Boussinesq-type model may struggle. In deep waters the underlying equations and assumptions become less valid (Zou, 1999). Therefore this type of model is particularly useful in intermediate water depths. The original Boussinesq equations have evolved and extended into several domains, for example enabling the inclusion of wave breaking and improving frequency dispersion (important for short waves).

Many models are of this type; examples include: MIKE21BW (DHI Group, N.D.) and TRITON (Deltares, 2008).

B.4 Mild slope models

These types of models have been specifically developed for uses in harbour or nearshore cases. The underlying mild slope equation describes the combined effect of diffraction and refraction, two of the most relevant processes in the nearshore and harbours. These mild slope equations are derived in a similar fashion as the Boussinesq equations discussed in the previous section. The model is again two-dimensional as the vertical dimension has now been eliminated under the assumption of purely Airy waves. Wave spectra are estimated by means of superposition of harmonic waves. Modified and extended formulas can be adopted to include effects of reflection, nonlinearities, bottom friction and wave breaking.

Mild slope models are computationally efficient due to their strategically simplified governing equation(s). Because of the specific target to model wave penetration into harbours, it is generally able to do so accurately. As the name already tells, the model is restricted to topographies with mild slopes. Obviously it is thus impossible to model overtopping over vertical quay walls with this type of model.

Examples of mild slope models are CGWAVE (Demirbilek & Panchang, 1998), PHAROS (Deltares, N.D.) and MILDwave (Stratigaki & Troch, 2012).

B.5 Nonlinear and non-hydrostatic wave models

Non-hydrostatic, nonlinear wave models are based on the nonlinear shallow water equations with some very relevant extensions. The governing equations are fairly different from the Boussinesq and mild-slope equations. The most important addition to the shallow water equations is the extra vertical momentum equation. This allows for variations over the depth, instead of a depth averaged approach. Furthermore the horizontal momentum equations contain non-hydrostatic pressure terms. This enables the modelling of short waves due to the ability to model frequency dispersion. (Zijlema, Stelling, & Smit, 2011).

Vertical variabilities of the flow are allowed for by implementing more depth-layers. The vertical structure of the flow can now be calculated instead of imposed on the solution as is done in the Boussinesq and mild-slope models.

This type of model solves the sea surface elevation in time. As every single (short) wave is solved, diffraction and reflection can be modelled accurately (Alabart, Sánchez-Arcilla, & Van Vledder, 2014).

A clear disadvantage of non-hydrostatic wave models is their high computational demand. They solve the nonlinear shallow water equations (potentially) in three dimensions. Furthermore by modelling every single wave a very high spatial resolution has to be adopted as a minimum amount of grid cells per wave length is required. The consequence is the necessity to model small to medium-sized features.

Examples of non-hydrostatic wave models are: SWASH (SWASH team, 2010), the non-hydrostatic module of the depth-averaged XBeach model (Smit, et al., 2010) and NHWAVE (Ma, Kirby, & Shi, 2014).

B.6 (Reynolds averaged) Navier Stokes-wave models

In this model type the governing equations are the full Navier-Stokes equations or the Reynolds averaged Navier-Stokes (RANS) equations. Of the discussed simplified governing equations the Reynolds averaged equations resemble the original Navier-Stokes equations the closest. The capabilities of this type of model is obviously very large. The main disadvantage of these models is the extremely high computational demand.

Often models of this class solve the Navier-Stokes by applying a turbulence closure model, thus averaging over the scale of the turbulent motion. It is possible to solve the entire Navier-Stokes equations but the computational demand is then even larger. Even the RANS-equations can already solve nonlinear flow phenomena very accurately, including a nearly exact estimation of wave

breaking. The very high computational demand and the complexity of this type of models are the largest disadvantages.

Some types of models falling within the Navier Stokes-type wave models are: FLOW-3D (Flow Science, N.D.) and IH2VOF (IH Cantabria, N.D.)

B.7 SPH Solvers

A completely different approach to all previously mentioned model classes is used by “smoothed-particle hydrodynamics” (SPH) solvers. The method is as old as 1977 (Gingold & Monaghan, 1977) (Lucy, 1977). In this method the entire domain is divided into small discrete elements: particles. Each particle has its own properties (e.g. density and pressure) and carries those properties along. In contrast to many models this approach is Lagrangian; i.e. the rates of change of the particle properties are calculated from a particle perspective. The rates of change are calculated from the neighbouring particles, where the flow properties (velocities and accelerations) are determined using the Lagrangian Navier-Stokes equations. These types of solvers have been proven to be very effective. An example of a model in this model class is SPHysics (Gesteira, Rogers, Dalrymple, Crespo, & Narayanaswamy, 2010).

Appendix C. Validity of SWASH for wave overtopping over vertical walls

This appendix will verify if the SWASH model (*Simulating Waves till Shore)* is able to accurately determine the overtopping discharge given the circumstances. This chapter will start by discussing the governing equations and other numerical aspects of SWASH (section C.1). Subsequently (C.2) the accuracy of SWASH for wave overtopping cases will be validated by comparing the SWASH outcomes to the EurOtop formulas (EurOtop, 2016). Ideally SWASH would be able to model the entire harbour and part of the hinterland. However, it will appear that this is not yet possible (see section C.2).

C.1 Governing equations and discretization in SWASH

This section will show the governing equations of SWASH, being (largely) based on the nonlinear shallow water equations. Furthermore some numerical aspects of SWASH will also be addressed.

C.1.1 Governing equations

As was stated in paragraph 3.4.1 SWASH is a nonlinear and non-hydrostatic shallow water model. Its governing equations are the nonlinear shallow water equations (NLSW) with the addition of a non-hydrostatic pressure term in the horizontal momentum equations and an additional equation for vertical momentum conservation for a multi-layered model. The NLSW equations are derived from the Navier-Stokes equations as follows:

1. Full Navier-Stokes equations
2. Incompressible flow assumption → Navier-Stokes equations for incompressible flow
3. Time-averaging over the turbulent period → Reynolds-averaged Navier-Stokes equations
4. Depth-averaging → Nonlinear Shallow Water equations

The governing equations for a depth-averaged, one layer approach are given in Equation C-1.

$$\frac{\partial \zeta}{\partial t} + \frac{\partial hu}{\partial x} + \frac{\partial hv}{\partial y} = 0$$

$$\frac{\partial u}{\partial t} + u\frac{\partial u}{\partial x} + v\frac{\partial u}{\partial y} + g\frac{\partial \zeta}{\partial x} + \frac{1}{h}\int_{-d}^{\zeta}\frac{\partial q}{\partial x}dz + c_f\frac{u\sqrt{u^2+v^2}}{h} = \frac{1}{h}\left(\frac{\partial \tau_{xx}}{\partial x} + \frac{\partial \tau_{xy}}{\partial y}\right) \quad \textbf{Equation C-1}$$

$$\frac{\partial v}{\partial t} + u\frac{\partial v}{\partial x} + v\frac{\partial v}{\partial y} + g\frac{\partial \zeta}{\partial y} + \frac{1}{h}\int_{-d}^{\zeta}\frac{\partial q}{\partial y}dz + c_f\frac{v\sqrt{u^2+v^2}}{h} = \frac{1}{h}\left(\frac{\partial \tau_{yx}}{\partial x} + \frac{\partial \tau_{yy}}{\partial y}\right)$$

C.1.2 Time- and space discretization of the governing equations

SWASH allows for various user-chosen discretization methods. The methods have an explicit and finite differencing character. All equations are discretized on a staggered grid for efficiency reasons. The order of accuracy depends on the choice of the user. Generally second order accuracy is achieved. The discretization methods used in SWASH will conserve mass and momentum on any discrete level (SWASH team, 2010). In cases of strong flow contraction, e.g. overtopping of vertical structure, SWASH will automatically switch to energy head conservation instead of momentum conservation.

By default SWASH applies the second order backward differencing BDF scheme for the momentum equations. It may be possible that this scheme or any other second order scheme induces wiggles on the solution. Where such instabilities grow too large a first order scheme may be the solution as a first order scheme is more robust. It is however not recommended as the numerical dissipation is considerable (SWASH team, 2010).

For time integration of the governing equation a second order (explicit) leapfrog scheme is applied in SWASH. Optionally a semi-implicit time integration method can be applied, however this method is only beneficial for large-scale flows. Due to the explicit character of the leapfrog scheme the time step is restricted according to the CFL-criterion. For a two-dimensional case this criterion reads:

$$Cr = \Delta t \left(\sqrt{gd} + \sqrt{u^2 + v^2}\right) \sqrt{\frac{1}{\Delta x^2} + \frac{1}{\Delta y^2}} \leq 1$$

SWASH is able to adapt the time step to the actual flow conditions by pre-set limits for the Courant number. The maximum limit for the Courant number for rapidly varying flow is advised to be 0.5 (SWASH team, 2010).

The non-hydrostatic pressure term in the horizontal momentum equations are discretized in a different fashion. SWASH allows for two options: the central differencing scheme and the Keller-box scheme. In terms of use the central differencing scheme is applied when rapidly varying flow is involved while the Keller-box scheme performs better on short wave propagation. For a case where overtopping is involved the central differencing scheme is likely to perform better when solely looking at accurate overtopping discharges. However this scheme may only be applied when a large number of vertical layers is involved. For the specific case of overtopping this is however not possible as it leads to critical instability (Vanneste, Altomare, Suzuki, Troch, & Verwaest, 2014). Therefore without further notice the Keller-box scheme will be applied in this thesis.

C.2 SWASH validation for wave overtopping

The numerical modelling software SWASH has not been extensively validated for wave overtopping. Previous researches (Vanneste, Altomare, Suzuki, Troch, & Verwaest, 2014) (Suzuki, et al., 2011) have shown its potential but also its (current) limitations. Currently SWASH has only been tested for very few cases. In this section the performance of SWASH will be verified for a wide range of geometries and settings. The procedure will be similar to the verification of ComFlow for wave overtopping as is done by Honda, Wellens en Van Gent (2011). This Section C.2.1 will describe the initial model set-up. The subsequent paragraphs in section C.2 will compare SWASH outcomes for various settings to predictions based on the EurOtop manual (EurOtop, 2016). The dependence of the SWASH outcomes on the following (geometrical) parameters are tested:

- Significant wave height at the incoming wave boundary, H_s → Section C.2.2
- Freeboard with respect to the water level of the vertical wall, R_c → Section C.2.3
- Slope angle of the overtoppable structure, cot(α) → Section C.2.4
- Peak wave period at the incoming boundary, T_p → Section C.2.5

The conclusions of the SWASH validation for wave overtopping are given and discussed in section C.2.6.

C.2.1 General SWASH model set-up

The model which is used to validate wave overtopping over a vertical structure in SWASH is a one-dimensional model. A schematization of the model set-up is given in Figure C.1.

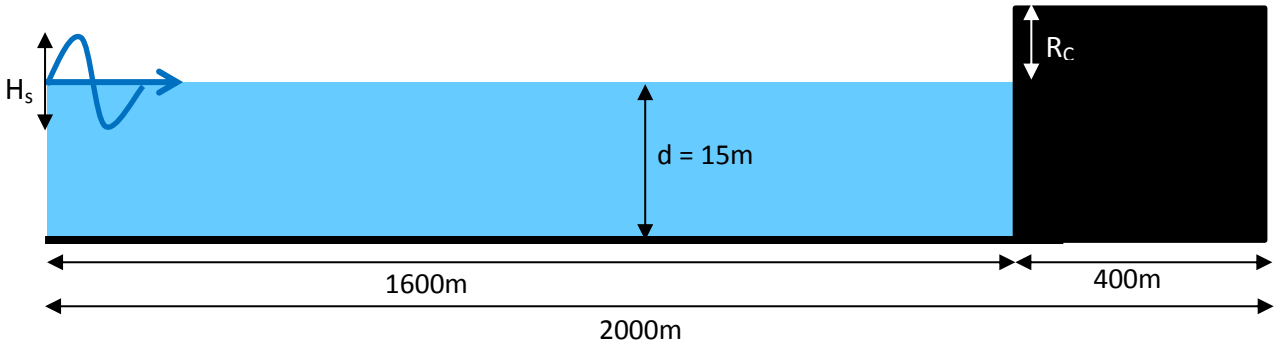

Figure C.1: Schematization of the SWASH model for wave overtopping validation

The numerical settings of the model are given below:

- One-dimensional grid with a cell length of 1m (2000 cells)
- One depth layer (as mentioned more depth layers results in an instable model)
- Initial time step of 0.01 seconds; low time step required in order to model the rapidly varying flow conditions near the wall
- Total simulation period of 45 minutes
- A weakly reflective wave boundary condition on the left side of the model
- A radiation stress boundary on the right side of the model to allow transmitted waves to leave the domain.
- First order upwind discretization of the governing equations to prevent instabilities
- The non-hydrostatic mode is turned on with the application of the Keller-box scheme to discretize the equation for the vertical pressure gradient.

A total number of 258 model runs were performed to achieve the results given in the following paragraphs.

C.2.2 SWASH validation for the significant wave height

This paragraph will analyse the performance of the SWASH model while varying the significant wave height at the incoming boundary. The model results are compared to the EurOtop formula for wave overtopping over vertical walls (see Equation 2-19) and its 90% confidence intervals. For this purpose use is made of the relative overtopping discharge, see Equation C-2.

$$Relative\ overtopping\ discharge = \frac{q}{\sqrt{gH_{m0}^3}} \qquad \textbf{Equation C-2}$$

Figure C.6 shows the results in a semi-logarithmic plot in which the (non-dimensional) local freeboard is on the horizontal axis. The wave height at the boundary is varied for three separate values of the freeboard of the structure.

A lot of the SWASH model results fall within the 90% confidence interval. Most of these have a local freeboard of 0.5 up to 1. It can be seen that for the largest value of the freeboard (R_C=2.0 m) SWASH

does not give similar results as the EurOtop formula. This is a result of (non-critical) wiggles near the vertical wall. For low values of the local freeboard (large significant wave height) the model produces critical instabilities, thereby not returning a value for the overtopping discharge. These critical instabilities arise for wave heights of approximately 4 meters.

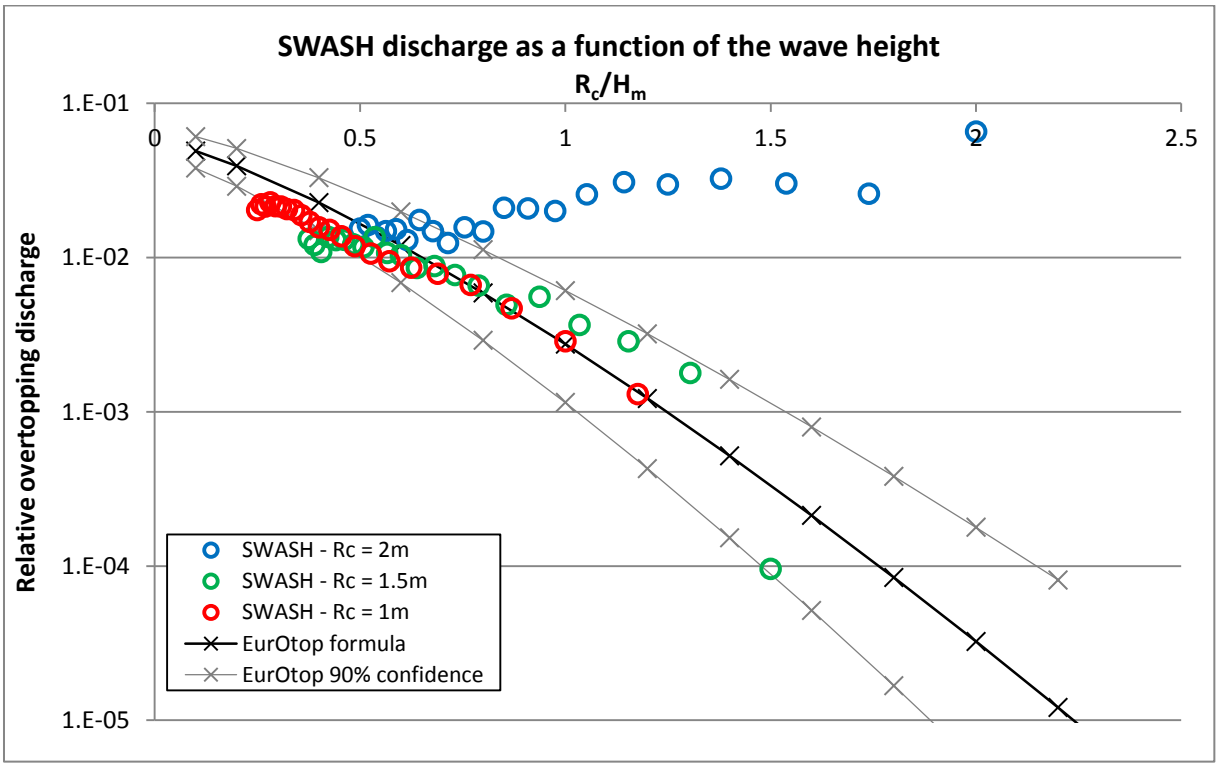

Figure C.2: Comparison of the SWASH results and the EurOtop formula. The significant wave height at the model boundary is varied for three values of the freeboard of the vertical structure.

C.2.3 SWASH validation for the freeboard of the vertical structure

This paragraph shows the SWASH validation of wave overtopping for a varying value of the freeboard of the vertical structure. The approach is similar as in the previous paragraph which analysed the SWASH results for a varying wave height. Again the results are plotted as relative overtopping discharges, see Equation C-2. These relative overtopping discharges, for three values of the significant wave height at the boundary, are plotted in Figure C.6. It can be seen that SWASH produces accurate results (within the 90% confidence interval), with respect to the EurOtop formula, for relative freeboards below 0.75. For a freeboard larger than 2 meters, independent of the wave height, the model produces wiggles which become critical for even larger values of the freeboard. These growing wiggles explain the deviating trend in the relative overtopping discharges for an increasing freeboard.

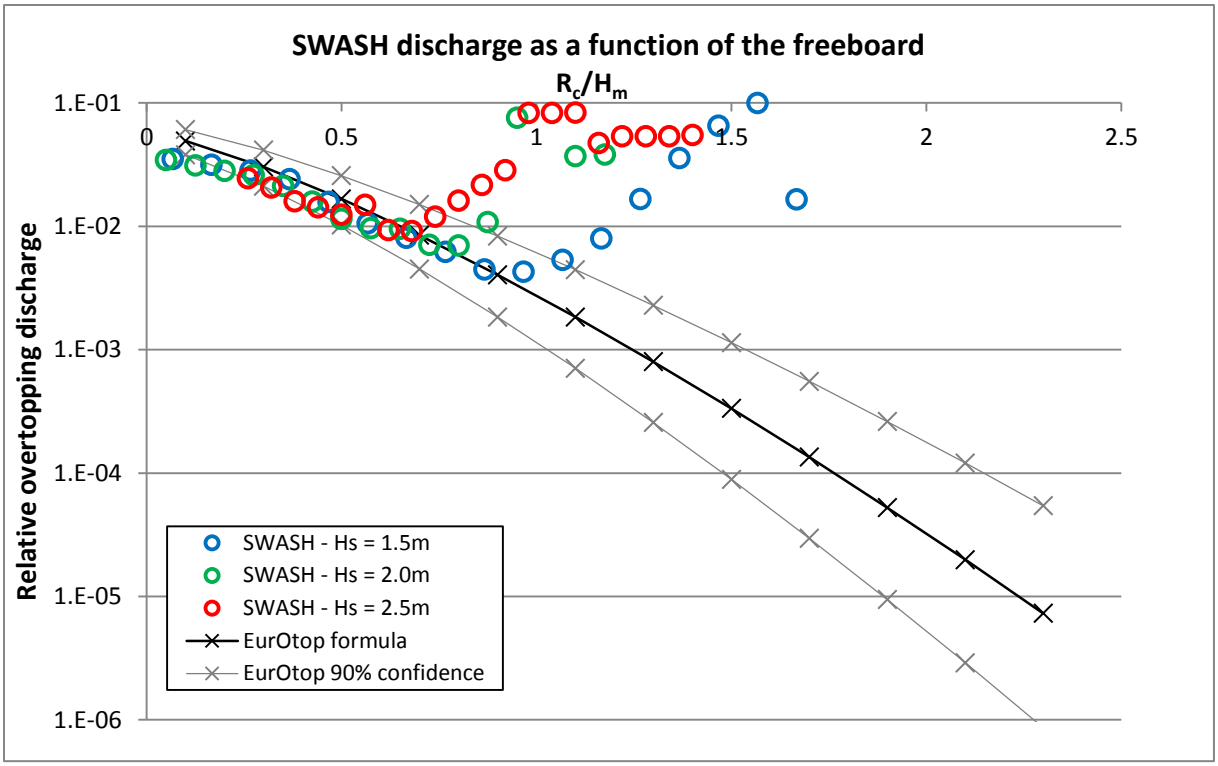

Figure C.3: Comparison of the SWASH results and the EurOtop formula. The freeboard of the vertical structure is varied for three values of the freeboard of the vertical structure

C.2.4 SWASH validation for the slope angle

This paragraph will test the effect of the slope angle of the structure on the overtopping discharge found by SWASH. The relevance is not directly linked to a harbour area as generally no sloped structures are found in a harbour. However, this validation may show the range of application of SWASH with respect to impulsive and non-impulsive wave overtopping.

Instead of a comparison with the EurOtop formula, the SWASH results are plotted together with the results of the Deltares Neural Network model (Deltares, 2010). For a varying slope angle different EurOtop formulas would have to be applied, such that the Neural Network allows for a better and more continuous comparison. The Neural Network model is based on the same CLASH database which lies at the basis of the EurOtop formulas.

For a sloping structure the relative overtopping discharge is defined slightly differently, see Equation C-3.

$$Relative\ overtopping\ discharge = \frac{q}{\sqrt{9.81 * H_{m0}^2 * L_0 * \tan(\alpha)}} \qquad \textbf{Equation C-3}$$

Figure C.6 plots this relative overtopping discharge for a varying slope angle as a function of the local freeboard and the breaker parameter: $\frac{R_C}{H_m * \xi_{m-1,0}}$.

It can be seen that SWASH generally produces accurate results with respect to the Neural Network predictions until the point where impulsive wave breaking is likely to occur ($2.5<\xi_{m-1,0}<5$). In this impulsive regime SWASH apparently underestimates the overtopping discharge.

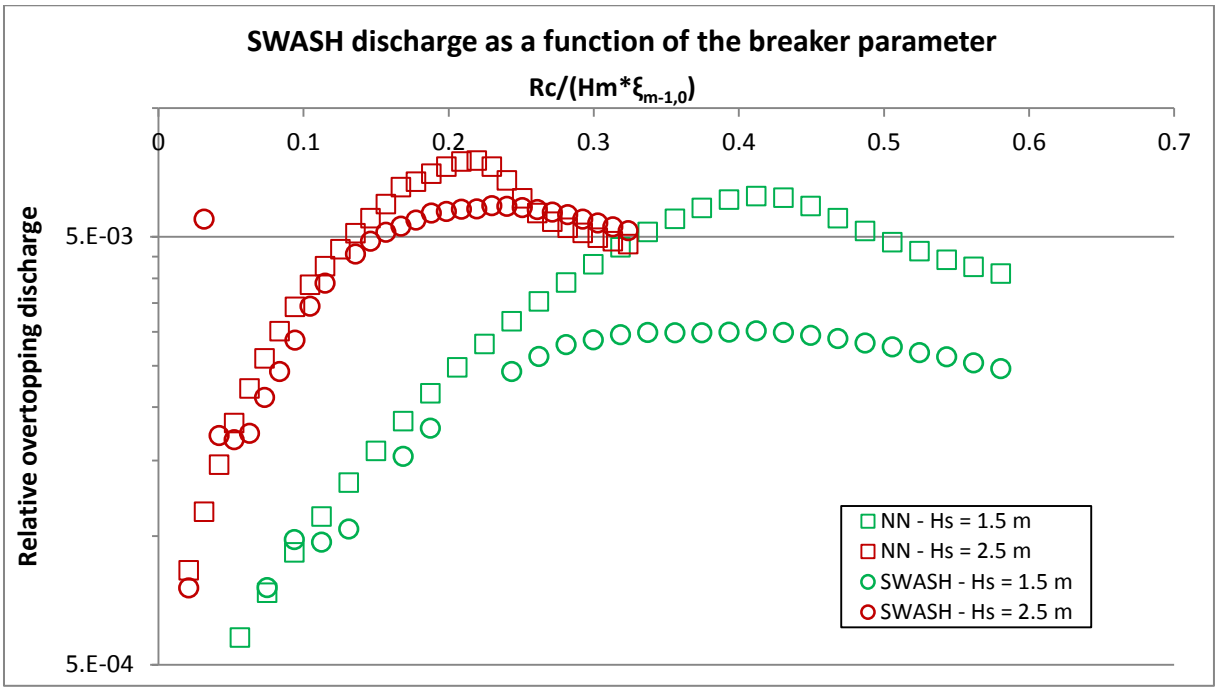

Figure C.4: Comparison of the SWASH results and the Deltares Neural Network model indications. The slope angle of the structure is varied for two values of the significant wave height at the model boundary and a freeboard of 1.5 meters.

C.2.5 SWASH validation for the wave period

According to the EurOtop manual the amount of wave overtopping is independent of the wave period for vertical structures and structures with a steep slope. For these types of structures non-impulsive wave overtopping can be expected. This paragraph will show whether the SWASH results are also independent of the wave period.

For this purpose SWASH runs were performed with varying wave periods. The results of these runs are shown in Figure C.5. It appears that for an increasing wave period the overtopping rate also increases. This can however be explained by a change in the incoming wave height near the vertical structure. Such a change in the wave height is a result of wave energy dissipation by whitecapping. This is illustrated in Figure C.5 in which the wave heights near the structure are plotted with a secondary vertical axis.

For the given conditions, a model with wave periods of over 12.5 seconds produces instabilities. This can be seen in Figure C.5 by an unexplainable increase of the incoming wave height and the overtopping rate. At a certain point the instabilities become critical.

C.2.6 Conclusions on the validity of SWASH for wave overtopping

This section (C.2) analysed the performance of the SWASH numerical model for wave overtopping scenarios. The main issue of using SWASH for these scenarios was the occurrence of unpredictable growth of wiggles (instabilities). Such instabilities arose in every set of model runs shown in the

previous paragraphs. This is also illustrated in Figure C.6 which plots the model results for varying relative freeboards (both by a varying freeboard and a varying wave height). These results are also shown in paragraphs C.2.2 and C.2.3. It can be seen that the workability range (in the context of instabilities) is independent of the relative freeboard but rather depends on the specific model conditions. Instable results are produced when either the freeboard is large (>2 meters) or the wave heights are large (>4 meters).

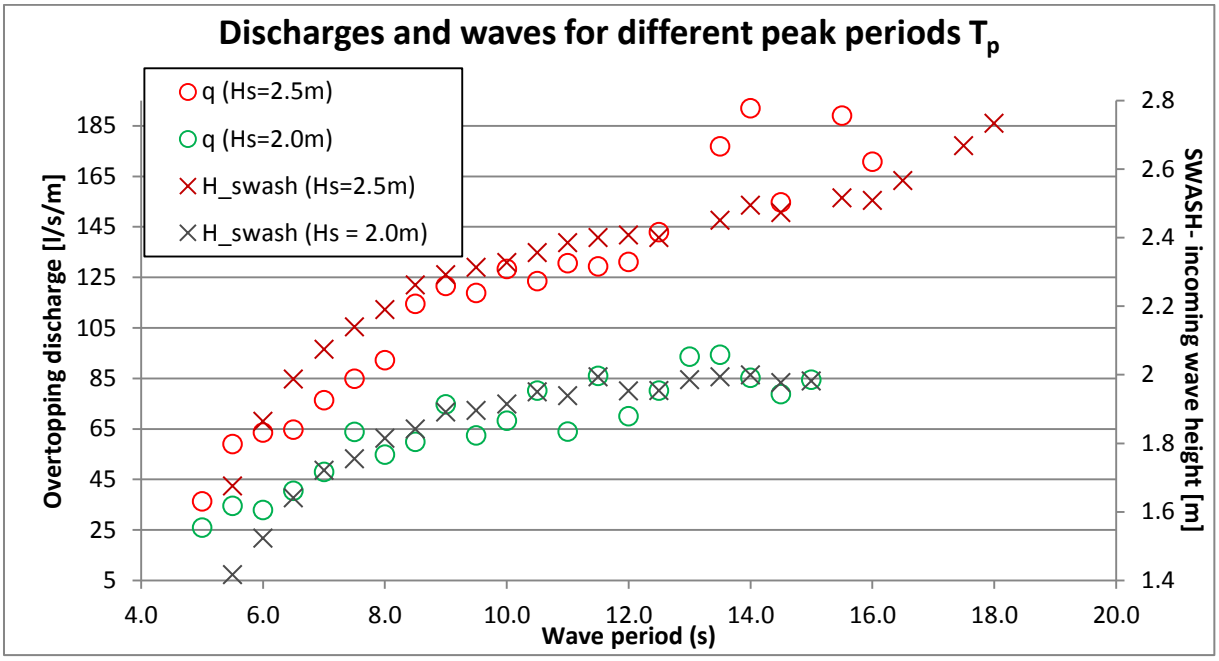

Figure C.5: Overtopping discharges and wave heights produced by SWASH for varying wave periods. The left axis shows the overtopping discharge and the right axis shows the incoming wave height near the vertical wall.

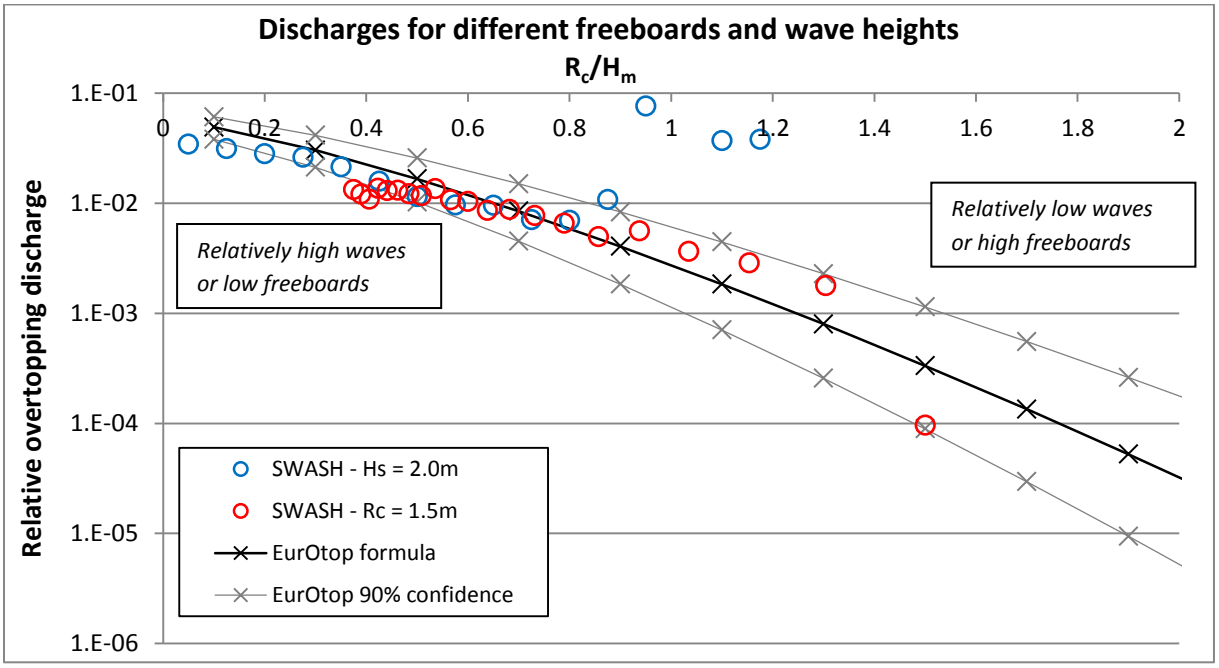

Figure C.6: Comparison of SWASH results with the EurOtop overtopping formula for variable freeboards and wave heights

Appendix D. Explanation of the scores on the assessment criteria

Due to the unavoidable subjectivity in the scores, this appendix will briefly explain how the scores the modelling approaches received on the assessment criteria, were chosen. For convenience, Table 3.4 which gives these scores is shown again (Table D.1).

Table D.1: Scoring of the methods on the various assessment criteria on a scale from 0 to 3.

	Physical model	Deterministic approach	Pragmatic approach	SWASH	SWASH+SWAN coupling	RANS model or SPH solver
Assessment criterion:	Non-numerical			Numerical		
Meeting the requirements (Table 3.3)	3	2	0	1	2	3
Expected accuracy in a harbour domain	3	1	0	2	2	3
Applicability range	2	1	3	2	3	2
Practicality: simplicity	2	3	3	1	0	0
Practicality: required (computational) effort	0	3	3	1	1	0
Practicality: required data availability	3	2	3	0	0	0
Interpretability of the results	3	3	0	2	1	1

Meeting the requirements

This assessment criterion is fairly objective. The number of requirements the modelling approach meets, is leading in the choice of a score. It can be seen (Table 3.3) that a physical model or a SPH solver is able to model most processes. Therefore these two modelling approaches have received the highest score (‘3’). Although a pragmatic approach is very useful in practice, it does not meet the formal requirements (‘0’)

Expected accuracy in a harbour domain

The expected accuracy in a harbour case is closely linked to the number of requirements a model meets. Differences occur due to the fact that a model may ignore certain processes, but that it produces accurate results for the processes it can actually model. An example is the application of SWASH. Although it cannot model wave overtopping accurately (see Appendix C), it is expected to accurately model the wave field inside the harbour. Therefore an approach with SWASH receives the score ‘2’. The reverse reasoning applies to the deterministic model. Although many of the most relevant processes can be taken into account, the expected accuracy is lower.

Applicability range

The score for the applicability range depends on the restrictions the modelling approach has on the cases which can be modelled. A pragmatic approach could be applied anywhere (such that it scores a ‘3’). In contrast, a deterministic approach is limited to fairly simple geometries, as it is impossible to model the wave processes for complex geometries (scoring a ‘1’).

Simplicity of the approach
The simplicity of the approach depends on the effort required to analyse a case. Obviously the non-numerical approaches score well on this criterion. It is relatively simple to implement a case in a non-numerical approach as it does not require a lot of specific technical knowledge. In order to be able to set up a (complex) case in a numerical modelling environment, experience with the model is required.

Required effort
The criterion of required effort is twofold. Firstly, the required resources (costs) play a role. Obviously building a physical model for every new harbour case, is very expensive (explaining the '0' score'). Secondly the required computational effort and computational time plays a role. For numerical methods this could add up to several (tens of) days, even when applying multi-core computers. Currently, it is practically impossible to run a harbour case in a RANS model or SPH solver due to a restriction on the computational capabilities ('0').

Required data availability
Data will always be required to analyse a case, independent of which approach is chosen. However, to set up a numerical model, more data is required compared to the non-numerical approach. At least a detailed bathymetry is required in order to be able to take advantage of the larger expected accuracy of numerical models. Often such detailed bathymetrical data is not (openly) available.

Interpretability of the results
The final assessment criterion is the interpretability of the results. It is evident that the pragmatic approach does not give any insight in the underlying processes. Therefore the results gained with such an approach are difficult to interpret ('0'). The same holds for the numerical models. A numerical model is often a 'black box' unless the user has a lot of experience in interpreting the results. For example, a numerical model usually does not give the option to separate the various wave components (e.g. incoming wave component vs. the reflected wave component). Furthermore the model may production of non-physical and non-critical wiggles, which may significantly change the outcomes (see Appendix C). Such wiggles may be difficult to detect, such that it becomes difficult to interpret the results.

Appendix E. Check on the validity of the diffraction diagrams for inland harbours

This appendix will briefly investigate the possibility to use the Goda diffraction diagrams (Goda, Takayama, & Suzuki, 1978), see paragraph 4.3.2, for an inland harbour configuration. A typical situation is given in Figure E.1 below.

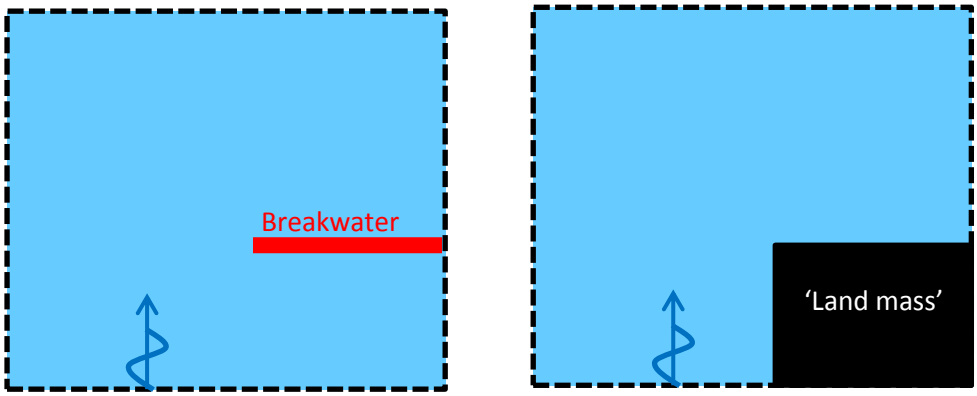

Figure E.1: *Left:* default semi-infinite breakwater configuration. *Right*: Inland harbour area configuration. Waves enter the domain from the southern border.

For this type of inland harbours the waves are expected to travel into the harbour via diffraction. However, the diffraction diagrams of Goda have been derived by assuming a fully reflective breakwater. These reflected waves also diffract around the tip of the breakwater; thereby contributing to the wave energy in the shadow zone. This reflection component is completely absent for the inland harbour configuration. To test the validity of the diagrams for this situation a SWASH model was set-up. Research shows that SWASH is able to accurately model the process of wave diffraction (Van Mierlo, 2014). It also matches well to the analytical Sommerfeld solution, which is also the basis of the derivation of the Goda diffraction diagrams.

The main settings of the SWASH model are:

- 1000x1000 grid with a grid size of 1x1m
- 2 equal vertical depth layers
- Constant water depth of 15 meters
- A weakly reflective boundary with an constant oscillation with an amplitude of 1.5 meters and a wave period of 5 seconds
- A closed boundary on the western edge (to prevent wave energy leaving the domain from this side)
- Default radiation stress boundaries on the north and east boundary with a 150 meter wide sponge layer in front of the northern boundary to prevent significant wave reflection
- The semi-infinite breakwater and the harbour area in the inland harbour configuration are modelled as a porous structure to prevent instabilities (n=0.01). The breakwater is located at y = 300m and in the harbour configuration the 'land mass' ends at y = 300m.

Figure E.2 shows the significant wave heights for the entire basin for both the semi-infinite breakwater model as the inland harbour model. Generally the two figures match well. A noticeable difference can be seen right along the wall of the harbour configuration where a slight focussing of wave energy can be distinguished. This is due the porous nature of the structure which draws in wave energy. This bundling of energy also has a consequence down the path of the wave rays and at the corner of the 'land mass'. However, it can still be concluded that for a course approximation of the diffraction pattern, the Goda diagrams may be applied for the harbour case.

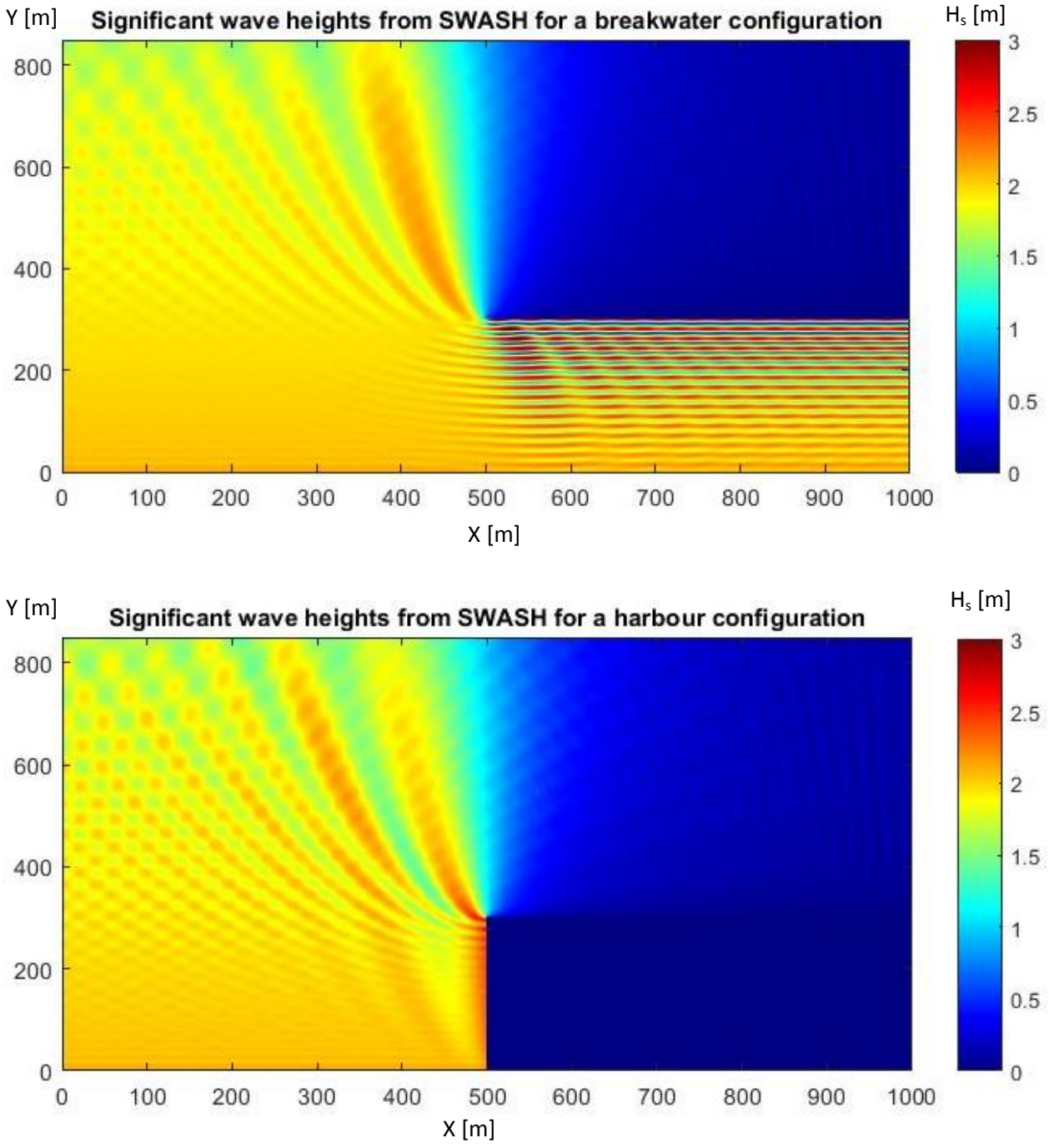

Figure E.2: Significant wave heights found by the SWASH model for the semi-infinite breakwater configuration (top figure) and the inland harbour configuration (bottom figure)

Appendix F. Analysis of 'Vlissingen Buitenhaven' case in the WGPO model

F.1 Introduction

The 'Vlissingen Buitenhaven' case was employed in order to validate the WGPO model with respect to the 'RIKZ' method *Golfbelasting in havens en afgeschermde gebieden* (Rijkswaterstaat, 2014). In paragraph 4.4 the table with the final wave heights for the six output location was shown. These values for the wave heights belonged to the design conditions. For these conditions the model performed well. The next section of this appendix will go deeper into the steps which lead to the wave heights in paragraph 4.4. It will show the comparison between the 'RIKZ' method and the WGPO model for various variables and coefficients.

In paragraph F.3 of this appendix overtopping scenarios have been analysed. Although they cannot be validated with other researches, they show the practicality of the model. The sensitivity of the wave overtopping discharges to several variables for this case is also explored.

F.2 Validation of model steps for 'Vlissingen Buitenhaven'

This paragraph will show the plots of the individual parts of the model for the case of the *Vlissingen Buitenhaven*. Firstly the bathymetry and the output locations are repeatedly shown in Figure F.1. The following processes/components are visualized:

- Figure F.2: Vlissingen outer harbour: maximum fetches in a sector of 60 degrees around the principal wind direction
- Figure F.3: Vlissingen outer harbour: Significant wave height of the locally wind-generated waves
- Figure F.4: Vlissingen outer harbour: diffraction coefficients (local diffracted wave height/outside wave height)
- Figure F.5: Vlissingen outer harbour: transmission coefficients (local transmitted wave height/outside wave height)
- Figure F.6: Vlissingen outer harbour: wave heights of the penetrated waves
- Figure F.7: Vlissingen outer harbour: combined wave height for the processes of wind-wave generation and wave penetration

For each component or process a comparison is made with the values shown in '*Golfbelasting in havens en afgeschermde gebieden'* (Rijkswaterstaat, 2014). The design conditions and representative dimensions are repeated below:

Table F.1: Boundary conditions for the WGPO model

Design conditions (outside the harbour)	Rijkswaterstaat (2014)	WGPO model
Design water level [m +NAP]	5.3	5.3
Representative bottom level in the basin [m+NAP]	-20.0	-20.0
Representative harbour area elevation [m+NAP]	4.5	4.5
H_s [m]	2.4	2.4
$T_{m-1,0}$ [s]	7.14	7.14
Wind direction [°N]	240	245
Wind speed [m/s]	33	33
Wave direction [°N]	235	240
Representative wave length [m]	77	77.1

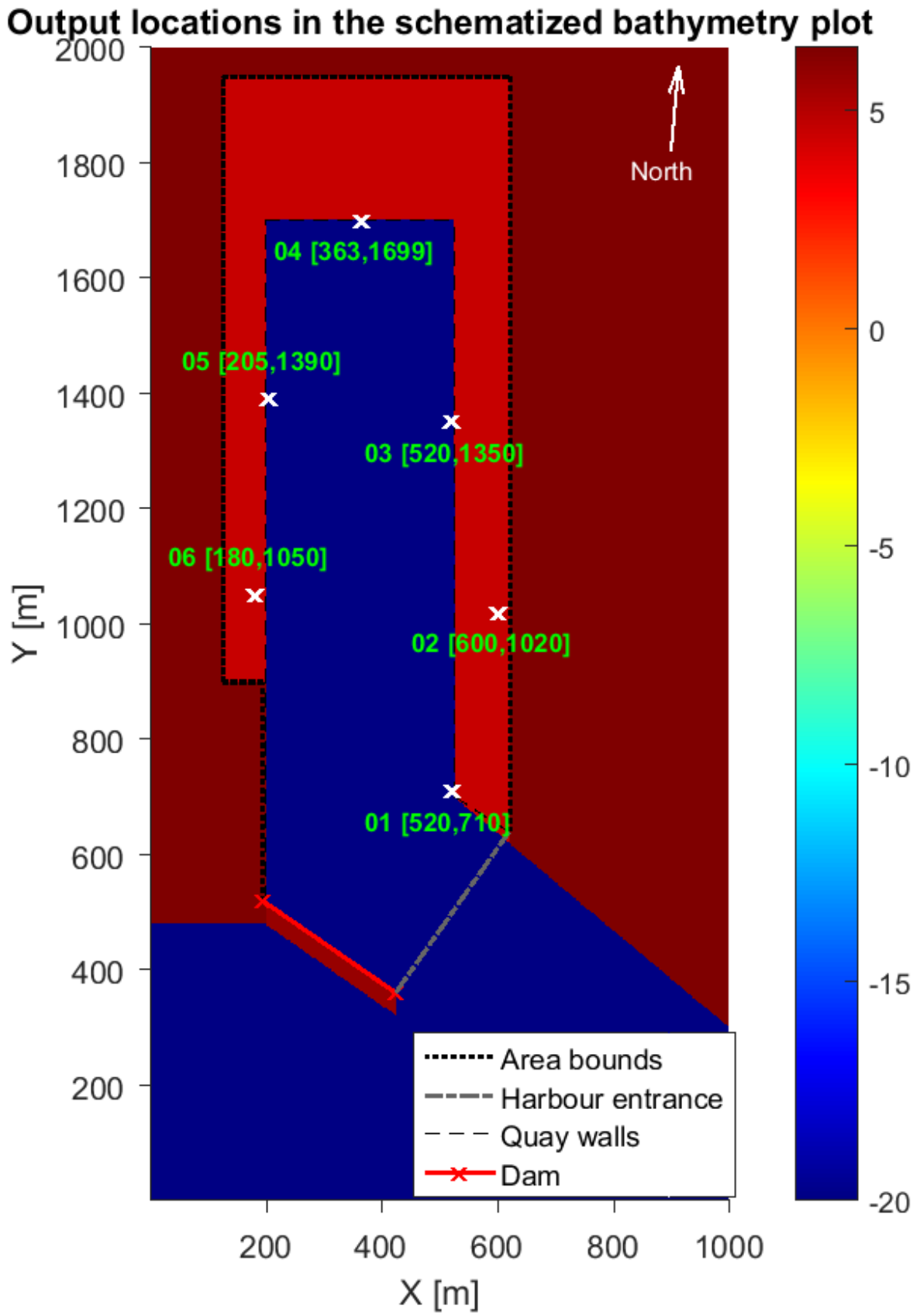

Figure F.1: Vlissingen outer harbour: Bathymetry and output locations

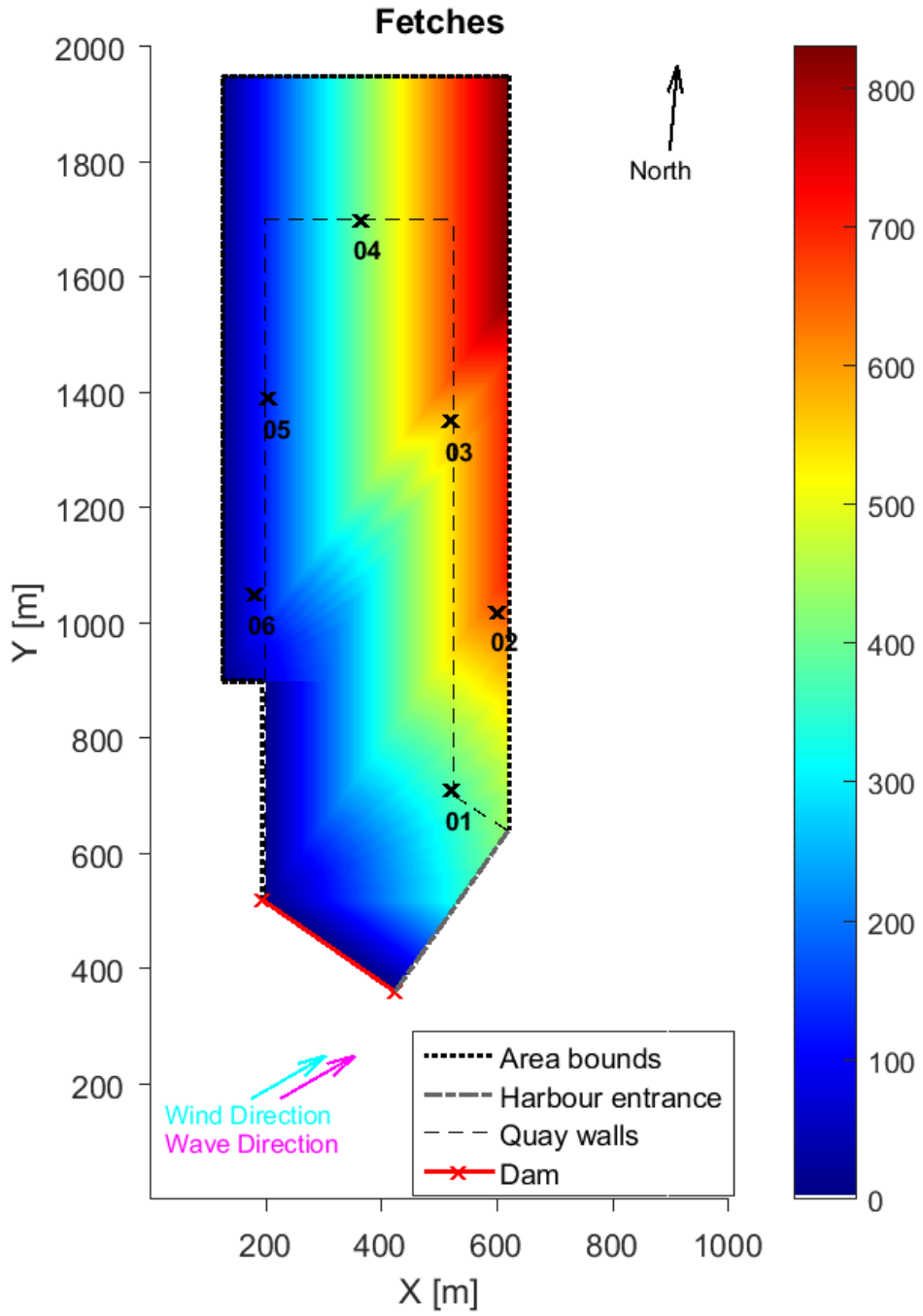

Figure F.2: Vlissingen outer harbour: maximum fetches in a sector of 60 degrees around the principal wind direction

Table F.2: Maximum fetches in a sector of 60 degrees for the six output locations

Maximum fetch at location:	01 [m]	02 [m]	03 [m]	04 [m]	05 [m]	06 [m]
WGPO model	368	640	565	400	135	95
RIKZ method	400	680	800	400	210	50

It can be seen that generally the fetches match up fairly well. The main exceptions are location 03 and 06. Both deviations can be explained by the geometry schematization in the WGPO model.

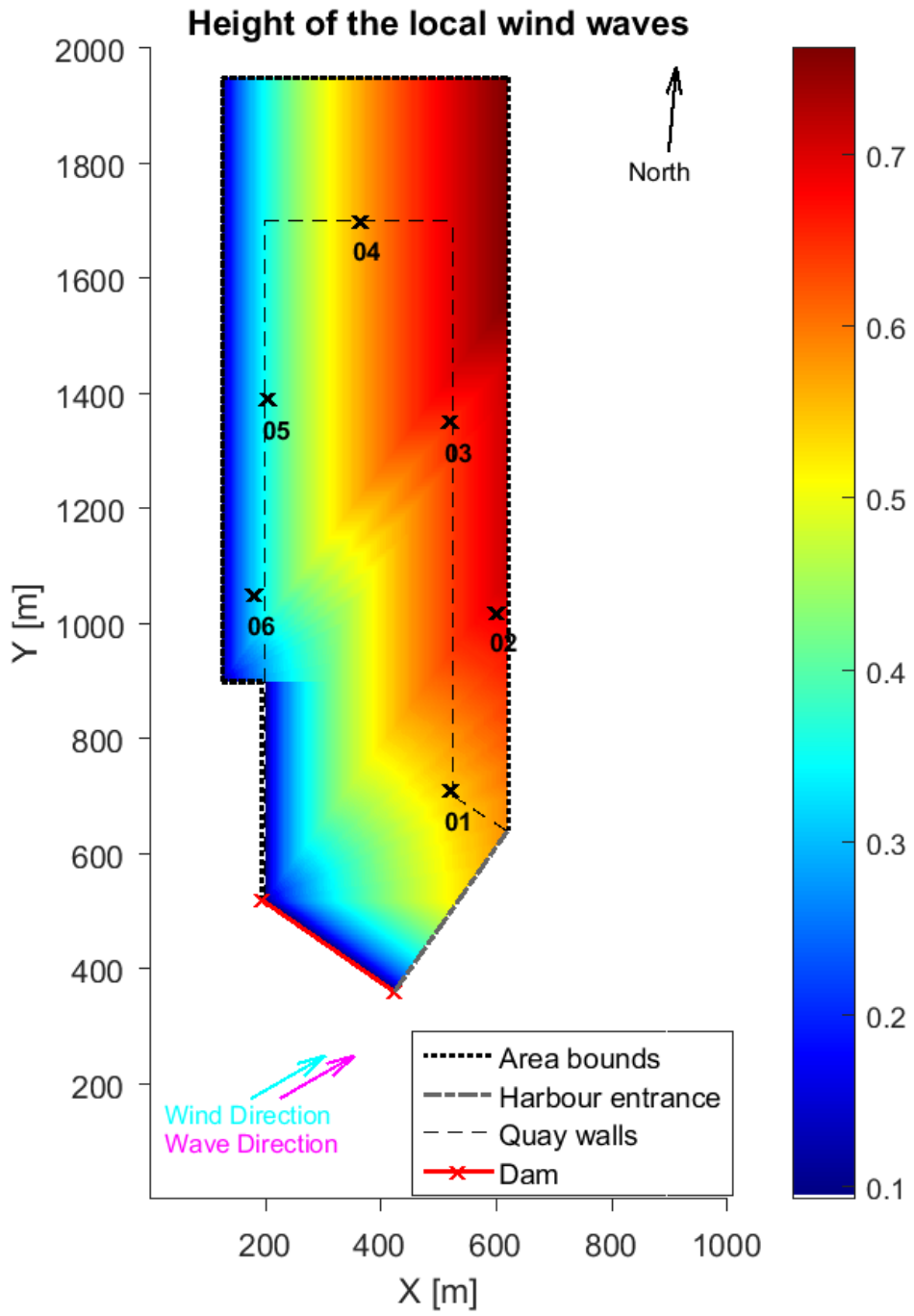

Figure F.3: Vlissingen outer harbour: Significant wave height of the locally wind-generated waves

Table F.3: Wave heights for the locally generated waves for the six output locations

$H_{s,wind}$ at location:	01 [m]	02 [m]	03 [m]	04 [m]	05 [m]	06 [m]
WGPO model	0.54	0.68	0.65	0.56	0.36	0.31
RIKZ method	0.50	0.55	0.60	0.42	0.31	0.15

The overestimation of the height of the locally wind-generated waves for every location can be explained by the use of a different formula in the two methods. For (very) short fetches the Wilson formula used in the RIKZ method (Rijkswaterstaat, 2014) gives a lower wave height compared to other wave growth formulas.

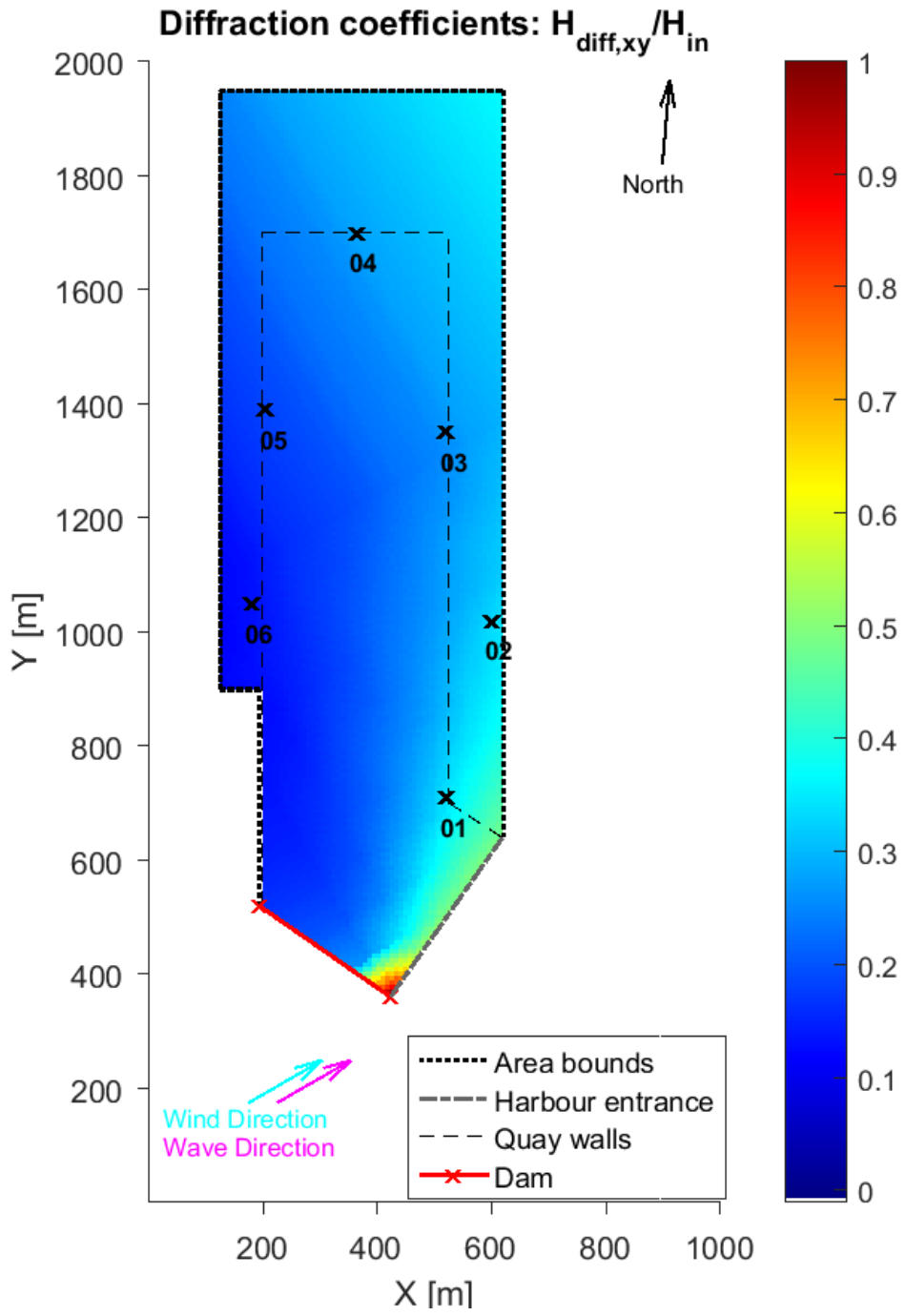

Figure F.4: Vlissingen outer harbour: diffraction coefficients (local diffracted wave height/outside wave height)

Table F.4: Diffraction coefficients for the six output locations

Diffraction coefficient at location:	01 [-]	02 [-]	03 [-]	04 [-]	05 [-]	06 [-]
WGPO model	0.34	0.33	0.26	0.24	0.17	0.14
RIKZ method	0.34	0.32	0.26	0.27	0.19	0.14

For every location a very similar value of the diffraction coefficient is found.

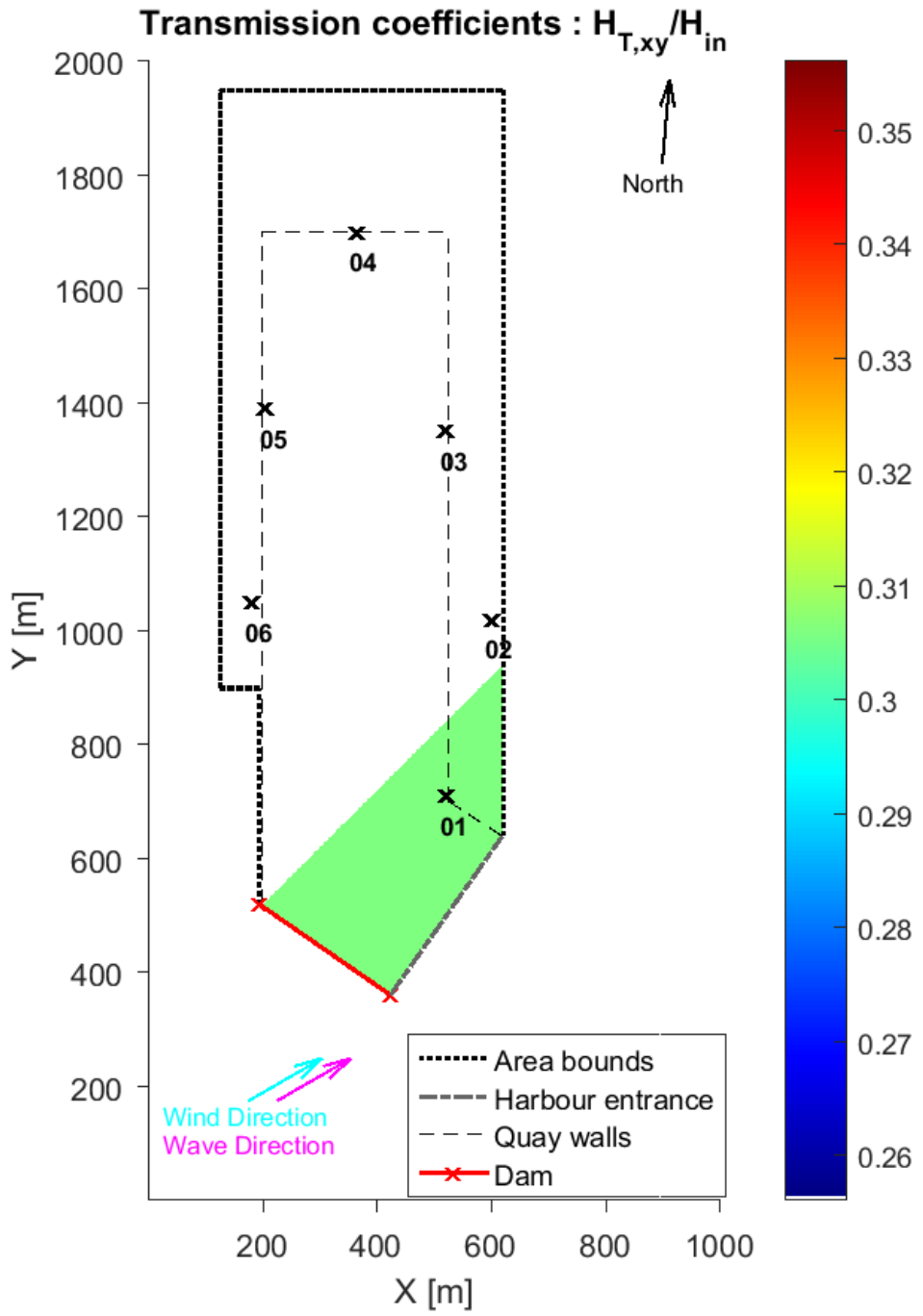

Figure F.5: Vlissingen outer harbour: transmission coefficients (local transmitted wave height/outside wave height)

Table F.5: Transmission coefficients for the six output locations

Transmission coefficient at location:	01 [-]	02 [-]	03 [-]	04 [-]	05 [-]	06 [-]
WGPO model	0.31	0	0	0	0	0
RIKZ method	0.31	0.31	0	0	0	0

In the WGPO model location 02 falls just outside of the transmission zone. This can be caused by a small deviation in the schematization of the harbour or a different location of the output location. As no gradual diminishing of the transmitted wave energy is applied outside of the transmission zone the difference is significant.

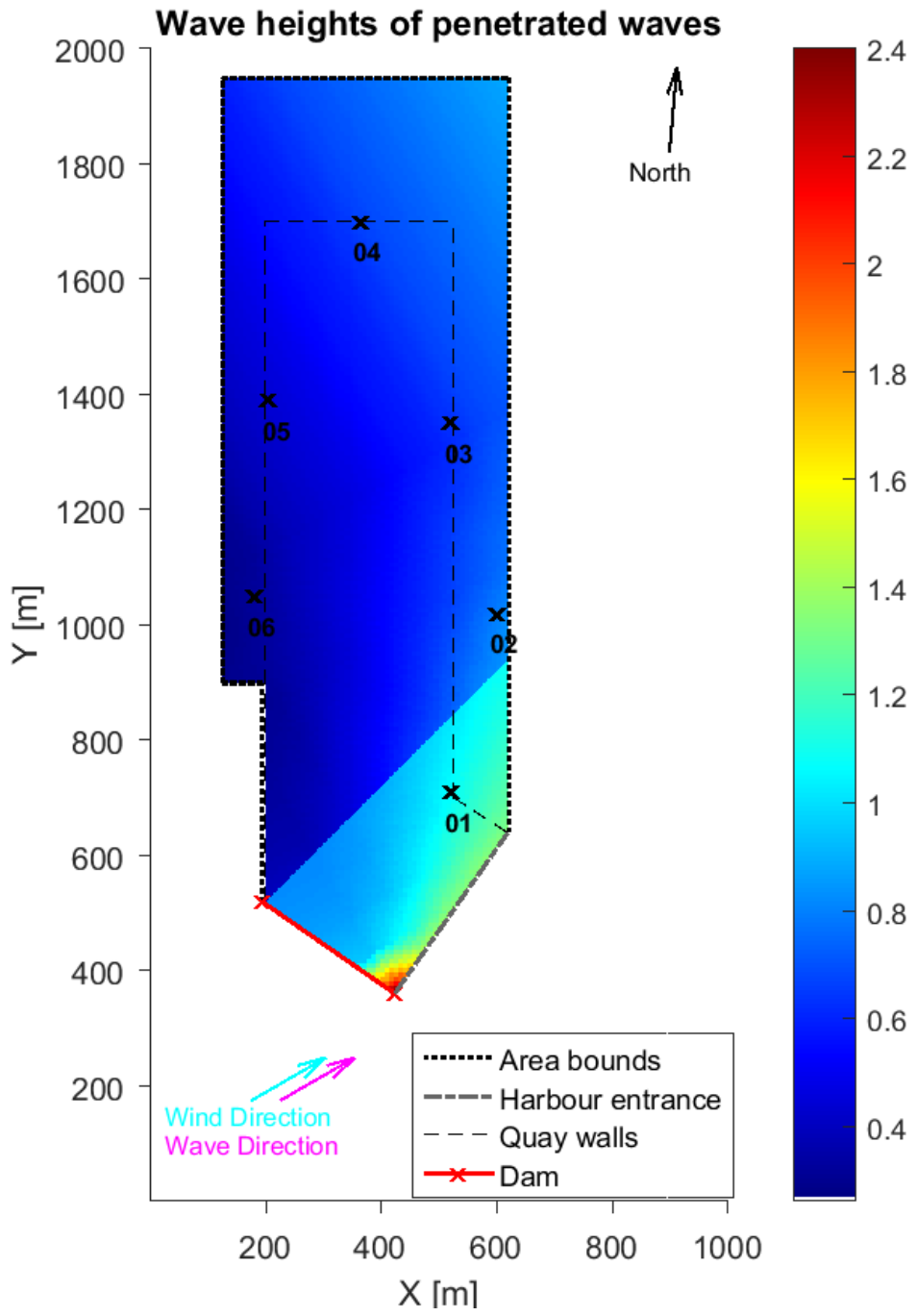

Figure F.6: Vlissingen outer harbour: wave heights of the penetrated waves

Table F.6: Significant wave heights of the penetrated waves for the six output locations

$H_{s,penetration}$ at location:	01 [m]	02 [m]	03 [m]	04 [m]	05 [m]	06 [m]
WGPO model	1.08	0.80	0.62	0.59	0.41	0.34
RIKZ method	1.07	1.04	0.62	0.64	0.46	0.33

The only clear mismatch between the model and the RIKZ method is found at location 02. This can readily be explained by the absence of the transmitted wave energy.

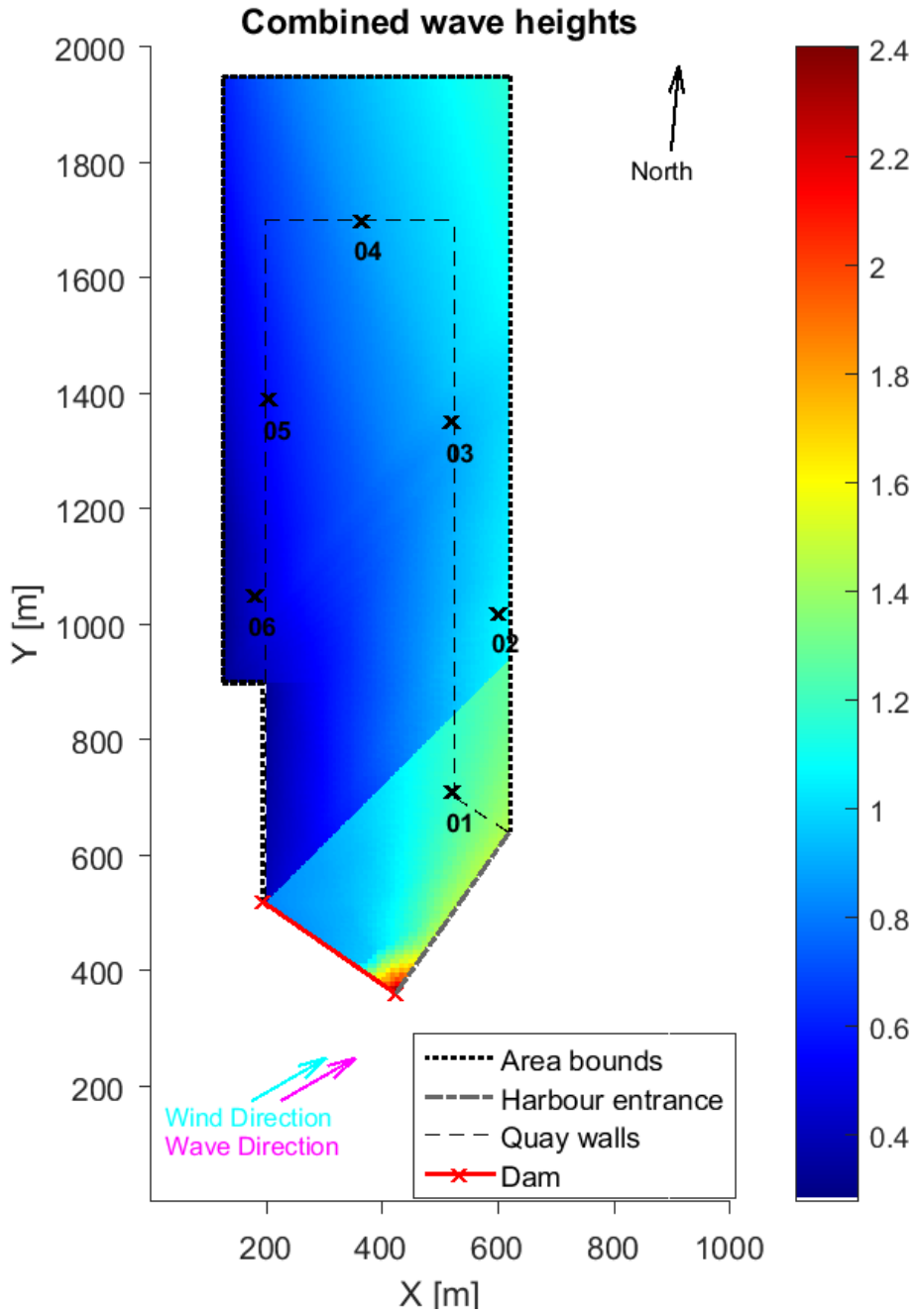

Figure F.7: Vlissingen outer harbour: combined wave height for the processes of wind-wave generation and wave penetration

Table F.7: Significant wave heights of the locally generated and penetrated waves combined for the six output locations

$H_{s,combined}$ at location:	01 [m]	02 [m]	03 [m]	04 [m]	05 [m]	06 [m]
WGPO model	1.20	1.05	0.90	0.83	0.55	0.56
RIKZ method	1.19	1.18	0.86	0.77	0.55	0.56

The values for the combined wave heights match up fairly well. The largest deviations are found at locations 02 and 04. At location 02 the deviation is again caused by the absence of transmitted wave energy in the WGPO model. At location 04 the difference can be explained by the use of a different formula for wave growth in which the Bretschneider formula (as applied in the WGPO model) sees faster wave growth compared to the Wilson formula in the RIKZ method.

F.3 Overtopping scenarios for 'Vlissingen Buitenhaven'

Using the 'Vlissingen Buitenhaven' case an analysis of wave overtopping can be undertaken. For various variables the sensitivity towards wave overtopping discharges will be evaluated after which some general conclusions can be drawn. For this purpose the still water level will be reduced to below the elevation level of the harbour areas (4.50 m+NAP). In this analysis the values of relevant parameters will be changed one by one. The base values and the range over which the sensitivity will be tested for the variables are:

Table F.8: Values for the variables in the sensitivity analysis

Variable	Base value	Minimum value	Maximum value
Still water level *h*	3.75 m +NAP	2.0 m+NAP	4.0 m+NAP
Wind speed u_{10}	33 m/s	20 m/s	35 m/s
Outside wave height $H_{s,outside}$	2.4 m	1.4 m	3.4 m

For the base values (equal to the design conditions except for the lower water level), the wave heights of the locally generated, penetrated and combined waves are shown in Figure F.8.

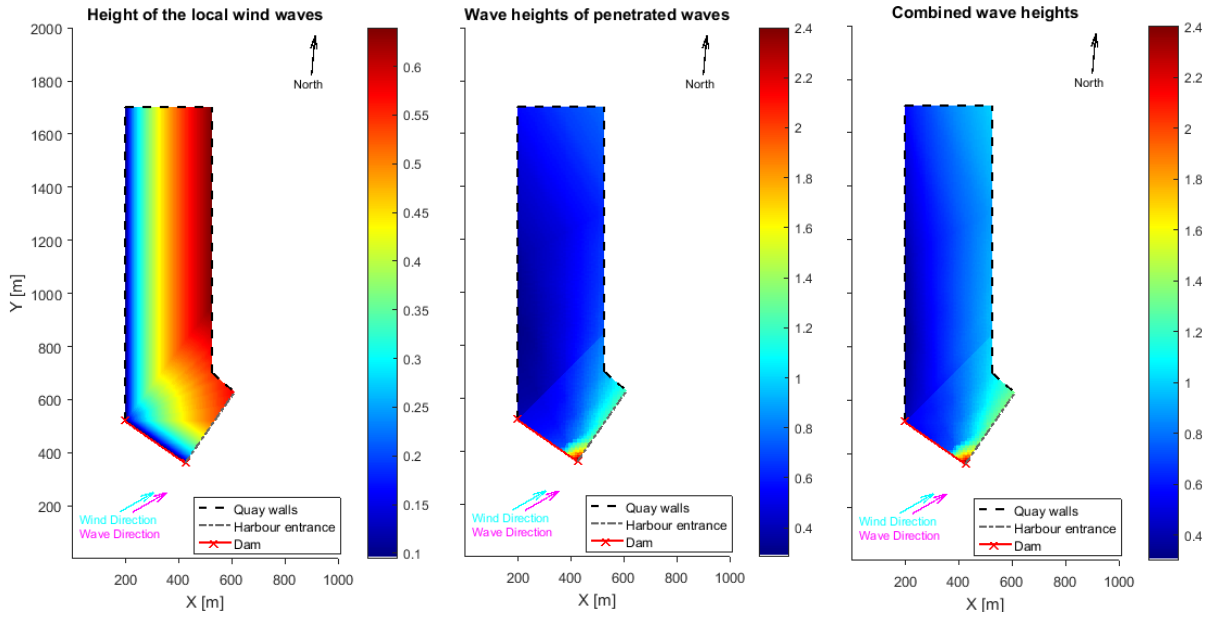

Figure F.8: Wave heights of the locally generated waves, penetrated waves and the combination of the two for a still water level of 3.75 m +NAP

For the four variables the effect on the mean wave heights, averaged over the entire basin, will be shown as well as the mean specific overtopping discharge (MSOD). This MSOD is the average of the specific overtopping discharges for the entire length of quay walls (2.6 kilometres)

F.3.1 Still water level

The dependency of the wave overtopping discharge occurs mainly via the freeboard. For higher water levels the freeboard will decrease such that more wave overtopping will occur. Slight dependencies on the wave height may also exist for a range of water levels. However, within the range of tested water levels the relative water depth will remain large. For relatively deep water

sensitivity to the water level is minor for both the wave length (and thus the diffraction) and the wind-wave generation.

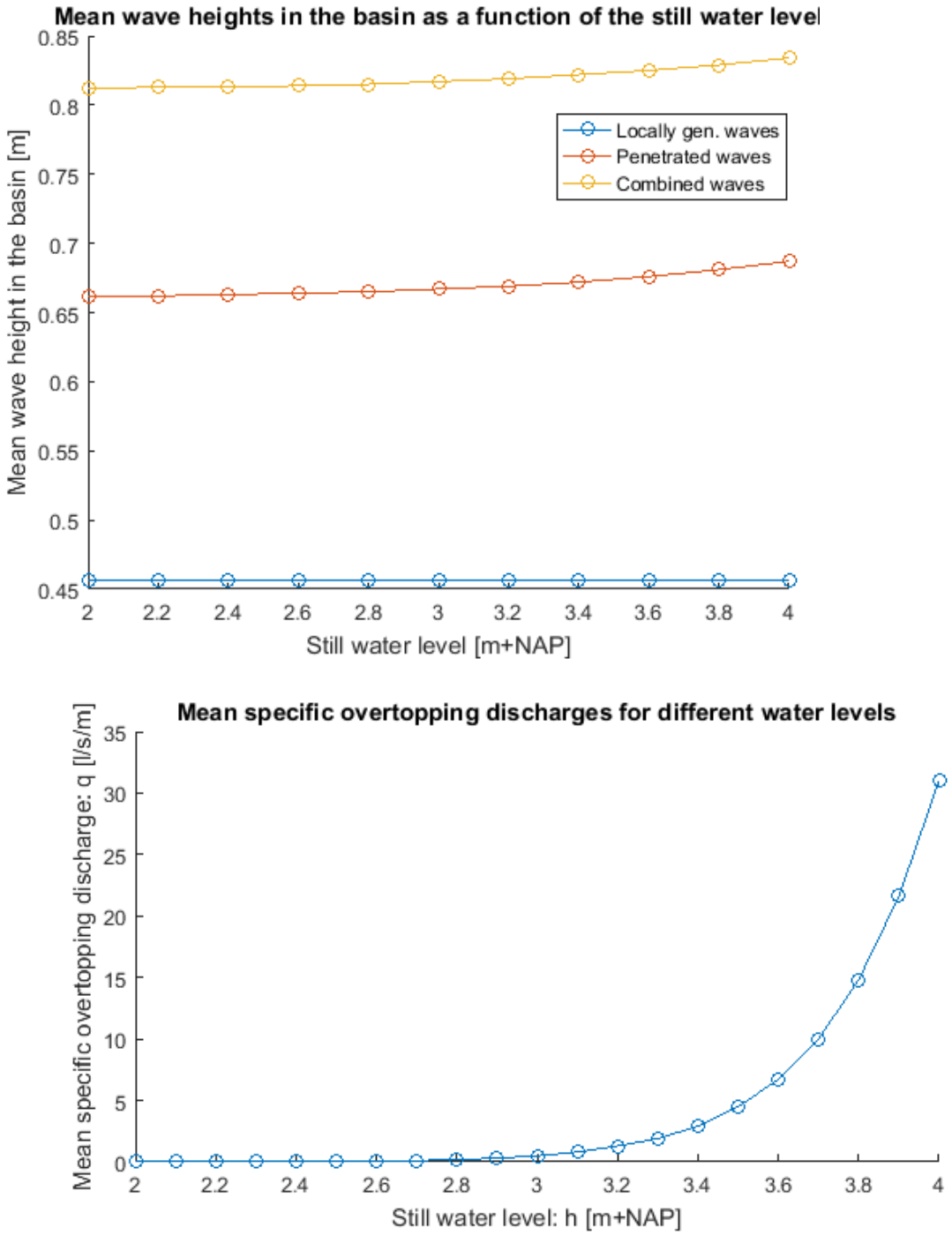

Figure F.9: Mean wave heights in the basin and the mean specific overtopping discharge for a range of still water levels for the *Vlissingen Buitenhaven* case. A bullet indicates the outcome of a model calculation.

F.3.2 Wind speed

The wind speed has a direct influence on the wind-generated waves in the basin. In its turn these increasing wave heights result in larger overtopping discharges.

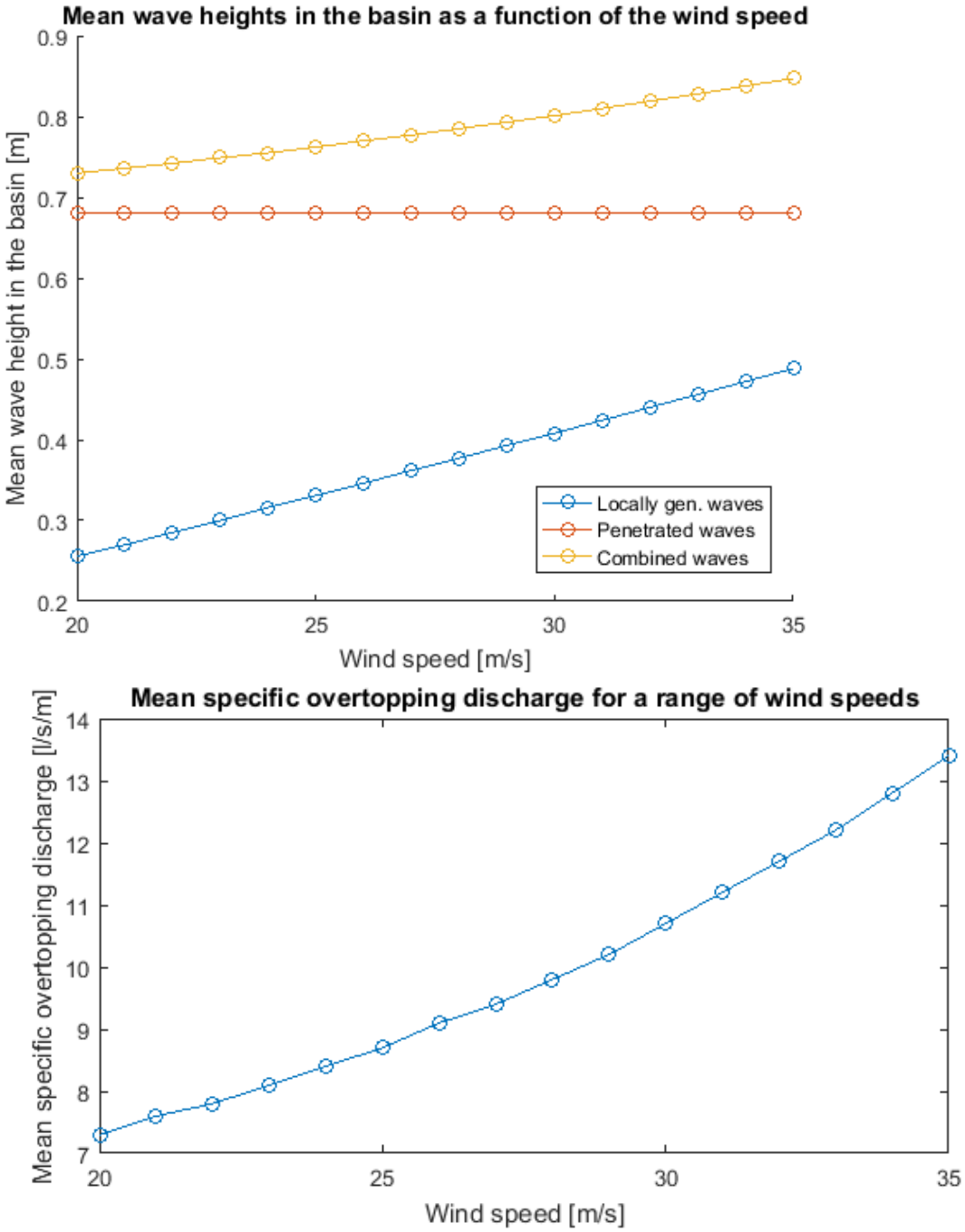

Figure F.10: Mean wave heights in the basin and the mean specific overtopping discharge for a range of wind speeds for the *Vlissingen Buitenhaven* case. A bullet indicates the outcome of a model calculation.

F.3.3 Outside wave height

The outside wave height has an obvious linear effect on the wave height inside the basin. No dependency of the wave diffraction coefficients on the outside wave height exists in the model. The larger wave heights inside the basin lead to an increase of the MSOD.

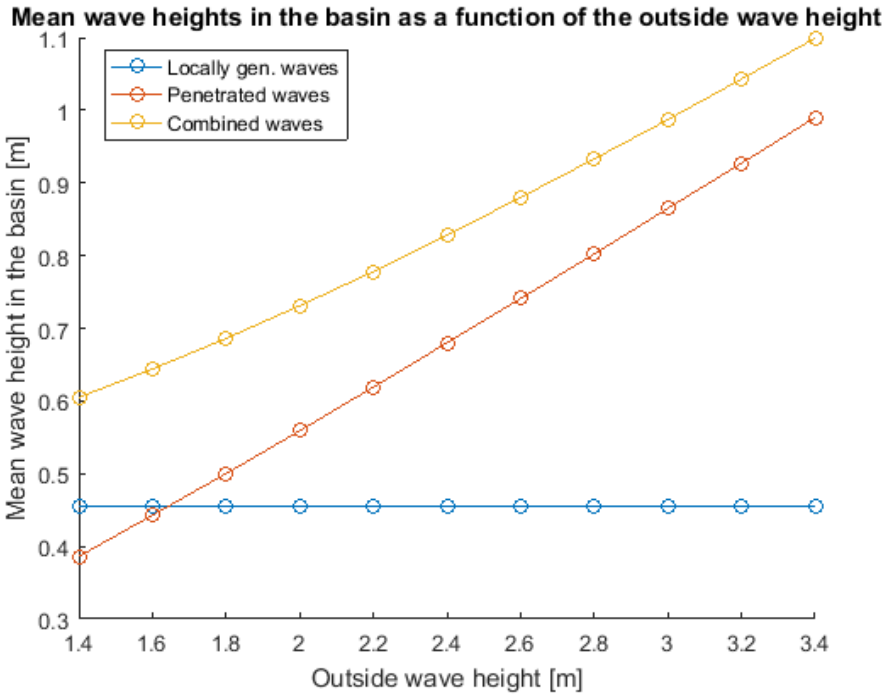

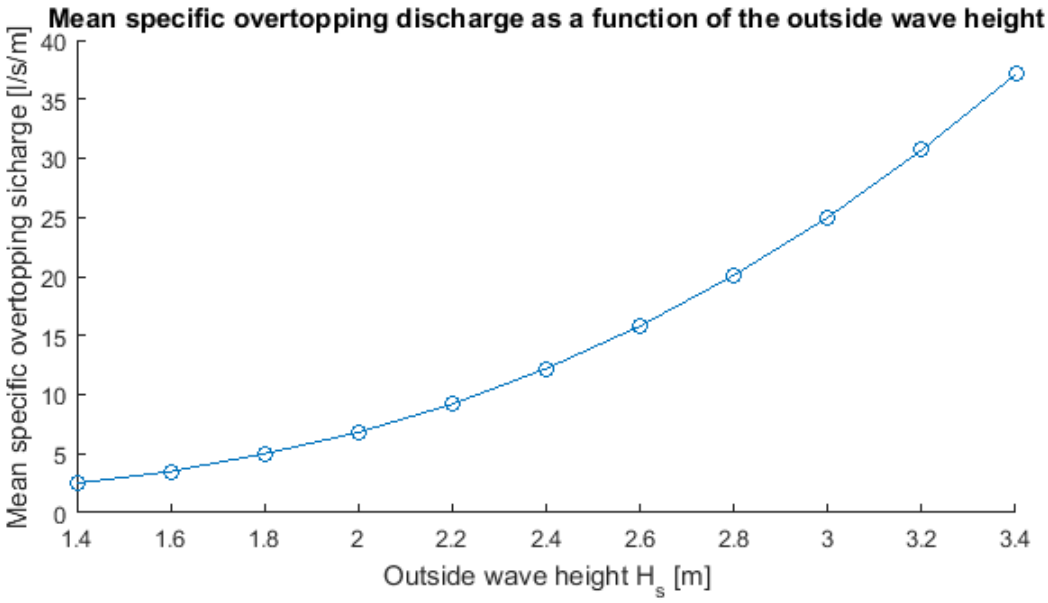

Figure F.11: Mean wave heights in the basin and the mean specific overtopping discharge for a range of outside wave heights for the *Vlissingen Buitenhaven* case. A bullet indicates the outcome of a model calculation.

Appendix G. Brittaniëhaven details

This appendix gives more background and results from the *Brittaniëhaven* case, studied in Chapter 5. Paragraph G.1 gives the Hydra-NL output breakdown for various return periods. This data is used as input for the flood risk analysis of paragraph 5.3. The second part of this appendix (G.2) shows the background of the model results, i.e. the wave height distributions in the basin.

G.1 Hydra-NL output breakdown

The Hydra-NL software is applied to find the input parameters for the WGPO model. The data which lies at the basis of this Hydra-NL calculation is found in the following database: '*CR2011_BenR_Rijndombuiten_oever_a_19_v01.mdb'*. The output location which is chosen is *´HRextra Europoort63´*. This location lies at the end of the *Brittaniëhaven* near the Calandbrug. This is also the end of the model domain as can be seen in Figure 5.4. The chosen output location is marked yellow in Figure G.1, which also shows the other possible output locations in green.

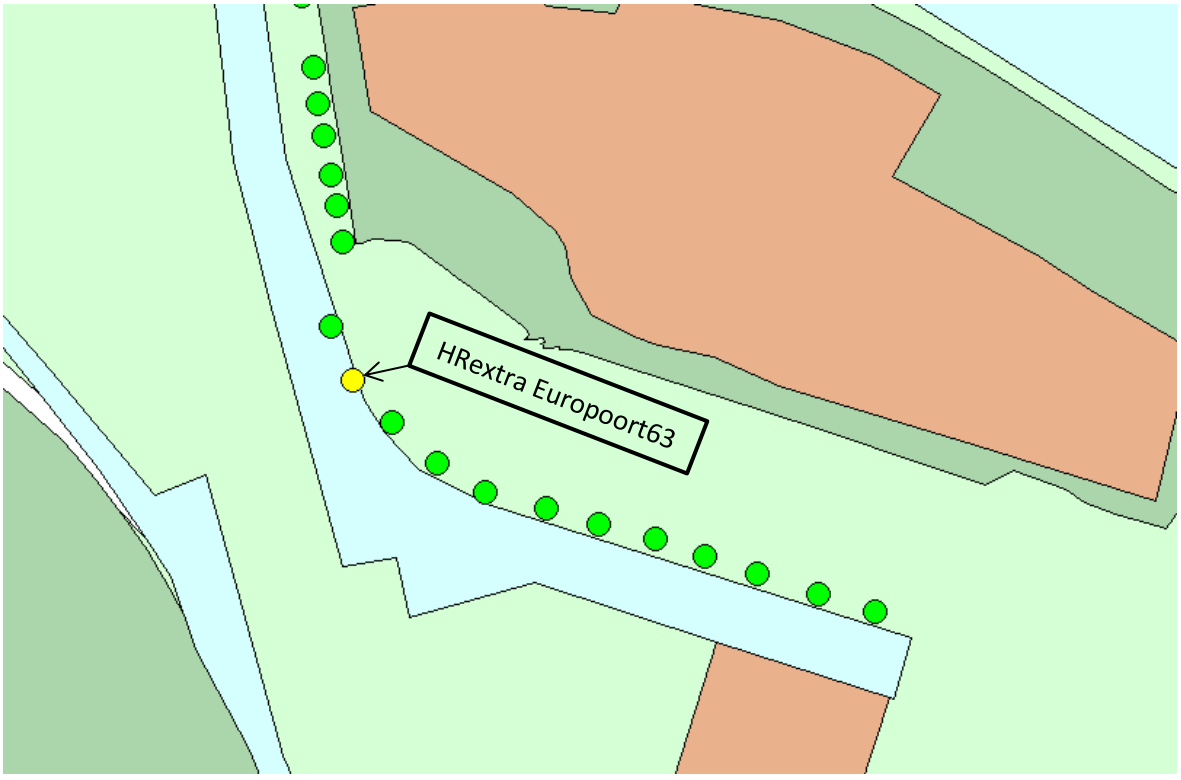

Figure G.1: Output locations of the Hydra database. The data used in the analyses originate from the yellow dot which marks location *´HRextra Europoort63´*

The water level statistics are covered in Figure G.2 which shows the still water level for various return periods. This graph corresponds to the values given in

Table 5.1. Subsequently, Figure G.3 up to Figure G.12 give the breakdown of the combinations of variables which lead to (critical) wave overtopping (a value of 1 l/s/m was chosen) with the given return period. Especially for low return periods many combinations of variables may lead to the same event. It can be seen that the western wind directions contribute most to the flood risk.

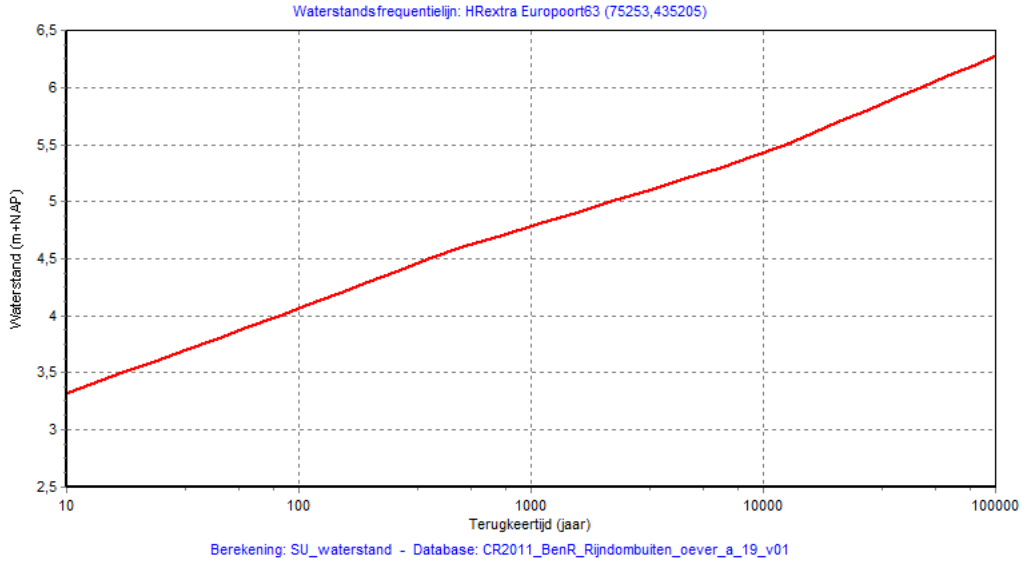

Figure G.2: Hydra output for water levels with a certain return period at location '*HRextra Europoort 63*'.

Geopende Europoortkering

r	zeews. m+NAP	q Rijn m³/s	q Maas m³/s	windsn. m/s	h,teen m+NAP	Hs,teen m	Tm-1,0,t s	golfr graden	ov. freq *0.001/whj	ov. freq %
NNO	1.33	10000	2095	26.7	2.37	0.56	2.3	345	0.000	0.0
NO	--	--	--	--	--	--	--	--	0.000	0.0
ONO	--	--	--	--	--	--	--	--	0.000	0.0
O	--	--	--	--	--	--	--	--	0.000	0.0
OZO	--	--	--	--	--	--	--	--	0.000	0.0
ZO	--	--	--	--	--	--	--	--	0.000	0.0
ZZO	--	--	--	--	--	--	--	--	0.000	0.0
Z	--	--	--	--	--	--	--	--	0.000	0.0
ZZW	1.33	2200	264	30.9	1.50	0.65	2.3	184	0.059	0.0
ZW	2.02	2250	276	22.9	2.19	0.40	1.8	199	24.213	2.4
WZW	2.21	2250	276	20.7	2.41	0.30	1.6	230	48.317	4.8
W	2.34	2000	217	18.0	2.55	0.26	1.5	289	104.459	10.4
WNW	2.30	2000	217	16.8	2.51	0.31	1.8	327	163.678	16.4
NW	2.26	2250	276	15.6	2.48	0.36	2.0	337	170.179	17.0
NNW	2.34	2200	264	15.0	2.54	0.37	2.0	340	77.269	7.7
N	2.40	2000	217	15.9	2.60	0.37	2.0	342	7.309	0.7
som									595.484	59.5

Figure G.3: Hydra output for a return period of T = 1 year. Note that these conditions are for an opened Europoortkering; at this water level the Europoortkering will generally not be closed and as the *Brittaniëhaven* lies outside of these protections it has no influence on the conditions for higher return periods (and is therefore assumed to be closed).

Gesloten Europoortkering

r	zeews. m+NAP	q Rijn m³/s	q Maas m³/s	windsn. m/s	h,teen m+NAP	Hs,teen m	Tm-1,0,t s	golfr graden	ov. freq *0.001/whj	ov. freq %
NNO	--	--	--	--	--	--	--	--	0.000	0.0
NO	--	--	--	--	--	--	--	--	0.000	0.0
ONO	--	--	--	--	--	--	--	--	0.000	0.0
O	--	--	--	--	--	--	--	--	0.000	0.0
OZO	--	--	--	--	--	--	--	--	0.000	0.0
ZO	--	--	--	--	--	--	--	--	0.000	0.0
ZZO	--	--	--	--	--	--	--	--	0.000	0.0
Z	--	--	--	--	--	--	--	--	0.000	0.0
ZZW	--	--	--	--	--	--	--	--	0.000	0.0
ZW	2.35	7600	1532	19.3	2.74	0.32	1.7	198	1.821	0.4
WZW	2.55	3800	640	18.3	2.84	0.26	1.5	229	17.379	3.5
W	2.60	3200	499	16.7	2.90	0.24	1.5	289	84.588	16.9
WNW	2.60	3750	628	15.0	2.90	0.28	1.7	327	120.260	24.1
NW	2.55	4750	863	14.0	2.87	0.32	1.9	337	109.665	21.9
NNW	2.60	4800	875	13.6	2.92	0.33	1.9	340	50.168	10.0
N	2.74	3250	511	13.0	3.04	0.30	1.8	342	6.509	1.3
som									390.390	78.1

Figure G.4: Hydra output for a return period of T = 2 years

Gesloten Europoortkering

r	zeews. m+NAP	q Rijn m³/s	q Maas m³/s	windsn. m/s	h,teen m+NAP	Hs,teen m	Tm-1,0,t s	golfr graden	ov. freq *0.001/whj	ov. freq %
NNO	--	--	--	--	--	--	--	--	0.000	0.0
NO	--	--	--	--	--	--	--	--	0.000	0.0
ONO	--	--	--	--	--	--	--	--	0.000	0.0
O	--	--	--	--	--	--	--	--	0.000	0.0
OZO	--	--	--	--	--	--	--	--	0.000	0.0
ZO	--	--	--	--	--	--	--	--	0.000	0.0
ZZO	--	--	--	--	--	--	--	--	0.000	0.0
Z	--	--	--	--	--	--	--	--	0.000	0.0
ZZW	--	--	--	--	--	--	--	--	0.000	0.0
ZW	2.58	3200	499	24.0	2.85	0.43	1.9	199	1.170	0.6
WZW	2.70	2600	358	22.5	3.01	0.34	1.6	230	7.784	3.9
W	2.80	2600	358	20.6	3.15	0.31	1.6	290	34.004	17.0
WNW	2.80	2600	358	18.5	3.14	0.35	1.9	327	58.727	29.4
NW	2.79	2600	358	17.0	3.13	0.39	2.0	337	67.034	33.5
NNW	2.82	2600	358	17.0	3.16	0.42	2.1	340	28.263	14.1
N	2.99	2750	393	16.1	3.33	0.38	2.0	342	2.251	1.1
som									199.232	99.6

Figure G.5: Hydra output for a return period of T = 5 years

Gesloten Europoortkering

r	zeews. m+NAP	q Rijn m³/s	q Maas m³/s	windsn. m/s	h,teen m+NAP	Hs,teen m	Tm-1,0,t s	golfr graden	ov. freq *0.001/whj	ov. freq %
NNO	--	--	--	--	--	--	--	--	0.000	0.0
NO	--	--	--	--	--	--	--	--	0.000	0.0
ONO	--	--	--	--	--	--	--	--	0.000	0.0
O	--	--	--	--	--	--	--	--	0.000	0.0
OZO	--	--	--	--	--	--	--	--	0.000	0.0
ZO	--	--	--	--	--	--	--	--	0.000	0.0
ZZO	--	--	--	--	--	--	--	--	0.000	0.0
Z	--	--	--	--	--	--	--	--	0.000	0.0
ZZW	--	--	--	--	--	--	--	--	0.000	0.0
ZW	2.67	2800	405	27.0	2.94	0.49	2.0	200	0.478	0.5
WZW	2.80	2600	358	25.1	3.14	0.39	1.7	230	3.198	3.2
W	2.95	2400	311	22.4	3.34	0.35	1.7	290	15.853	15.9
WNW	2.95	2400	311	20.6	3.33	0.40	2.0	327	28.987	29.0
NW	2.97	2250	276	18.6	3.34	0.43	2.1	337	36.323	36.3
NNW	3.01	2250	276	18.6	3.38	0.47	2.2	340	14.262	14.3
N	3.19	2750	393	18.0	3.55	0.43	2.1	342	0.897	0.9
som									99.997	100.0

Figure G.6: Hydra output for a return period of T = 10 years

Gesloten Europoortkering

r	zeews. m+NAP	q Rijn m³/s	q Maas m³/s	windsn. m/s	h,teen m+NAP	Hs,teen m	Tm-1,0,t s	golfr graden	ov. freq *0.001/whj	ov. freq %
NNO	--	--	--	--	--	--	--	--	0.000	0.0
NO	--	--	--	--	--	--	--	--	0.000	0.0
ONO	--	--	--	--	--	--	--	--	0.000	0.0
O	--	--	--	--	--	--	--	--	0.000	0.0
OZO	--	--	--	--	--	--	--	--	0.000	0.0
ZO	--	--	--	--	--	--	--	--	0.000	0.0
ZZO	--	--	--	--	--	--	--	--	0.000	0.0
Z	--	--	--	--	--	--	--	--	0.000	0.0
ZZW	--	--	--	--	--	--	--	--	0.000	0.0
ZW	2.78	2750	393	29.6	3.08	0.55	2.1	201	0.147	0.3
WZW	2.93	2250	276	27.4	3.31	0.44	1.8	231	1.235	2.5
W	3.09	2250	276	24.5	3.52	0.39	1.8	290	7.332	14.7
WNW	3.10	2400	311	22.6	3.52	0.44	2.1	327	14.375	28.7
NW	3.13	2250	276	20.6	3.53	0.48	2.3	337	19.669	39.3
NNW	3.21	2250	276	20.3	3.60	0.52	2.3	340	6.895	13.8
N	3.45	2750	393	19.0	3.83	0.46	2.2	342	0.347	0.7
som									50.000	100.0

Figure G.7: Hydra output for a return period of T = 20 years

Gesloten Europoortkering

r	zeews. m+NAP	q Rijn m³/s	q Maas m³/s	windsn. m/s	h,teen m+NAP	Hs,teen m	Tm-1,0,t s	golfr graden	ov. freq *0.001/whj	ov. freq %
NNO	--	--	--	--	--	--	--	--	0.000	0.0
NO	--	--	--	--	--	--	--	--	0.000	0.0
ONO	--	--	--	--	--	--	--	--	0.000	0.0
O	--	--	--	--	--	--	--	--	0.000	0.0
OZO	--	--	--	--	--	--	--	--	0.000	0.0
ZO	--	--	--	--	--	--	--	--	0.000	0.0
ZZO	--	--	--	--	--	--	--	--	0.000	0.0
Z	--	--	--	--	--	--	--	--	0.000	0.0
ZZW	--	--	--	--	--	--	--	--	0.000	0.0
ZW	2.92	2750	393	32.7	3.25	0.63	2.2	202	0.030	0.1
WZW	3.12	2250	276	30.3	3.54	0.50	1.9	231	0.339	1.7
W	3.33	2250	276	27.0	3.79	0.44	1.9	290	2.515	12.6
WNW	3.37	2250	276	24.5	3.83	0.49	2.1	327	5.576	27.9
NW	3.37	2250	276	22.5	3.81	0.54	2.3	337	8.861	44.3
NNW	3.50	2200	264	21.8	3.93	0.56	2.4	340	2.582	12.9
N	3.75	2750	393	21.0	4.16	0.51	2.3	342	0.097	0.5
som									20.000	100.0

Figure G.8: Hydra output for a return period of T = 50 years

Gesloten Europoortkering

r	zeews. m+NAP	q Rijn m³/s	q Maas m³/s	windsn. m/s	h,teen m+NAP	Hs,teen m	Tm-1,0,t s	golfr graden	ov. freq *0.001/whj	ov. freq %
NNO	--	--	--	--	--	--	--	--	0.000	0.0
NO	--	--	--	--	--	--	--	--	0.000	0.0
ONO	--	--	--	--	--	--	--	--	0.000	0.0
O	--	--	--	--	--	--	--	--	0.000	0.0
OZO	--	--	--	--	--	--	--	--	0.000	0.0
ZO	--	--	--	--	--	--	--	--	0.000	0.0
ZZO	--	--	--	--	--	--	--	--	0.000	0.0
Z	--	--	--	--	--	--	--	--	0.000	0.0
ZZW	--	--	--	--	--	--	--	--	0.000	0.0
ZW	3.02	2568	350	35.0	3.36	0.70	2.3	202	0.009	0.1
WZW	3.29	2250	276	31.9	3.73	0.54	2.0	231	0.128	1.3
W	3.50	2400	311	29.0	4.00	0.48	2.0	290	1.120	11.2
WNW	3.56	2250	276	26.1	4.05	0.53	2.2	326	2.666	26.7
NW	3.56	2250	276	23.9	4.03	0.58	2.4	337	4.808	48.1
NNW	3.71	2250	276	23.0	4.18	0.60	2.5	340	1.232	12.3
N	3.96	2750	393	22.5	4.41	0.56	2.4	342	0.036	0.4
som									10.000	100.0

Figure G.9: Hydra output for a return period of T = 100 years

Gesloten Europoortkering

r	zeews. m+NAP	q Rijn m³/s	q Maas m³/s	windsn. m/s	h,teen m+NAP	Hs,teen m	Tm-1,0,t s	golfr graden	ov. freq *0.001/whj	ov. freq %
NNO	--	--	--	--	--	--	--	--	0.000	0.0
NO	--	--	--	--	--	--	--	--	0.000	0.0
ONO	--	--	--	--	--	--	--	--	0.000	0.0
O	--	--	--	--	--	--	--	--	0.000	0.0
OZO	--	--	--	--	--	--	--	--	0.000	0.0
ZO	--	--	--	--	--	--	--	--	0.000	0.0
ZZO	--	--	--	--	--	--	--	--	0.000	0.0
Z	--	--	--	--	--	--	--	--	0.000	0.0
ZZW	--	--	--	--	--	--	--	--	0.000	0.0
ZW	3.20	2400	311	36.6	3.55	0.74	2.4	202	0.002	0.0
WZW	3.48	2250	276	33.1	3.94	0.57	2.0	231	0.046	0.9
W	3.68	2250	276	30.7	4.20	0.52	2.0	290	0.491	9.8
WNW	3.75	2250	276	27.7	4.27	0.57	2.3	326	1.256	25.1
NW	3.78	2200	264	25.0	4.29	0.61	2.5	336	2.611	52.2
NNW	3.91	2250	276	24.5	4.40	0.64	2.6	340	0.581	11.6
N	4.25	2750	393	23.7	4.66	0.59	2.5	342	0.012	0.2
som									5.000	100.0

Figure G.10: Hydra output for a return period of T = 200 years

Gesloten Europoortkering

r	zeews. m+NAP	q Rijn m³/s	q Maas m³/s	windsn. m/s	h,teen m+NAP	Hs,teen m	Tm-1,0,t s	golfr graden	ov. freq *0.001/whj	ov. freq %
NNO	--	--	--	--	--	--	--	--	0.000	0.0
NO	--	--	--	--	--	--	--	--	0.000	0.0
ONO	--	--	--	--	--	--	--	--	0.000	0.0
O	--	--	--	--	--	--	--	--	0.000	0.0
OZO	--	--	--	--	--	--	--	--	0.000	0.0
ZO	--	--	--	--	--	--	--	--	0.000	0.0
ZZO	--	--	--	--	--	--	--	--	0.000	0.0
Z	--	--	--	--	--	--	--	--	0.000	0.0
ZZW	--	--	--	--	--	--	--	--	0.000	0.0
ZW	3.39	2600	358	39.0	3.76	0.81	2.4	203	0.000	0.0
WZW	3.62	2250	276	36.0	4.11	0.64	2.1	232	0.012	0.6
W	3.92	2250	276	32.5	4.48	0.56	2.1	289	0.177	8.8
WNW	4.01	2250	276	29.7	4.57	0.62	2.4	326	0.476	23.8
NW	4.05	2200	264	26.7	4.58	0.66	2.5	336	1.137	56.9
NNW	4.25	2200	264	26.0	4.72	0.69	2.6	340	0.195	9.7
N	4.62	2750	393	25.6	4.97	0.65	2.6	342	0.003	0.1
som									2.000	100.0

Figure G.11: Hydra output for a return period of T = 500 years

Gesloten Europoortkering

r	zeews. m+NAP	q Rijn m³/s	q Maas m³/s	windsn. m/s	h,teen m+NAP	Hs,teen m	Tm-1,0,t s	golfr graden	ov. freq *0.001/whj	ov. freq %
NNO	--	--	--	--	--	--	--	--	0.000	0.0
NO	--	--	--	--	--	--	--	--	0.000	0.0
ONO	--	--	--	--	--	--	--	--	0.000	0.0
O	--	--	--	--	--	--	--	--	0.000	0.0
OZO	--	--	--	--	--	--	--	--	0.000	0.0
ZO	--	--	--	--	--	--	--	--	0.000	0.0
ZZO	--	--	--	--	--	--	--	--	0.000	0.0
Z	--	--	--	--	--	--	--	--	0.000	0.0
ZZW	--	--	--	--	--	--	--	--	0.000	0.0
ZW	3.65	2400	311	39.4	4.03	0.82	2.5	203	0.000	0.0
WZW	3.82	2250	276	37.4	4.33	0.67	2.2	232	0.005	0.5
W	4.07	2250	276	34.3	4.66	0.61	2.2	289	0.080	8.0
WNW	4.18	2250	276	31.3	4.73	0.66	2.4	325	0.228	22.8
NW	4.24	2250	276	28.2	4.75	0.70	2.6	336	0.600	60.0
NNW	4.50	2200	264	27.3	4.93	0.73	2.7	340	0.086	8.6
N	4.94	2750	393	26.3	5.23	0.68	2.6	342	0.001	0.1
som									1.000	100.0

Figure G.12: Hydra output for a return period of T = 1000 years

G.2 Breakdown of the model results

In this paragraph of Appendix G examples of the interim model results are shown. This should give insight in the contribution of certain processes and the spatial distribution of these contributions. Two sets of conditions are considered. These correspond to the western wind direction and a return period of 2 years and a return period of 200 years. The boundary conditions which correspond to these return periods are given in Table G.1 below

Table G.1: Boundary conditions for the *Brittaniëhaven* case which apply to return periods of 2 and 200 years.

Return period T [years]	Still water level [m+NAP]	Wind direction [°N]	Wind speed [m/s]	Incoming wave height [m]
2	2.81	270	18.5	0.27
200	4.25	270	30.2	0.52

For convenience the schematization of the bathymetry of the *Brittaniëhaven* is repeated in Figure G.13. The results are broken down and visualized for the following variables:

- Fetch (G.2.1)
- Wave heights of the locally wind generated waves (G.2.2)
- Wave heights of the penetrated waves (G.2.3)
- Combined wave heights (G.2.4)
- Overtopping discharges (G.2.5)

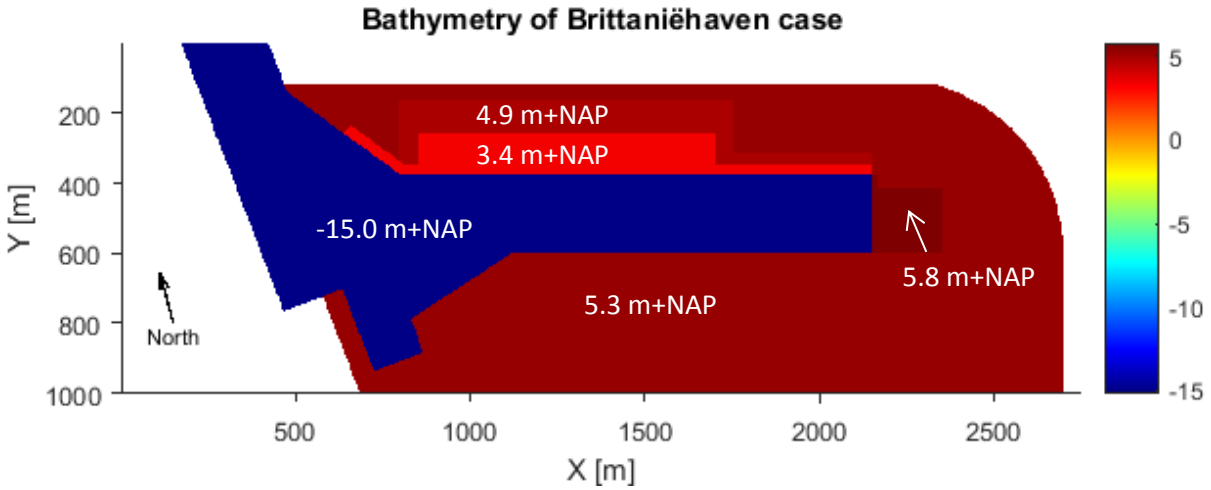

Figure G.13: Bathymetry of the *Brittaniëhaven* case

G.2.1 Fetches

Figure G.14 and Figure G.15 show the fetches for the return periods of 2 and 200 years respectively. The only difference between the two figures is the result of the inundation of the northern quay walls. The maximum fetch occurring in the entire basin is equal for both return periods and is approximately 1800 meters.

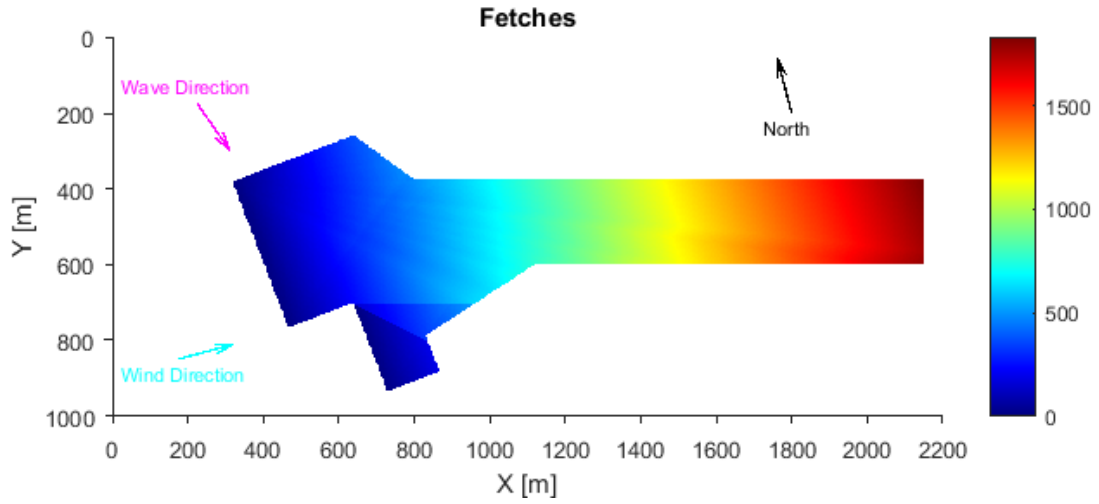

Figure G.14: (Maximum) Fetches in the *Brittaniëhaven* case for T = 2 years

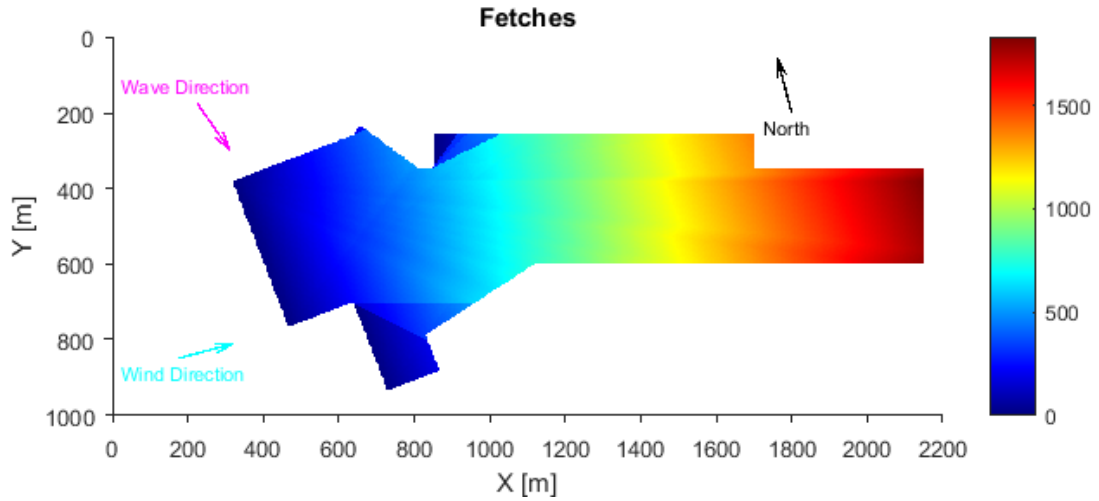

Figure G.15: (Maximum) Fetches in the *Brittaniëhaven* case for T = 200 years

To illustrate the difference between the maximum fetch and the effective fetch approach, Figure G.16 shows the effective fetch for a return period of 2 years. The largest fetch now occurring in the basin reduces to approximately 700 meters. The large difference is mainly due to the fact that the *Brittaniëhaven* is a narrow harbour, such that the fetches in the sector around the principle wind direction are fairly small. The effects of the effective fetch principle on the probability of flooding were tested in paragraph 5.4.1.

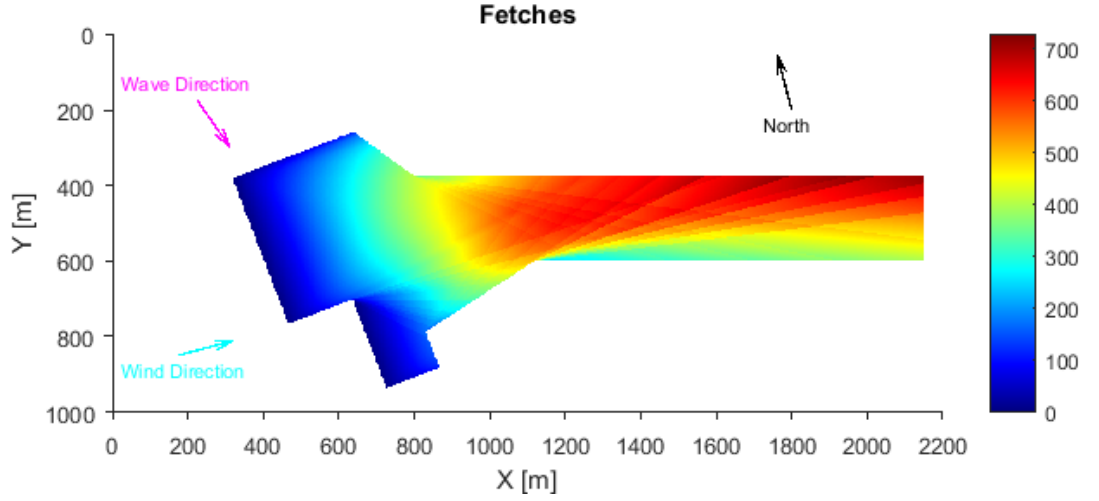

Figure G.16: Effective fetches in the *Brittaniëhaven* for T = 2 years.

G.2.2 Wave heights of the locally generated waves

Figure G.17 and Figure G.18 show the wave heights for the locally generated waves for the return periods of 2 and 200 years. The spatial distribution remains fairly the same. However, due to the increased wind speed for a return period of 200 years, the wave heights are approximately a factor 1.5 higher in Figure G.18.

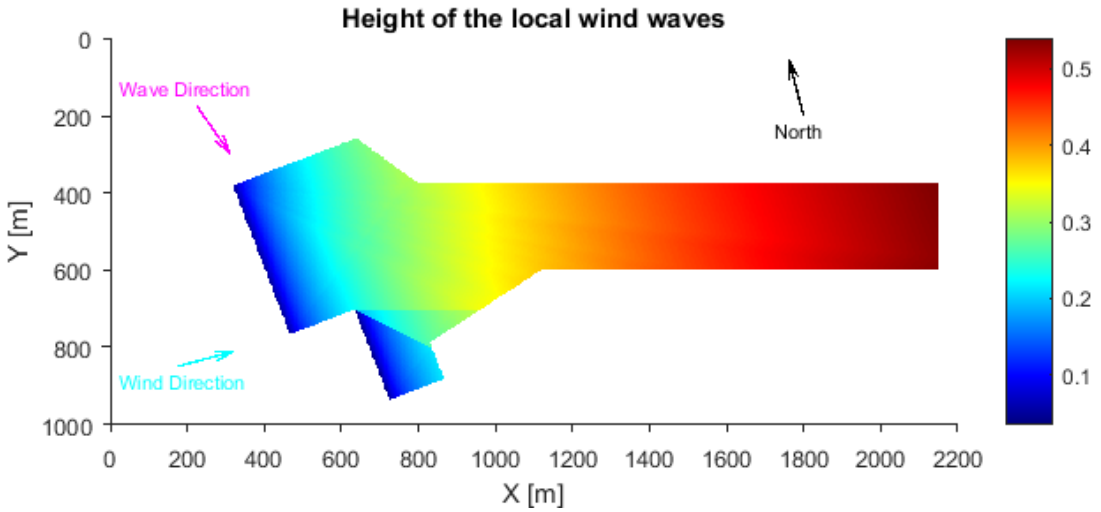

Figure G.17: Wave heights of the locally generated waves for T = 2 years

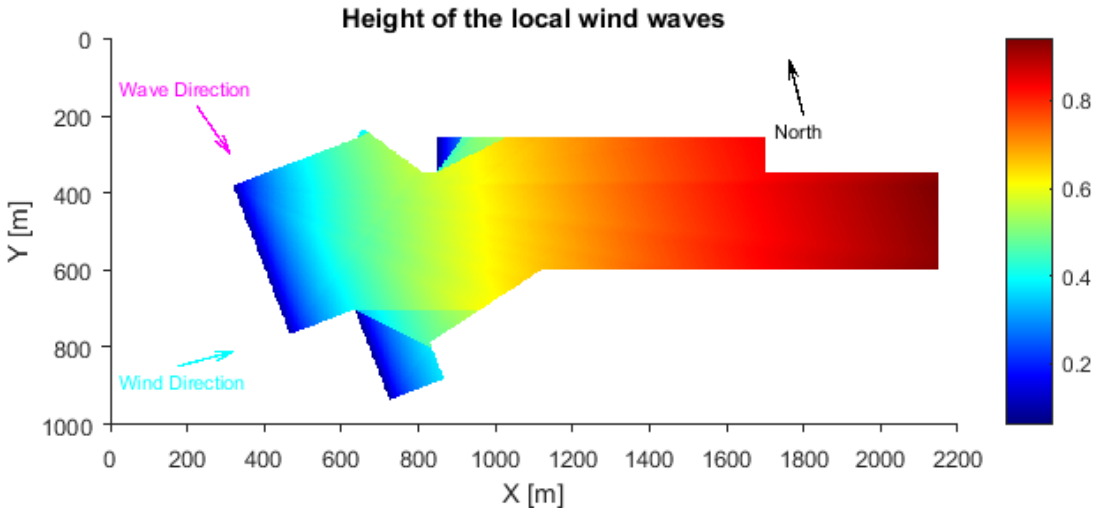

Figure G.18: Wave heights of the locally generated waves for T = 200 years

G.2.3 Wave heights of the penetrated waves

Figure G.19 and Figure G.20 show the modelled penetrated wave heights in the *Brittaniëhaven*. These figures show that the wave penetration into the harbour is little compared to the locally generated waves. This is mainly due to the low wave heights at the harbour entrance and the low wave period of these waves. Such waves with low periods diffract less. It must be noted that the size of the *Brittaniëhaven* exceeds the limits of the diffraction diagrams, again (mainly) as a result of the low wave periods. Behind these limits it was assumed that the minimum diffraction coefficient of the shadow zone is valid for the remainder of the basin. This likely results in an overestimation of the wave heights of the penetrated waves. However, the assumption of no wave diffraction outside of the diagram limits and thus no wave penetration into the *Brittaniëhaven* at all, also seems invalid.

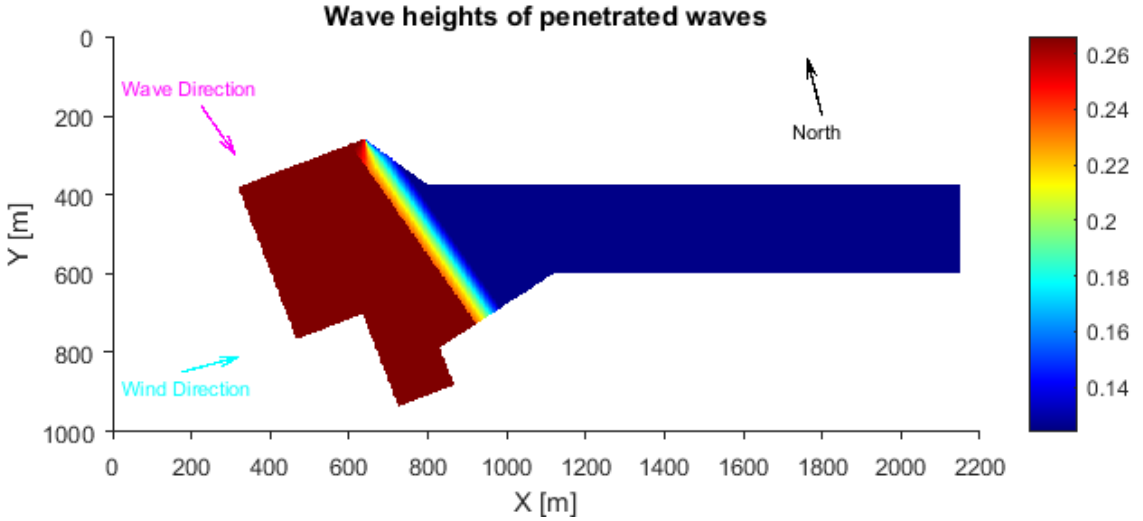

Figure G.19: Penetrated wave heights for T = 2 years

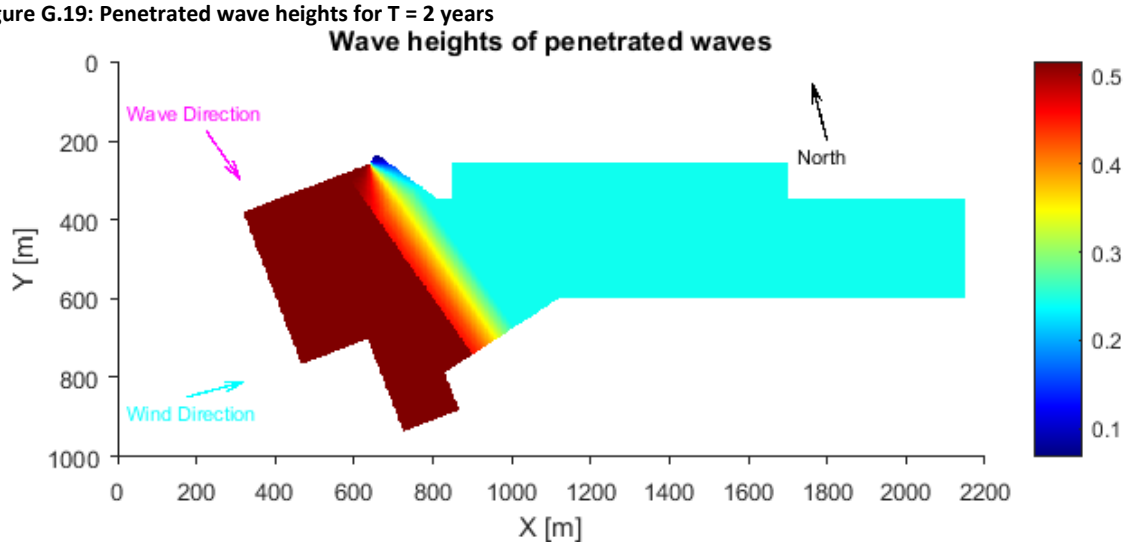

Figure G.20: Penetrated wave heights for T = 200 years

G.2.4 Combined wave heights

The combined wave heights from the two sources of locally generated waves and penetrated waves are shown in Figure G.21 and Figure G.21. The figures are an obvious result when looking at the figures for the two individual sources. The seemingly irregular pattern is therefore also explainable. It can be seen that the wind waves dominate the wave heights in the eastern part of the basin.

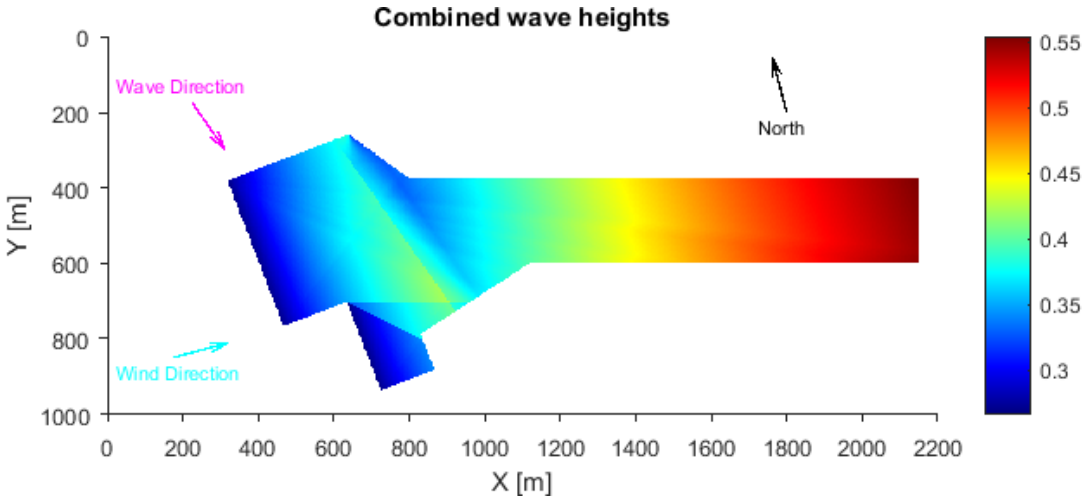

Figure G.21: Combined wave heights for T = 2 years

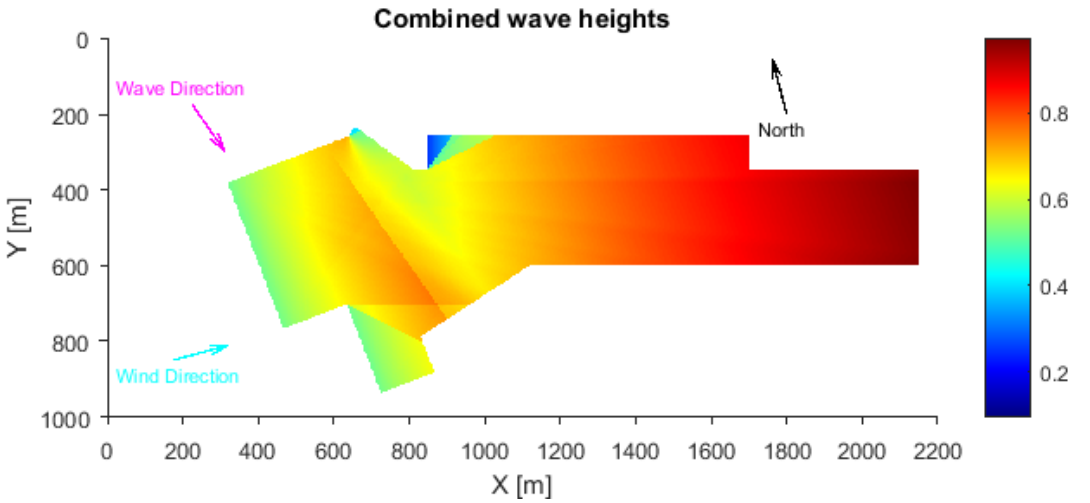

Figure G.22: Combined wave heights for T = 200 years

G.2.5 Overtopping discharges

The spatial distribution of the overtopping discharges along the quay walls of the *Brittaniëhaven* are shown in Figure G.23 and Figure G.24. It can be seen that for a return period of 2 years only the northern quay wall is overtopped. Wave overtopping for this northern quay wall increases in eastern direction. This is due to the increase in wave heights towards the east. The maximum overtopping discharge occurring for T = 2 years is 0.49 l/s/m. For the conditions with a return period of 200 years the primary northern quays are completely inundated. Also the sloping (1:50) harbour area behind these experiences large inundation (>5 l/s/m). The eastern and southern quays experience overtopping discharges of 0.4 l/s/m up to 1.5 l/s/m.

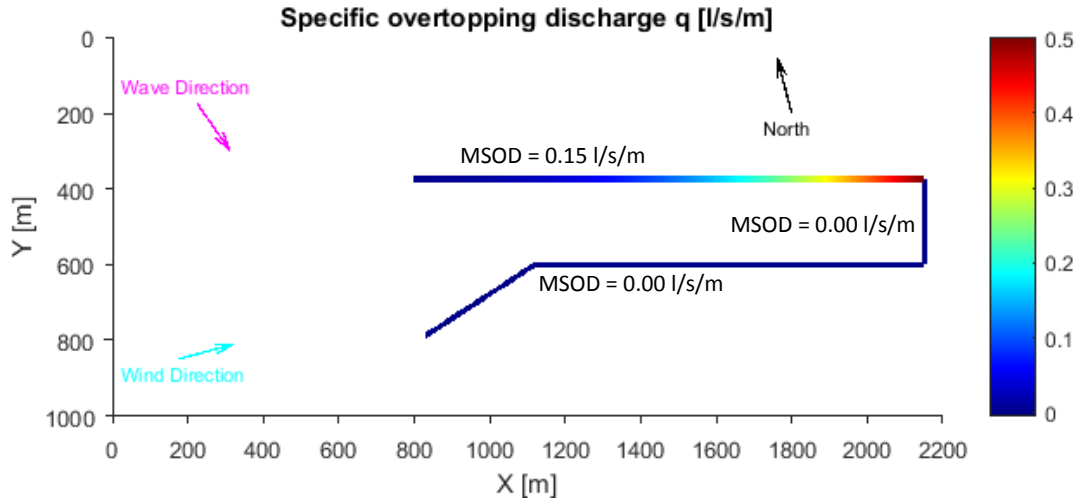

Figure G.23: Overtopping discharges over the quays of the *Brittaniëhaven* for T = 2 years

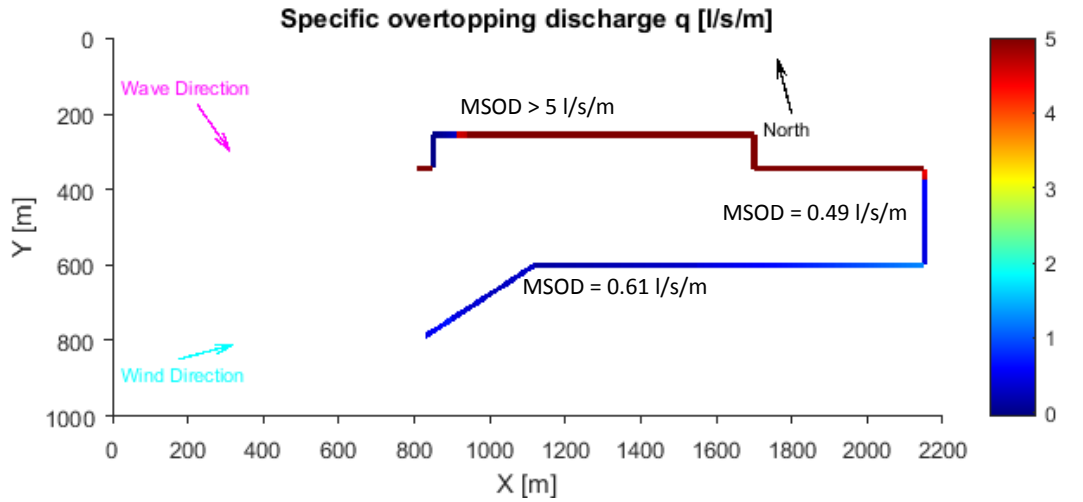

Figure G.24: Overtopping discharges over the quays and structures of the *Brittaniëhaven* for T = 200 years

Appendix H. Maps and images of the Rotterdam harbour

The following areas and other points of interest have been indicated in Figure H.1: *Map of the western part of the Rotterdam harbour area. Source: Google Maps (2016).*

Areas:

- Maasvlakte and Maasvlakte 2
- Europoortgebied
- Botlekgebied
- Vondelingenplaat

Bodies of water:

- Nieuwe Waterweg
- Calandkanaal
- Hartelkanaal
- Brittaniëhaven
- Seinehaven

Other:

- Maeslant storm surge barrier
- Hartelkering
- Europoortkering (Maeslant barrier + Hartelkering + dikes between the two barriers)
- Rozenburgse sluis

The following areas and other points of interest have been indicated in Figure H.2: *Aerial picture of the Brittaniëhaven and its surroundings. Source: Google Maps (2016)*

Areas and harbours:

- Rozenburg (town inside dike ring 19)
- Brittaniëhaven
- Seinehaven
- Botlekgebied

Channels:

- Nieuwe Waterweg
- Calandkanaal
- Hartelkanaal

Other:

- Rozenburgse sluis
- Calandbrug wind shield (discontinuous, 1750 meter long and 25 meters high wind shield)

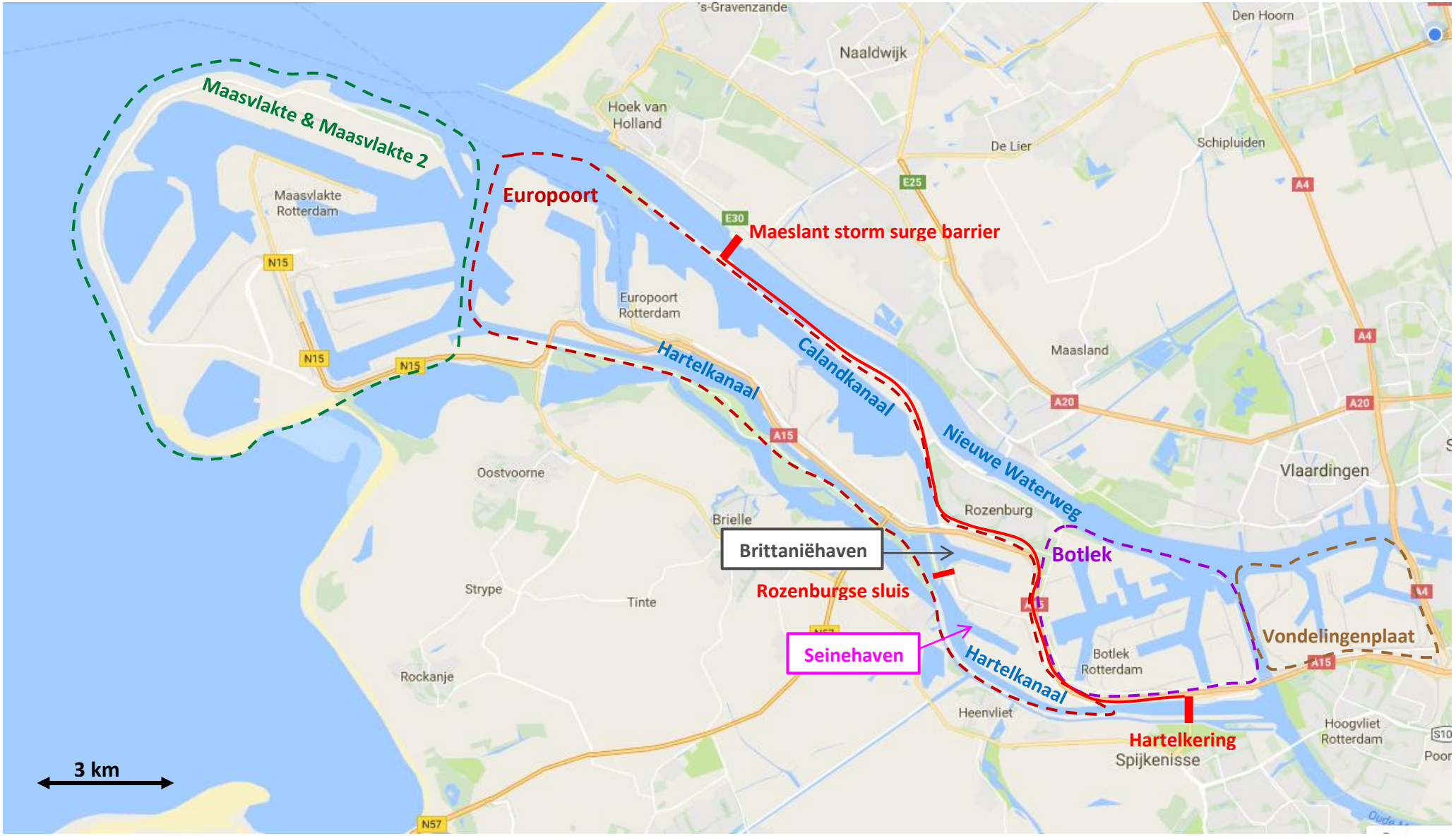

Figure H.1: Map of the western part of the Rotterdam harbour area. Source: Google Maps (2016)

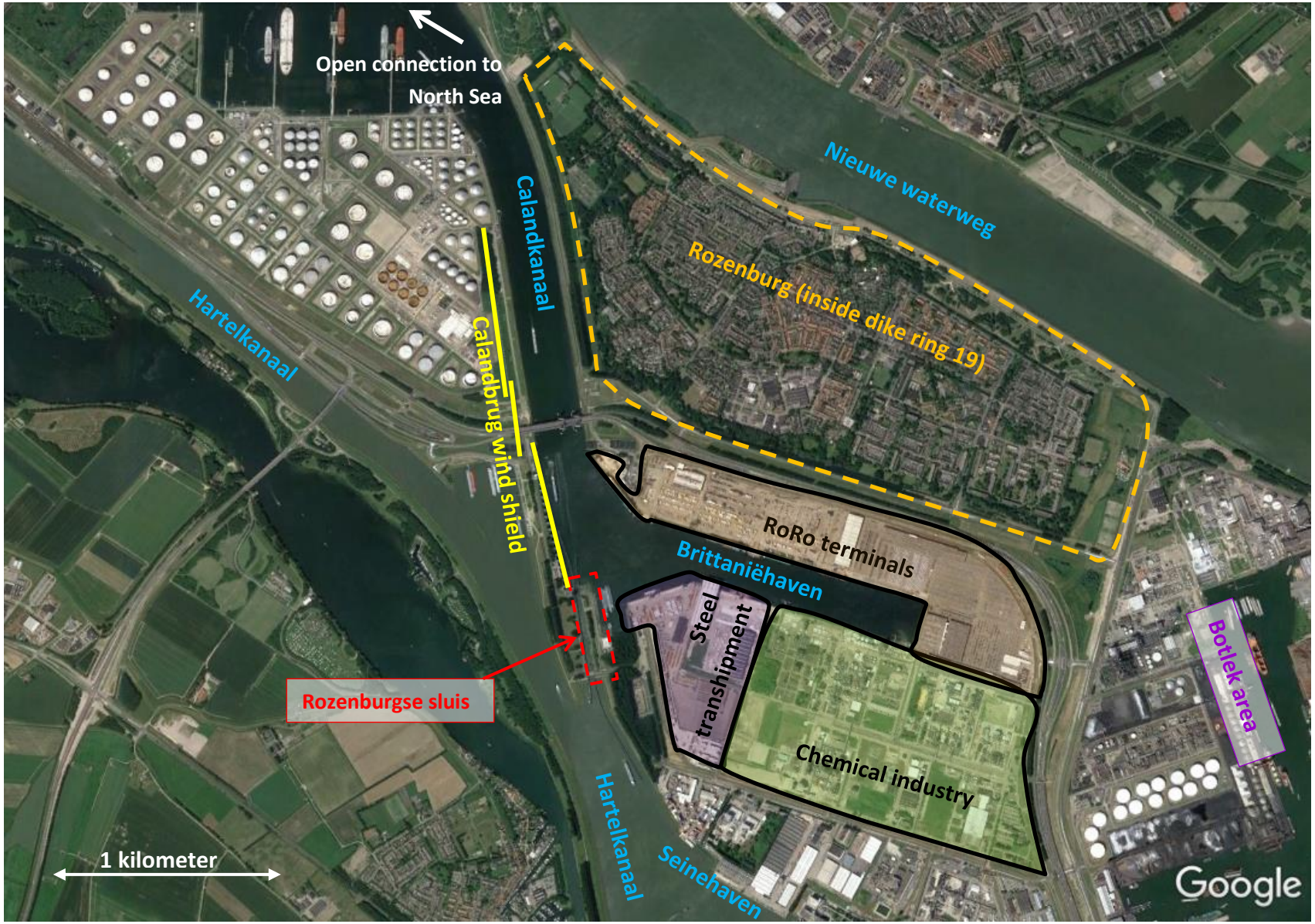

Figure H.2: Aerial picture of the Brittaniëhaven and its surroundings. Source: Google Maps (2016)